

Synopsis:

Title: "Development and Utilisation of a Novel Rat Model of Ischemic Stroke for Assessment of the Effect of Rehabilitative Onset Time post Stroke on Gait Function"

Theme: "Applied Biomedical Engineering and Informatics"

Project period: 3rd - 4th semester,
Autumn 2011 - Spring 2012

Project group: 1084

Participants: 3

Katrine Leander Soerensen

Daniel Simonsen

Rasmus Kragh Nielsen

Advisor:

Winnie Jensen

Number of copies: 6

Number of pages: 104

Ended: 1st of June 2012

The content of this report is freely available, but publication (with sources) may be made after agreement with the authors.

Cerebral ischemia is caused by occlusion of the vascular supply in a local region of the brain, and 85 % of all strokes are ischemic of nature. One of the major consequences of ischemic stroke is motor dysfunction such as a decrease in the walking ability. In relation to rehabilitation post stroke, two terms are used "true recovery", implying restoration of the neurological circuitry, and "behavioral compensation", implying alterations of the neurological circuitry, which was in place pre stroke. The aim of rehabilitative training is to obtain the largest possible degree of "true recovery", and has previously been related to the onset time of rehabilitation. The aim of the present study was to investigate the effects of ischemic stroke and onset of subsequent rehabilitation related to gait function in rats, by development and utilisation of a novel rat model of ischemic stroke. Nine male Sprague-Dawley rats (350 - 400 g) were instrumented with a 16-channel intracortical (IC) electrode array. Stroke was induced by the photothrombosis method, within the hindlimb area of the left hemisphere, and rehabilitation consisted of a repetitive training paradigm over 28 days, initiated on day one and seven for intervention group 1 and 2, respectively. Data were obtained from IC microstimulation tests, treadmill walking tests, and beam walking tests. Results revealed an expansion of the hindlimb representation, and an increased firing rate modulation size post stroke for intervention group 1, but not for intervention group 2. Residuals and centre of gravity for marker trajectories revealed a significant change pre to post stroke for both intervention groups. Results from the beam walking test showed functional performance deficits, which though returned to baseline level. The results from the present study emphasise the existence of a critical period. In conclusion, the results indicate that rehabilitation onset time within the critical period is related to a higher degree of "true recovery". Further, a novel rat model of ischemic stroke was successfully developed.

Resume

Hvert år rammes ca. 13.000 mennesker af en iskæmisk blodprop grundet okklusion af en eller flere blodårer i hjernen. Som en følge heraf lider imellem 30.000 – 40.000 personer af følgevirkninger relateret til iskæmiske blodpropper. Halvdelen af disse følgevirkninger er af kronisk karakter, og en af de mest udbredte følgevirkninger er nedsat eller manglende kontrol af gang funktionen. Den akutte behandling af iskæmiske blodpropper består af rekanalisering igennem trombolytisk behandling, hvilket har til formål at reetablere blod forsyningen til det ramte område. Hvis behandlingen påbegyndes inden for de første fire timer efter indtræf af en iskæmisk blodprop, kan 10 % af patienterne undgå alvorlige komplikationer relateret til den iskæmiske blodprop [1], [2]. Rehabilitering handler i første omgang om at mobilisere patienten. Efterfølgende gennemgår patienten et struktureret træningsforløb. Rehabilitering, der har til formål at styrke patientens muskelstyrke og funktion, består af en række fysiske træningsformer, heriblandt repetitiv fysisk træning. Formålet med rehabilitering er at reetablere så meget af det beskadigede neurologiske netværk i hjernen som muligt ("true recovery"), dog er det ikke muligt at opnå komplet "true recovery", da nogle neurologiske systemer er blevet forvoldt så stor skade, at det ikke er muligt at genoprette funktionen i dette område. Derfor er den reelle effekt af rehabilitering et sammenspil mellem "true recovery" og "behavioral compensation", hvilket består i at andre områder af hjernen overtager funktionen fra det skadede område [3]. Studier har vist at den største effekt af rehabilitering opnås igennem opstart af rehabilitering indenfor en kritisk periode, som strækker sig fra 5 til 14 dage efter indtræf af en iskæmisk blodprop [4], [5]. Dette leder frem til følgende problemstilling for denne rapport: Undersøgelse af om gangfunktionen efter iskæmisk blodprop er påvirket af starttidspunktet for rehabilitering, ved udvikling og benyttelse af en rotte model relateret til iskæmiske blodpropper.

I dette studie blev ni Sprague-Dawley rotter (350 – 400 g) benyttet. Alle rotter fik implementeret et intrakortikalt elektrode array bestående af 16 kanaler. Iskæmisk blodprop blev induceret i området, der repræsenterer bagbensfunktion i motor cortex ved brug af fototrombose metoden [6]. Rehabiliteringen bestod i repetitiv træning over et forløb på 28 sammenhængende dage, med start på dag et for interventionsgruppe 1 og dag syv for interventionsgruppe 2 efter inducering af iskæmisk blodprop. Dataopsamlingen omhandlede udførelse af intrakortikale mikrostimulationstest, gang test på løbebånd samt gang funktionstest på bom både før og efter inducering af iskæmisk blodprop. Resultaterne, der er relateret til intrakortikale mikrostimulationstest, viste en signifikant ændring i den kortikale repræsentation af bagbensbevægelse for interventionsgruppe 1, hvilket ikke var tilfældet for interventionsgruppe 2. Desuden blev en signifikant forøgelse i modulationen af fyringsfrekvens observeret for interventionsgruppe 1. Dette kunne ikke ses for interventionsgruppe 2. I relation til bevægelsesmønstret for højre bagben blev der, igennem analyse af

kinematisk data fra gang på løbebånd, set signifikante ændringer i denne for begge interventionsgrupper. For interventionsgruppe 2 blev det dog observeret, at denne ændring var mindre udtalt end for interventionsgruppe 1. Resultater for funktionstesten på bom viste at begge interventionsgrupper havde nedsat gangfunktion efter inducering af iskæmisk blodprop. Ved afslutning af forsøget havde begge interventionsgrupper dog nået et niveau, der svarede til deres funktionsniveau før inducering af iskæmisk blodprop. Resultaterne observeret i dette forsøg underbygger eksistensen af en kritisk periode i relation til start af rehabilitering. Således kan det konkluderes at der er indikationer for forøget effekt af rehabiliteringen, hvis opstarten sker indenfor den kritiske periode. Dette vil sige at interventionsgruppe 2 har en højere grad af "true recovery" end interventionsgruppe 1. Ydermere dokumenterer resultaterne, at en rotte model relateret til iskæmisk blodprop blev udviklet.

Kildeliste

[1] http://www.hjerteforeningen.dk/hjertestatistik/fakta_om_apopleksi/, besøgt: 19.05-2012.

[2] T. V. Schroeder et al., "Basisbog i Medicin og Kirurgi". Munksgaard Danmark, 4. udgave; ISBN: 978-87-628-0573-6, 2008

[3] T. H. Murphy & D. Corbett. "Plasticity during stroke recovery: from synapse to behaviour". *Neuroscience*, 10:861–872, 2009.

[4] J. Biernaskie et al. "Efficacy of Rehabilitative Experience Declines with Time after Focal Ischemic Brain Injury". *Journal of Neuroscience*, 24: 1245–1254, 2004.

[5] A. W. Dromerick et al. "Very Early Constraint-Induced Movement during Stroke Rehabilitation (VECTORS): A single-center RCT". *Neurology*, 73: 195–201, 2009.

[6] P. Wester et al. "A Photothrombotic 'Ring' Model of Rat Stroke-in-Evolution Displaying Putative Penumbra Inversion". *Stroke*, 26: 444–450, 1987.

Preface

This report has been composed by project group 1084, in the project period of 3rd - 4th semester, of the master education in Biomedical Engineering and Informatics with specialisation in Medical Systems, at Aalborg University.

This report reflects a long-term study spanning three semesters, and was initiated 1st of February 2011. Work conducted on the 2nd semester of the master is documented in the form of an abstract submitted for the 2012 IFESS Conference.

Work conducted during the 3rd and 4th semester of the master education concerned development of an ischemic stroke model which makes use of a novel approach to investigate the effects of stroke and rehabilitation. Thus, the work was documented in the form of an article, which is prospectively aimed at publication in IEEE Transactions on Neural Systems and Rehabilitation Engineering. In this way the article concerning stroke and rehabilitation serves as the main documentation of the project groups work, and all other chapters are supplementary chapters (e.g. chapters concerning relevant physiology, the experimental protocol, results obtained from pilot experiments, additional discussion, and conclusion) that compliment the article.

The reference style used in the article and abstract is according to standards specified by the journal, and supplementary chapters is according to the Harvard method [Last name, Year]. The figures and tables are numbered with reference to the chapter, e.g. figure 1 in chapter 3 is 3.1.

We would like to thank Jens Soerensen, Ole Soerensen, and Torben Madsen at Pathological Institute at Aalborg Sygehus Nord for assistance, while carrying out surgeries and animal experiments. Further, we would like to thank our supervisor Winnie Jensen for technical assistance during the project.

Contents

| | | |
|------------|--|-----------|
| 1 | Introduction | 1 |
| 1.1 | Methodological Choices | 2 |
| 1.2 | Solution Strategy | 3 |
| I | Articles | 5 |
| 2 | Modulation of Intracortical Motor Cortex Responses During Walking in Rats | 7 |
| 3 | Assessment of the Effect of Rehabilitative Onset Time post Stroke on Gait Function - A Novel Rat Model of Ischemic Stroke | 11 |
| II | Background Knowledge | 21 |
| 4 | The Neocortex of the Rat | 23 |
| 4.1 | Cellular Composition | 23 |
| 4.2 | Cortical Connectivity | 24 |
| 4.3 | Characteristics of the Motor Cortices | 25 |
| 4.4 | Correlations and Discrepancies between the Human and Rat Motor Cortices | 28 |
| 5 | Gait | 31 |
| 5.1 | Central Pattern Generators | 32 |
| 5.2 | Gait Adjustments as a Result of Peripheral Input | 33 |
| 5.3 | Gait Adjustments as a Result of Supraspinal Processes | 34 |
| 5.4 | Correlations and Discrepancies between Human and Rat Gait | 34 |
| 6 | Ischemic Stroke Induction and Recovery | 37 |
| 6.1 | Ischemic Stroke Induced by the Photothrombosis Method | 37 |
| 6.2 | Plasticity post Ischemic Stroke | 38 |
| 6.3 | Correlations and Discrepancies between Human and Rat Stroke | 42 |
| III | Intervention Study | 45 |
| 7 | Pilot Experiment | 47 |
| 7.1 | Aim of Pilot Experiment | 47 |

| | | |
|-----------|--|-----------|
| 7.2 | Results | 48 |
| 7.3 | Experiences from the Pilot Experiment | 50 |
| 8 | Experimental Protocol | 51 |
| 8.1 | Setup | 53 |
| 8.2 | Experimental Procedures | 59 |
| 9 | Data Analysis | 65 |
| 9.1 | Intracortical Microstimulation Test | 65 |
| 9.2 | Treadmill Walking Test | 65 |
| 9.3 | Beam Walking Test | 73 |
| 9.4 | Statistics | 74 |
| 10 | Results | 75 |
| 10.1 | Intracortical Microstimulation Test | 76 |
| 10.2 | Treadmill Walking Test - Intracortical Signals | 78 |
| 10.3 | Treadmill Walking Test - Kinematics | 83 |
| 10.4 | Beam Walking Test | 90 |
| 10.5 | Summary of Results | 92 |
| 11 | Additional Discussion | 95 |
| 11.1 | Methodological Considerations | 95 |
| 11.2 | Results | 96 |
| 12 | Additional Conclusion | 99 |
| 12.1 | Future Perspectives | 99 |

In Denmark, approximately 13,000 people each year suffer from occlusion of one or several blood vessels, within the brain (ischemic stroke). As a consequence, around 30,000 - 40,000 people are currently suffering from impacts related to stroke incidents. Around 50 % of these impacts, are permanent dysfunctions, and one of the most frequently observed dysfunctions is lack of muscle control resulting in impaired walking ability [Hjerteforeningen, 2011; Yonggang et al., 2008].

Within the first seconds, post ischemic stroke onset, brain cells at the site of infarction cease to function, due to decreased levels of oxygen and glucose supply to the area. Structural damage of the neurons, within the ischemic region, is observed within minutes after the onset of ischemic stroke (fig. 1.1). Irreversible damage occurs in the ischemic core, since the neurons within this region are unable to sustain homeostasis, due to the lack of sufficient blood supply. The damage in the penumbra is less severe, due to some degree of oxygen and glucose supply to the area, enabling neurons within this region to sustain homeostasis in a time-limited period. Thus, without proper treatment, the neurons within the penumbra will progress to infarction due to several mechanisms following the ischemic stroke, and as a result irreversible damage will occur [Dirnagl et al., 1999; Murphy and Corbett, 2009].

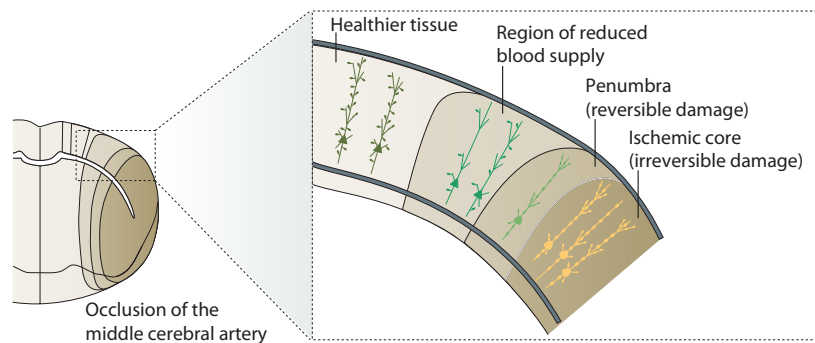


Figure 1.1: Cross-section of the cortex of the rat, depicting the effects of experimental occlusion of the middle cerebral artery. The dark brown region depicts the core of the ischemic stroke. The penumbra, which is the targeted area of rehabilitation, is depicted as the light brown region. Modified from [Murphy and Corbett, 2009].

Recanalisation, which aims at re-establishing blood supply to the affected regions, by use of thrombolytic agents, is currently the only acute treatment of ischemic stroke. Approximately, 10 % of patients, suffering from an ischemic stroke, will avoid severe impacts related to the stroke, if thrombolytic intervention is conducted, within four hours post stroke. Earlier initiation of thrombolytic intervention is correlated with an even higher success rate related to avoidance of severe impacts fol-

lowing ischemic stroke [Hjerteforeningen, 2011].

Rehabilitation initially concerns mobilisation of the patient. Prospectively, the patient is subjected to different types of training, related to motor dysfunctions, in order to improve muscle function and control [Sundhed.dk, 2010]. Concerning rehabilitation, the penumbra is of special interest, since it has been documented that the largest gains post stroke are correlated with the degree of conservation of penumbral regions. Rehabilitation techniques focusing on conservation of brain function, make use of repetitive movement exercises (hebbian synaptic learning), through which synaptic connections are restored and enhanced by repeated associated inputs, i.e. long-term potentiation (LTP). Further, endogenous neurons and glia from subventricular zones may migrate to the site of infarction, as a response to the neuronal activity, within the penumbra. The glia and endogenous neurons will aid in the regeneration of neurons, once arrived at the penumbral region [Dobkin, 2004]. In relation to rehabilitation onset, a study by Biernaskie et al. [2004] has documented different degrees of recovery post stroke. Significant levels of recovery, were observed, when rehabilitation was initiated on day 5 or 14, compared to rehabilitation initiated on day 30 post stroke. Additionally, increased levels of growth-promoting genes have been documented within the same period post stroke, resulting in suggestion of a critical period from day 5 - 14 post stroke, where optimal effects of rehabilitation can be achieved [Murphy and Corbett, 2009]. Further, results from a study by Dromerick et al. [2009] support the existence of a critical period, since very early onset of rehabilitation (three days post stroke) resulted in less motor improvement, compared to later onset.

On the basis of the aforementioned studies by Murphy and Corbett [2009], Dromerick et al. [2009], and Biernaskie et al. [2004], it would be of high relevance to assess, if rehabilitation onset post stroke, within the critical period, would result in a more pronounced regain of gait function, compared to rehabilitation onset prior to the critical period. Thus, the aim of the present work was to:

Assess if gait function post stroke was affected by different onset times of rehabilitation, through development and utilisation of a novel rat model of ischemic stroke.

1.1 Methodological Choices

As a result of the aim, the rehabilitative focus in the present work concerned gait dysfunction, since it is one of the most frequently observed disabilities, related to ischemic stroke in humans. Further, the experimental model was build around a previously, established rat model of ischemic stroke, featuring a novel approach to assessment of neuronal activity, within the motor cortex during gait, utilising a 16-channel intracortical (IC) electrode array, and induction of stroke by the photothrombosis method [Wester et al., 1987]. The model has previously been used for assessment of the effect of rehabilitation of upper extremities through repetitive grasping training. The use of laboratory rats as subjects has several advantages, since they are quite homogenous within strains, and can easily be monitored during experiments [Woodruff et al., 2011].

1.2 Solution Strategy

Initial work concerned verification of neuronal firing rate modulations related to gait in healthy rats, and was conducted on the 2nd semester of the master education in Biomedical Engineering and Informatics. The physical task was changed from a grasping exercise to walking on a motorised treadmill. The initial work documented that the firing rate of neurons, within the motor cortex of the rat, similarly to other quadrupeds, did modulate according to the gait cycle. Hence, the results from this study were comparable to results from studies utilising single-unit recordings in cats [Armstrong and Drew, 1984; Drew, 1988]. The initial work resulted in an abstract submission to the conference *IFESS Smart Machines - Neural Evolution in Banff, Alberta, Canada, September 9 - 12, 2012* (ch. 2).

In the present work, several methodological components were added to the rat ischemic stroke model, hereby enabling recording of data, related to rehabilitation post stroke. Thus, a beam walking test was added to the model, in order to assess if motor performance alterations did occur as a consequence of the photothrombosis intervention and subsequent rehabilitation. Further, a more extensive analysis of kinematic data, related to the treadmill walking test was performed, in order to document if gait patterns were modified as a consequence of the stroke. Two intervention groups, only differing in the time of rehabilitation onset, were included in the study, in order to verify if significant differences were related to rehabilitation onset. The study was conducted during the 3rd and 4th semester of the master education in Biomedical Engineering and Informatics, and is documented through an article, aimed at publication in *IEEE Transactions on Neural Systems and Rehabilitation Engineering* (ch. 3).

In this way, the articles located in **Part I**, document the initial study (ch. 2) and the major work of the 3rd and 4th semester of the master education of Biomedical Engineering and Informatics (ch. 3). Additional chapters function as supplementary information, supporting the content of the major article, and more thoroughly documenting aspects related to the experimental protocol and the obtained results. **Part II** describes the different physiological aspects related to the experiment, whereas **Part III** documents all aspects related to the experimental protocol and results. Further, an additional discussion, conclusion, and perspective are included in the supplementary chapters, in order to account for considerations, related to the methodological choices made prior to onset of the study, and results that are not displayed within the article. It should be noted that the experimental protocol reflects the intended experiment. In cases, where the experimental study deviated from the experimental protocol, the nature of the deviation and following consequences are described.

Articles

I

Modulation of intracortical motor cortex responses during walking in rats

Nielsen RK¹, Simonsen D¹, Soerensen KL¹, Jensen W¹¹. Center for Sensory-Motor Interaction, Dept. Health Science and Technology, Aalborg University, Aalborg, Northern Jutland, Denmark

Abstract

Single-unit firing rate alterations has been observed in the motor cortex of walking cats, suggesting some degree of cortical control of gait. Further, recent studies have shown altered gait patterns as a result of corticospinal damage in quadrupeds, suggesting that the motor cortex has a function in relations to gait patterns. Our objective was to investigate if similar motor cortex firing patterns could be observed using a multi-unit recording approach in rats, walking on a treadmill. Two Sprague-Dawley rats were instrumented with a 16-channel intracortical electrode array. Neuronal firing rates were recorded at three different gait velocities. ANOVA and Kruskal-Wallis tests were utilised to test for significant differences in the firing rates, recorded by the channels. Results revealed that mean firing during stance and swing, for the majority of the channels, was significantly different for both rats. Further, the occurrence of the peak of the PSTH, within both the stance and swing phase, modulated according to gait velocity in the majority of the channels. Alterations in the actual peak firing rate were only observed in a few of the channels. Results were comparable to results from studies utilising single-unit recording, conducted in cats.

Keywords: motor cortex, gait, intracortical recording, descending input, rat model

Introduction

Evidence suggests that human gait is a result of a basic rhythmic walking activity generated, within neuronal circuitries in the spinal cord, and modulated by supraspinal control and sensory feedback [1]. Therefore, one of the possible consequences of ischemic stroke in humans is motor dysfunction, such as a decrease in walking ability [2]. On the contrary, integration of motor cortex input has been reported as being nonessential with regards to control of gait in experimental animals such as cats and nonhuman primates, since rhythmic walking has been experimentally elicited in spinalised animals [3] [4]. As a result, little research has been conducted to investigate gait alterations as a consequence of corticospinal damage [4] [5], even though studies of single-unit motor cortex firing patterns in cats showed a rhythmic activity modulation, synchronised to a specific event within the gait cycle (phase-locked firing) [6] [7]. Though, recently analysis of kinematic data from cortically injured mice, walking on a treadmill, has shown that motor cortex lesions in mice affects gait. During the experiment several impaired parameters gradually recovered to near-control levels, whereas others did not improve [5]. Similar findings were reported in cats, where the lateral descending pathway was lesioned, resulting in difficulties in regards to the execution of the swing phase (paw drag) of the affected hindlimb [3]. Our group has previously reported on multi-unit changes in motor cortex responses related to reaching and grasping in a chronic rat model of ischemic stroke [8]. In the present study we aimed to obtain and characterise multi-unit intracortical (IC) signals from rats walking on a treadmill, thus assessing if similarities in multi-unit recordings from rats, compared to single-unit data from walking cats, exist. Hereby, obtaining a base of comparison within the same animal model, which in the long-term perspective could be used for assesment of cortical damage affecting gait in rats.

Materials and Methods

Animals and training

Approval for all experimental procedures was obtained from the Danish Committee for the ethical use of animals. Two male Sprague-Dawley rats (350 - 400 g) were included in the experiment. Animals were trained to walk on a treadmill (Letica Scientific Instrument) with a perspex cover (running surface: length = 0.4 m, width = 0.1 m). Once the rats exhibited a satisfactory gait at speeds of 0.27 - 0.37 m/s, they were considered ready for entering the study.

Surgical procedures

Prior to the surgical procedure, rats were anaesthetised with a subcutaneous injection of 0.1 ml /100 g body weight of Rumpun (Ketamine: 100 mg/kg, Xylazine: 5 mg/kg, and Acepromazine: 2.5 mg/kg). A dose of approximately 0.05 ml/100 g body weight were administrated every 30 minutes to maintain the anaesthesia. A craniectomy was performed over the hindlimb area in the left hemisphere. A 16-ch IC electrode array (**array dimension:** width = 2 mm, length = 2 mm, **electrode:** Φ = 100 μ m, spacing = homogeneous) was lowered 1.8 mm into the cortex at position; 0:2 mm caudally to bregma, and 1:3 mm laterally to the midline [9]. Two stainless steel bone screws, serving as mechanical stabilisation and grounding, were inserted in the skull caudally to the electrode.

Data acquisition and analysis

IC microstimulation tests were conducted on day 2 after the surgical procedure. Each electrode within the array was consecutively stimulated (stimulus train = 100 Hz, pulse duration = 200 μ s, pulse amplitude = 70 - 280 μ A). Motor responses were visually observed and grouped into hindlimb-, forelimb-responses or responses not related to hind- or fore-limb. The IC microstimulation test revealed that 6/16 channels for rat 1 and 11/16 channels for rat 2 were related to hindlimb activation. The IC signals were acquired through a Tucker-Davis Technologies (TDT) RX5. IC signals were filtered (800 Hz - 8 kHz) prior to sampling at 24 kHz. On-line spike detection was performed using a lower threshold of \approx 1.5 x RMS of the raw data. Threshold for each channel was adjusted prior to conduction of treadmill test, and was based on spontaneous motor cortex firing activity, while the rat was sitting still. Kinematic data was recorded by a Basler A602fc-2 camera (frame rate = 100 Hz, clocking = external DT340 PCI board). Synchronisation of kinematic- and IC-data was controlled by a digital clock signal from the DT340 PCI board. Initial- and terminal-stance, within the gait cycles, were determined based on three markers, positioned on the hindlimb of the rat (knee joint, ankle joint, and distal part of paw).

The gait experiment was conducted at three different gait velocities (0.29 m/s, 0.32 m/s, 0.35 m/s). Three recordings of 30 s were captured at each gait velocity. The mean duration of the gait cycle, swing, and stance phase for the different gait velocities was estimated based on the kinematic data (tab. 1).

| —Gait cycle and phase duration— | | | |
|---------------------------------|----------------|-----------------|-----------------|
| —Rat 1— | | | |
| Treadmill velocity | Duration (ms) | | |
| | Gait | Swing | Stance |
| 0.29 m/s (N=87) | 59.51±5.21 STD | 24.76 ±3.64 STD | 34.75 ±3.74 STD |
| 0.32 m/s (N=100) | 53.03±4.30 STD | 24.91 ±2.84 STD | 28.12 ±3.25 STD |
| 0.35 m/s (N=119) | 46.53±3.96 STD | 22.30 ±3.14 STD | 24.24 ±3.31 STD |

| —Rat 2— | | | |
|--------------------|----------------|-----------------|-----------------|
| Treadmill velocity | Duration (ms) | | |
| | Gait | Swing | Stance |
| 0.29 m/s (N=87) | 64.33±6.00 STD | 28.17 ±4.64 STD | 36.16 ±6.04 STD |
| 0.32 m/s (N=90) | 59.10±4.64 STD | 23.58 ±2.56 STD | 35.52 ±3.86 STD |
| 0.35 m/s (N=76) | 53.11±7.44 STD | 25.03 ±6.44 STD | 28.08 ±5.65 STD |

Table 1: Mean duration and standard deviation of the gait cycle, swing, and stance phases for both rat 1 and rat 2.

The time window of the Peri-Stimulus Time Histograms (PSTH) was normalised according to the mean gait cycle duration for the session, and the mean firing rate, within the PSTH, was subtracted from the instantaneous firing rates in the PSTH (fig. 1). Excitatory firing rates were defined as firing rates > 0 and inhibitory firing rates were defined as firing rates < 0. A Poisson distribution was estimated from the data, and the upper and lower 95 % confidence intervals were determined. Channels that recorded neuronal firing rates, which exceeded the 95% confidence limits, were selected for further analysis.

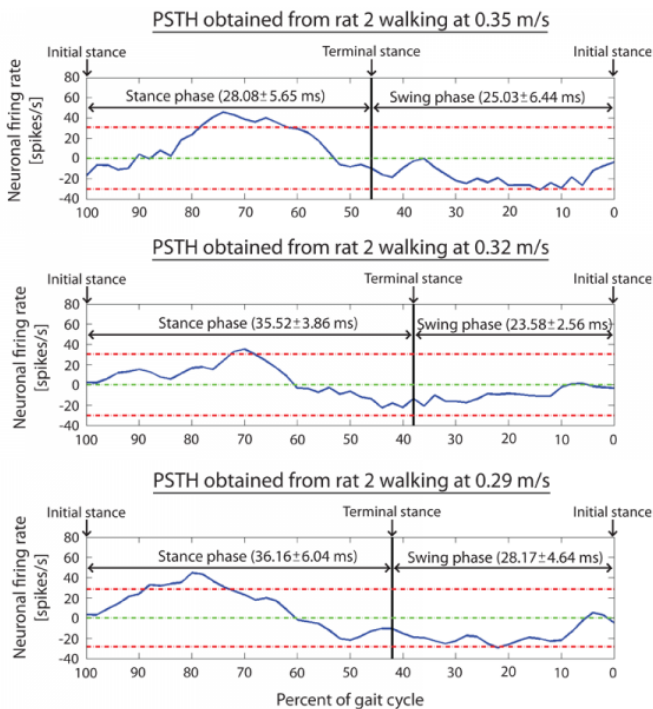


Figure 1: Neuronal firing rates during the gait cycle, recorded by channel 9 of rat 2. The mean duration ± STD for both swing and stance is indicated. Limits of the Poisson distribution is depicted as the read dashed lines. Note that events are expressed as percent of the gait cycle duration.

The mean firing rate, within the PSTH, was chosen as a feature for study. Two-way ANOVA (gait phase, gait velocity) was used to test if any differences between the firing rate, within the phases of the gait cycle exists, and if the mean firing rate did change as a function of gait velocity. The amplitude and temporal position of the peak firing rate (inhibitory/excitatory), within stance and swing, was detected and used as a

feature in order to obtain detailed information on specific events within the gait cycle, and assess if alterations of events did occur as a consequence of gait velocity changes. Kruskal-Wallis test (gait velocity) was used to test the firing rate modulation, since the data did not suffice a normal distribution.

Results

Modulation within the gait cycle

Two-way ANOVA (gait phase, gait velocity) revealed that phase was a significant main effect in the channels of interest for rat 1 (fig. 2). No significant interaction effect was observed. Gait velocity was not a significant main effect related to the neuronal firing for rat 1 (tab. 2). Two-way ANOVA for rat 2 revealed that phase was a significant main effect for the mean firing rate in 3/4 channels (ch.5, ch.6 and ch.9) (fig. 2). Channel 2 and 9 showed a significant interaction effect. Gait velocity was not a significant main effect related to the neuronal firing for rat 2 (tab. 2).

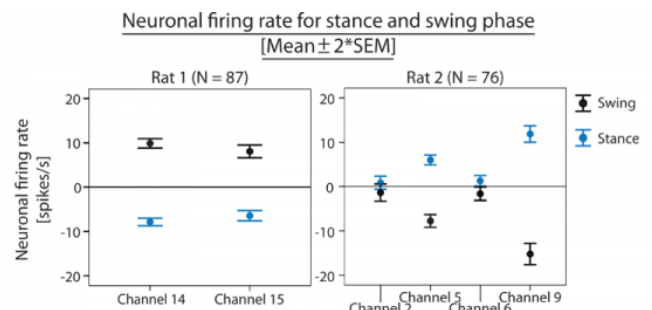


Figure 2: Mean firing rate within the stance and swing phase, calculated across the three gait velocities. Black errorbars indicate mean firing ± SEM for swing, whereas blue errorbars indicates mean firing ± SEM for stance.

Post-hoc test revealed that gait phase*gait velocity at 0.35 m/s was significantly different from gait phase*gait velocity at 0.29 m/s and 0.32 m/s for channel 2. Post-hoc test for channel 9 revealed that gait phase*gait velocity at 0.32 m/s was significantly different from phase*gait velocity at 0.29 m/s and 0.35 m/s (fig. 3).

Neuronal firing rate for channels exhibiting firing rate alterations due to gait velocity*gait phase interaction

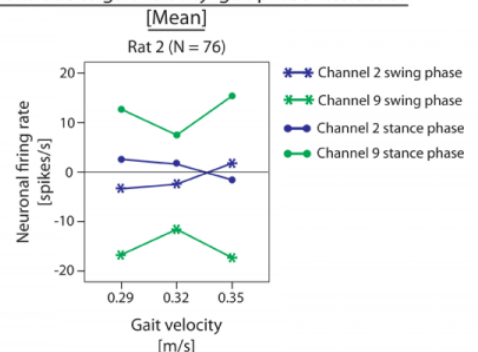


Figure 3: Mean firing rate alterations for channel 2 and 9 of rat 2 as a result of a gait phase*gait velocity interaction.

—p-values related to mean firing within the gait cycle—

—Rat 1(Summary of p-values)—

| Channel | Gait velocity | Phase | Gait velocity*Phase |
|---------|---------------|--------|---------------------|
| 14 | 0.406 | 0.000* | 0.076 |
| 15 | 0.797 | 0.000* | 0.072 |

—Rat 2 (Summary of p-values)—

| Channel | Gait velocity | Phase | Gait velocity*Phase |
|---------|---------------|--------|---------------------|
| 2 | 0.920 | 0.067 | 0.004 |
| 5 | 0.722 | 0.000* | 0.302 |
| 6 | 0.998 | 0.003 | 0.331 |
| 9 | 0.796 | 0.000* | 0.001 |

Table 2: Summary of p-values from the two-way ANOVA (gait phase, gait velocity) test of mean firing. * indicates p-values < 0.001.

Based on the results, the overall neuronal firing between stance and swing differed, where one was inhibitory, whereas the other was excitatory, since the mean firing between the phases was statistically different. Furthermore, the results from a couple of channels (2/6 channels in all) showed that the mean firing rate, within each phase, did change as a result of increased gait velocity, and thus that the mean firing rate ratio of the neurons between swing and stance in some cases was affected by the gait velocity. This effect though, was not observed to have a linear relationship with gait velocity.

Modulation of the peak firing rate

The Kruskal-Wallis test revealed that the gait velocity was a significant main effect related to changes in the timing of the peak firing rate for the stance phase in both channels of rat 1. Significant changes in the timing of peak firing rate, within the swing phase, was only seen on channel 15. Significant changes of the amplitude of peak firing rate was observed as a function of gait velocity for the stance phase in channel 14 (tab. 3). Results from rat 2 showed that gait velocity was a significant main effect related to changes in the timing of the peak firing rate for both gait phases of all channels. Channel 2 exhibited a significant change in the amplitude of peak firing rate in the stance phase as a function of gait velocity, whereas channel 6 had significant peak firing rate alterations of the amplitude in the swing phase (tab. 3).

Post-hoc test on data from rat 1 revealed that the temporal position of peak firing, within the stance phase for channel 14, was significantly different for gait velocity at 0.29 m/s compared to gait velocity at 0.32 m/s and 0.35 m/s. For channel 15, all temporal positions of peak firing as a function of gait velocity were significantly different for both swing and stance. Post-hoc test on data from rat 2 revealed that the temporal position of peak firing as a function of gait velocity was significantly different for both swing and stance for all channels (fig. 4).

Post-hoc test on data from rat 1 revealed that the amplitude of peak firing, within the stance phase for channel 14, was significantly different for gait velocity at 0.32 m/s compared to gait velocity at 0.35 m/s. Post-hoc test on data from rat 2 revealed that the amplitude of peak firing, within the stance phase for channel 2, was significantly different for gait velocity at 0.29 m/s compared to gait velocity at 0.35 m/s, and 0.32 m/s compared to gait velocity at 0.35 m/s. For the swing phase in channel 6 significant differences was observed for gait velocity at 0.32 m/s compared to gait velocity at 0.35 m/s (fig. 5).

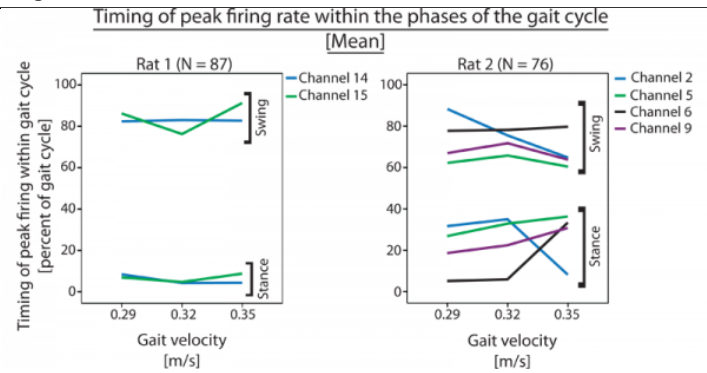


Figure 4: Temporal modulation of the peak firing rate as a function of gait velocity.

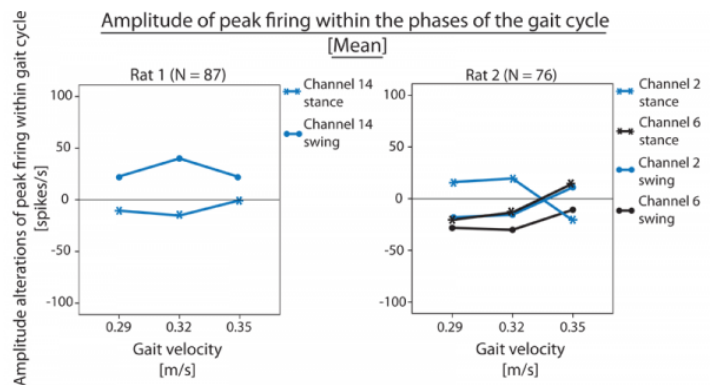


Figure 5: Amplitude alterations of the peak firing rate within the gait cycle as a function of gait velocity.

Based on the results it is apparent that the timing of peak firing rate, within both phases, did change as a consequence of gait velocity for the majority of channels (5/6 channels in all). This observation applies to both timing of inhibitory and excitatory peak firing rates. Though, it should be noted that the timing of the peak modulatory firing rate did not appear to have a linear relationship with gait velocity when measured as percent of gait cycle. The amplitude of the peak modulatory firing rate did only change as a function of gait velocity for a few channels (3/6 channels in all). Similar to the timing of peak firing, amplitude of peak firing was not observed to have a linear relationship with gait velocity.

—p-values for peak firing rate events within the gait phases—

| —Rat 1 (Summary of p-values)— | | | |
|-------------------------------|----------------------------|--------|---------------|
| Channel | | | Gait velocity |
| 14 | Timing of peak firing rate | Swing | 0.844 |
| | | Stance | 0.000* |
| | Peak firing rate | Swing | 0.979 |
| | | Stance | 0.032 |
| 15 | Timing of peak firing rate | Swing | 0.000* |
| | | Stance | 0.000* |
| | Peak firing rate | Swing | 0.120 |
| | | Stance | 0.250 |

| —Rat 2 (Summary of p-values)— | | | |
|-------------------------------|----------------------------|--------|---------------|
| Channel | | | Gait velocity |
| 2 | Timing of peak firing rate | Swing | 0.000* |
| | | Stance | 0.000* |
| | Peak firing rate | Swing | 0.114 |
| | | Stance | 0.004 |
| 5 | Timing of peak firing rate | Swing | 0.000* |
| | | Stance | 0.000* |
| | Peak firing rate | Swing | 0.072 |
| | | Stance | 0.343 |
| 6 | Timing of peak firing rate | Swing | 0.000* |
| | | Stance | 0.000* |
| | Peak firing rate | Swing | 0.021 |
| | | Stance | 0.120 |
| 9 | Timing of peak firing rate | Swing | 0.000* |
| | | Stance | 0.000* |
| | Peak firing rate | Swing | 0.642 |
| | | Stance | 0.358 |

Table 3: Summary of p-values from the Kruskal-Wallis test (gait velocity) for peak firing rate and temporal position of peak firing rate. Phases written in red indicates firing modulations, where an excitatory firing rate was detected. Phases written in blue indicates firing modulations, where an inhibitory firing rate was detected. Phases written in black indicates modulation intervals that changed from inhibitory to excitatory firing or vice versa as a function of gait velocity. * indicates p-values < 0.001.

Discussions

Analysis of the IC multi-unit responses obtained from two rats walking on a treadmill, documented that neuronal firing rates, within the hindlimb area, contained modulations, which were not a results of random firing rate fluctuations, since the PSTH responses exceeded the limits of the Poisson distribution. Significant differences in the mean firing rate was found between the stance and swing phase across all gait velocities for both rats, implying that cortical neurons, within the multi-unit recording site, fired at different rates during the stance phase compared to swing. These observations are in line with data from mice and cats, suggesting that the motor cortex may play a role in the initiation of the swing phase, and fine-tuning of movement during the swing phase [5] [10]. It should be noted that the pattern of mean firing rate during stance and swing is opposite between the two rats (stance = excitatory and swing = inhibitory or vice versa), and that all channels, which recorded significant firing rate differences, displayed the same phase pattern for the individual rat (all channels exhibited excitation in the same phase and inhibition in the other). The lack of channels exhibiting excitatory firing rates in the swing phase, as well as channels exhibiting excitatory firing rates within the stance phase for the individual rat, may be owing to imprecise electrode placement resulting in a low count of electrodes related to hindlimb. For rat 2, a significant interaction effect was observed for two channels. No pattern related to the interaction effect was obvious by inspection of the firing rate versus gait velocity plot. Analysis of the peak firing rate modulation (excitatory/inhibitory), within both the swing and stance phase, revealed that the timing of peak firing rate (percent of gait cycle) did change as a function of gait velocity. No consistent pattern of firing rate timing as a function of gait velocity can be visually determined from the

plots. Though, still the changes in timing document that some cortical neurons do fire in relation to some aspect related to the gait velocity. In order to investigate this alteration in peak firing rate timing it would be of interest to include electromyographical recording from muscles in the hindlimb related to the targeted cortical area. Only few examples of significant peak firing rate changes were observed. These results are in line with single-unit recordings from cats walking on a treadmill at different velocities. Here the peak firing rate for the majority of neurons was found to be approximately constant despite changes in gait velocity. Firing rates of neurons exhibiting alterations of peak firing as a function of gait velocity did not show any characteristic pattern, since significant firing rate alterations could be observed between two gait velocity levels, whereas no alterations were observed between all other gait velocities [6].

Conclusions

IC multi-unit recording by use of a 16-channel electrode array implanted, within the hindlimb area of the motor cortex in the rat, documented that firing rate modulations does occur during gait. Further, it was observed that timing of the peak firing rate modulation did change as a function of gait velocity, and that in a few cases did the amplitude of the peak firing change as a function of gait velocity. The results from the present study is in line with results from single-unit recordings of cats, walking on a treadmill. Future studies should include simultaneous recording of electromyography, in order to allow a closer investigation of the correlation between kinematics, muscle activity, and the cortical neuronal discharge related to gait.

References

- [1] J. B. Nielsen. "How we Walk: Central Control of Muscle Activity during Human Walking". *The Neuroscientist*, 9:195–204, 2003.
- [2] W. Yonngang, B. Bontempi, S. M. Hong, K. Mehta, P. R. Weinstein, G. M. Abrams, and J. Liu. "A comprehensive analysis of gait impairment after experimental stroke and the therapeutic effect of environmental enrichment in rats". *Journal of Cerebral Blood Flow and Metabolism*, 28:1936–1950, 2008.
- [3] T. Drew, W. Jiang, and W. Widajewicz. "Contributions of the motor cortex to the control of the hindlimbs during locomotion in the cat". *Brain Research Reviews*, 40:178–191, 2002.
- [4] G. Orlovsky, T. G. Deliagina, and S. Grillner. "Neuronal Control of Locomotion". 1st edition. Oxford University Press, 1999. ISBN 978-0-19- 852405-2.
- [5] M. Ueno and T. Yamashita. "Kinematic analyses reveal impaired locomotion following injury of the motor cortex in mice". *Experimental Neurology*, 230:280–290, 2011.
- [6] D. M. Armstrong and T. Drew. "Discharges of pyramidal tract and other motor cortical neurones during locomotion in the cat". *The Journal of Physiology*, 346:471–495, 1984.
- [7] T. Drew. "Motor cortical cell discharge during voluntary gait modification". *Brain Research*, 457:181–187, 1988.
- [8] L. C. Fjeldborg, M. V. Nielsen, K. J. G. Ottesen, and W. Jensen. "Characterization of peri-infarct, intra-cortical motor cortex responses during reaching task in a chronic animal model of ischemic stroke. Proceedings of the 10th Vienna International Workshop on Functional Electrical Stimulation and 15th IFESS Annual Conference, 8-12 September, 2010, Vienna, Austria, 154–156, 2010.
- [9] E. J. Neafsey, E. L. Bold, G. Haas, K. M. Hurley-Gius, G. Quirk, C. F. Sievert, and R. R. Terrence. "The Organization of the Rat Motor Cortex: A Microstimulation Mapping Study". *Brain Research Reviews*, 11:77–96, 1986.
- [10] D. M. Armstrong and T. Drew. "Locomotor-related Neuronal Discharges in Cat Motor Cortex Compared with Peripheral Receptive Fields and Evoked Movements". *The Journal of Physiology*, 346:497–517, 1984.

Acknowledgements

Jens Soerensen, Ole Soerensen, and Torben Madsen at Pathological Institute at Aalborg Sygehus Nord for assistance during experiments.

Authors Address

Winnie Jensen, Center for Sensor-Motor Interaction, Department of Health Science and Technology, Aalborg University, Fredrik Bajersvej 7D-3, 9220 Aalborg, Denmark, wj@hst.aau.dk

Assessment of the Effect of Rehabilitative Onset Time post Stroke on Gait Function A Novel Rat Model of Ischemic Stroke

Katrine Leander Soerensen, Daniel Simonsen, Rasmus Kragh Nielsen, and Winnie Jensen

Abstract—The aim of the present study was to investigate the effects of ischemic stroke and onset of subsequent rehabilitation related to gait in rats. Nine male Sprague-Dawley rats (350 - 400 g) were instrumented with a 16-channel intracortical (IC) electrode array. Stroke was induced by the photothrombosis method, within the hindlimb area of the left hemisphere, and rehabilitation consisted of a repetitive training paradigm over 28 days, initiated on day one and seven for intervention group 1 (five rats) and intervention group 2 (four rats), respectively. Data were obtained from IC microstimulation tests, treadmill walking tests, and beam walking tests. Results revealed an expansion of the hindlimb representation, and an increased firing rate modulation size post stroke for intervention group 1, but not for intervention group 2. Kinematic data revealed a significant change pre to post stroke for both intervention groups. However, this difference was larger for intervention group 1. Results from the beam walking test showed functional performance deficits, following stroke, which though returned to pre stroke level. The results from the present study is in line with results from previous studies, suggesting a critical period, where onset of rehabilitative training is more effective. In conclusion the results indicate that rehabilitation onset time within the critical period is related to a higher degree of "true recovery".

Index Terms—motor cortex, gait, intracortical recording, plasticity, rat ischemic stroke model, rehabilitation onset time.

I. INTRODUCTION

DEFICITS in motor function is a frequent consequence of ischemic stroke, caused by local thrombosis. The possible subsequent inability to control a group of muscles can produce severe gait deficits [1], since human gait is a result of a basic rhythmic walking activity, generated within neuronal circuitries of the spinal cord, and modulated by supraspinal control and sensory feedback [2]. Recovery post stroke can be subdivided into two terms; "true recovery" and "behavioral compensation". "True recovery" is often referred to as the re-emergence of the exact motor and sensory patterns in the brain, which were in place before the stroke. "Behavioral compensation" covers the situation, where function is regained through a modification of neuronal connectivity, resulting in an altered execution of motor patterns. The proportion of "true recovery" and "behavioral compensation" is dependant on the severity of the stroke. The aim of rehabilitative training is to obtain the largest possible degree of "true recovery" [3]. In relation to rehabilitation, existence of a critical period, where the brain is more susceptible to plastic changes, has been postulated on the basis of findings from comparing early brain development mechanisms with mechanisms following stroke. Increased levels of growth promoting compared to growth inhibiting

genes and proteins, were found in a period from day 5 to 14 post stroke, suggesting that rehabilitative training, if initiated within this period, might have a larger effect [4].

Knowledge concerning neuronal control of gait in healthy humans is still modest, compared to experimental animals, due to the limited amount of recording techniques, which can be applied in humans [5]. However, limitations of deductions from animal experiments exist, due to the bipedal nature of human walking, which has been shown to be under a larger degree of modulation from supraspinal levels, compared to gait of experimental animals [2]. For instance, cats have been shown to be able to walk on a flat surface upon lesion of the motor cortex, and only encounter difficulties, when traversing a horisontal ladder or avoiding obstacles [6], whereas for humans, much more severe outcomes are seen [5]. Recently though, analysis of kinematic data from cortically injured mice, walking on a treadmill, has shown that motor cortex lesion in mice affects gait performance. During the experiment, several impaired parameters gradually recovered to near-control levels, whereas others did not improve [7]. Thus, animal experiments are still valuable for understanding fundamental principles of neuronal control related to gait, even though supraspinal inputs does not have the same crucial function in animals, as in humans. Further, in animal studies a diverse range of experimental techniques can be utilised, hereby enabling optimal data acquisition circumstances.

Several animal studies have investigated the possibility of restoring motor functions, related to gait post stroke, and how different motor training paradigms affect the recovery process [7], [8], [9]. Common for the majority of these studies is that they make use of functional or endogenous assessments to draw conclusions about motor system improvements. These assessment types limit the interpretation of the ongoing plasticity in the brain, and thus also limit the possibility for investigation of the correlation between the plastic changes and obtained performance measures. However, the use of intracortical (IC) recordings has the possibility to study intricate changes of the neural activity and plasticity on a cellular level [10]. We have previously developed a novel rat gait model suitable for assessing the effects of ischemic stroke. The model is based on IC recordings and tracking of kinematic parameters of the hindlimb during treadmill walking in healthy rats. In the present study the model was expanded, in order to include ischemic stroke and rehabilitation, for assessing the effects of ischemic stroke and onset of rehabilitation on gait function. The effects of stroke and rehabilitation were assessed through analysis of the relationship between neuronal modulation, beam walking performance, and kinematics related to the gait pattern.

R. K. Nielsen, K. L. Soerensen, D. Simonsen and W. Jensen are with Center for Sensory-Motor Interaction, Dept. Health Science and Technology, Aalborg, Northern Jutland, Denmark (e-mail: wj@hst.aau.dk)

Thus, the objective of this study was to investigate if a higher amount of "true recovery" was obtained both on a cellular level and in gait function, when rehabilitation onset is within the critical period.

II. MATERIALS AND METHODS

A. Animals

All experimental procedures were approved by the Animal Experiments Inspectorate under the Danish Ministry of Justice. 24 male Sprague-Dawley rats (350 - 400 g) were initially enrolled in the experiment.

B. Experimental design

All animals went through a three week training period, where they were familiarised with being handled, trained to walk on a motorised treadmill (Letica Scientific Instrument) with a perspex cover (running surface: length = 0.4 m, width = 0.1 m) for 3 x 1 min per day, and to conduct five traversions per day on a ledged beam. The performance criteria for inclusion in the experiment was a stable gait pattern at velocities of 0.24 - 0.28 m/s on the treadmill, and a stable foot drop rate on the ledged beam. At the end of the training phase, nine rats were included in the experiment. The rats were instrumented with a 16-channel IC electrode array, and randomly divided into two intervention groups, consisting of five and four rats. The two intervention groups were subjected to identical rehabilitation paradigms, only differing in the time of rehabilitation onset. Intervention group 1 started rehabilitation on day one after ischemic stroke induction (photothrombosis intervention), whereas intervention group 2 started rehabilitation on day seven after photothrombosis intervention (fig. 1.A). IC microstimulation tests were performed upon initiation and termination of the experiment. Beam walking and treadmill walking test baseline recordings were conducted pre stroke (B1 and B2). Further, seven recordings were conducted post photothrombosis intervention (D1 - D7).

C. Surgical procedure

Prior to the surgical procedure, rats were anaesthetised with a subcutaneous injection of 0.2 ml/100 g body weight of Hypnorm-Dormicum (Hypnorm: fentanyl = 0.315 mg/ml; fluanisone = 10 mg/ml, and Dormicum: midazolam = 5 mg/ml). A dose of approximately 0.05 ml/100 g body weight were administrated every 30 min to maintain the anaesthesia. Rats were fixated in a stereotactic frame. A craniectomy was performed over the hindlimb area of the left hemisphere. A 16-channel IC electrode array, with a guiding tube (array dimension: width = 2 mm, length = 2 mm, electrode: ϕ = 100 μ m, spacing = homogenous, guiding tube: ϕ = 4 mm), was lowered 1.8 mm into the cortex at position 1:3 mm caudally to bregma, and 1:3 mm laterally to the midline (fig. 1.C) [11]. Three stainless steel bone screws, serving as mechanical stabilisation and reference for recording, were inserted in the skull (two located caudally and one rostrally with respect to the electrode), and the IC electrode array was anchored to the screws and skull by use of dental acrylic.

D. Stroke induction and rehabilitation

Prior to the photothrombosis intervention, rats were anaesthetised according to the procedure described in section II-C. Stroke was induced just rostrally to the IC electrode array (fig. 1.C). A light probe (ϕ = 3 mm) was lowered into the guiding tube, until it was located approximately 1.5 mm above the surface of the cortex. Rose bengal dye (concentration = 20 mg dye/ml saline, injection dose = 0.3 ml/100 g body weight) was injected through a catheter (ϕ = 0.7 mm, length = 19 mm) in the vein of the tail, over a 2 min timespan. The light source (λ = 560 nm), was turned on upon initiation of rose bengal dye injection, and remained on for a total of 30 min, hereby illuminating the dye, circulating within the blood vessels, supplying the cortical region, situated just beneath the light probe [12].

The rehabilitative training consisted of 25 beam traversions and 3 x 1 min of treadmill walking per day, five days a week. The motivation for the amount of rehabilitative training was based on former observations, where declined performance level was seen as a function of increased training duration, starting at approximately 3 min of treadmill walking and 25 beam traversions.

E. Data acquisition and analysis

Intracortical microstimulation test: The motivation for conduction of IC microstimulation tests upon initiation and termination of the experiment, was to produce an estimate of the cortical mapping, within the implementation site of the IC electrode array, hereby verifying correct electrode placement and if plastic changes had occurred during the experiment. Each electrode, within the array, was consecutively stimulated (stimulus train = 100 Hz, pulse duration = 200 μ s, pulse amplitude 100 - 500 μ A). Motor responses were visually observed and grouped into hindlimb-, forelimb- motor responses, or no-motor-responses. Precautions were taken, in order to assure that the rat was relaxed prior to each stimulation. Thus, the observed motor activity was related to the elicited IC microstimulation. The percentage, of all channels and channels in each row of the IC electrode array, corresponding to hindlimb evoked response, was calculated (channel grouping can be seen on fig. 1.C).

Beam walking test: The motivation, for conducting the beam walking test, was to assess functional performance changes as a result of stroke and the subsequent rehabilitation, while restricting the amount of behavioral compensation [13]. The beam walking test consisted of 20 traversions per recording day. Additional beam traversions were conducted after end of the beam walking test, in order to reach the rehabilitative level of 25 traversions per day. Upon each test the rat was placed on the broad end of the beam and then traversed the beam. Each beam walking test was recorded by a Basler A602fc-2 camera (frame rate = 100 Hz, clocking = external DT340 PCI board) for off-line analysis. The beam walking test was quantified by the number of foot drops per

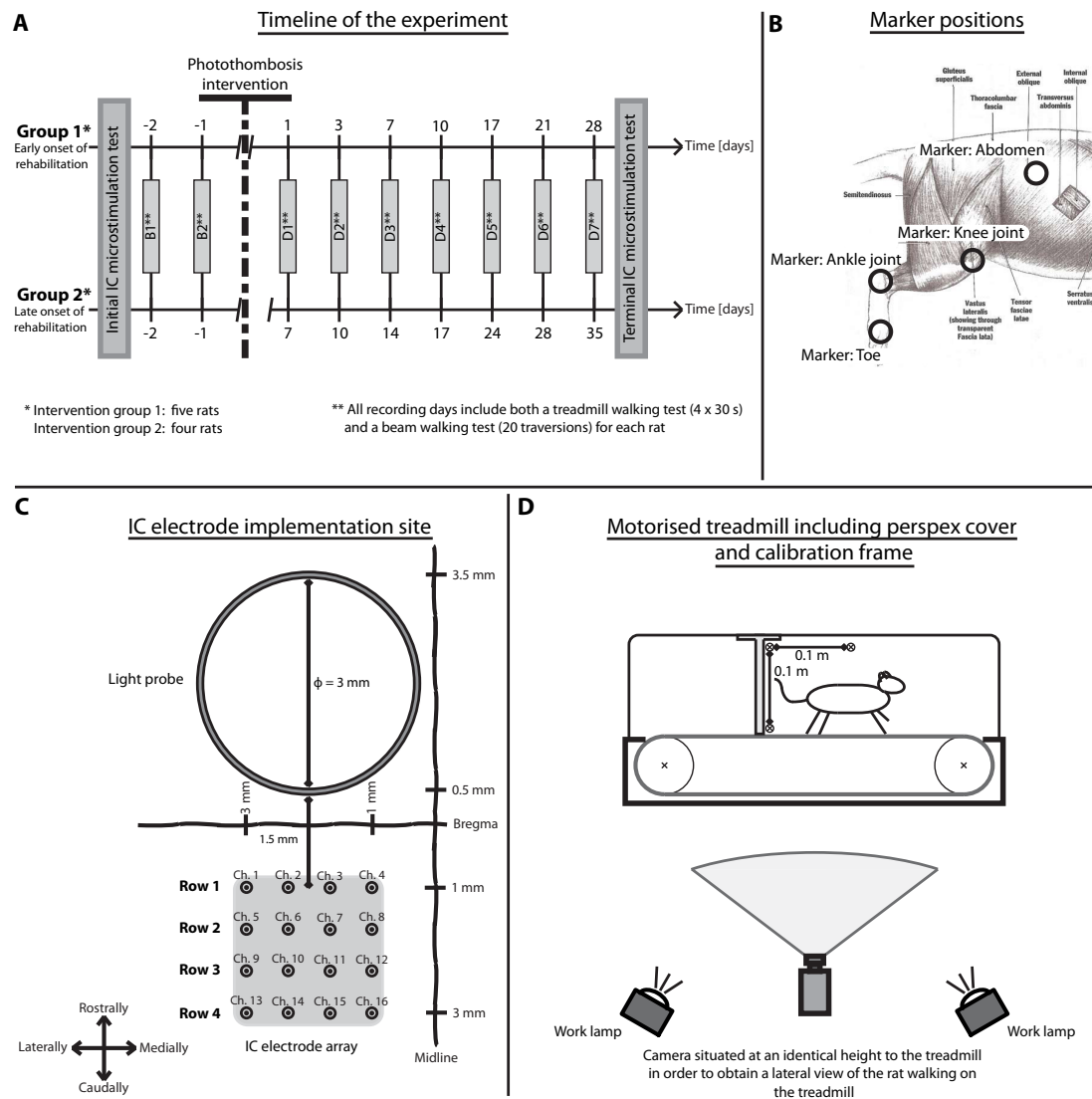


Fig. 1: **A:** timeline of the experiment: IC microstimulation tests were conducted at both initiation and termination of the experiment. Treadmill walking tests, and beam walking tests were conducted on two consecutive days pre stroke (B1 and B2) and on seven specific days post stroke (D1 - D7) for the two groups. After baseline measurements the rats underwent a photothrombosis intervention during which an ischemic stroke was induced within the hindlimb area of the left primary motor cortex. The recording days, relative to stroke induction, are displayed above the time axes for intervention group 1 and below for intervention group 2. **B:** marker positions on the hindlimb. **C:** implementation site of IC electrode and light probe position. **D:** experimental setup for treadmill walking test.

traversal.

Treadmill walking test: The motivation, for conducting the treadmill walking test, was to obtain IC signals and hindlimb kinematics related to walking, hereby assessing if neuronal activity and hindlimb movement were affected by the stroke intervention and subsequent rehabilitation. The treadmill walking test consisted of 4 x 30 s sessions per recording day and was conducted at a gait velocity of 0.26 m/s. Additional training on the treadmill was conducted after end of the treadmill walking test, in order to reach the rehabilitation level of 3 min per day. The IC signals were acquired through a Tucker-Davis Technologies (TDT) RX5. IC signals were filtered (800 Hz - 8 kHz) prior to sampling at 24 kHz. On-line spike detection was performed using a lower threshold of

1.5 x RMS of the raw data. Threshold for each channel was adjusted prior to conduction of treadmill test, and was based on spontaneous motor cortex firing activity, while the rat was sitting still. Kinematic data were recorded by a Basler A602fc-2 camera (fig. 1.D). Synchronisation of kinematic- and IC- data was controlled by a digital clock signal from the DT340 PCI board.

Initial and terminal stance, within the gait cycles, were determined on the basis of three markers, positioned on the hindlimb of the rat (knee joint, ankle joint, and toe). A fourth marker was positioned at the lateral part of the stomach (denoted as abdomen), where no bones could be sensed, hereby allowing for alignment of the individual marker trajectories (fig. 1.B). In order to enable calculation of peri-stimulus time histogram (PSTH), timing of firing rates was

Neuronal and kinematic characteristic during the gait

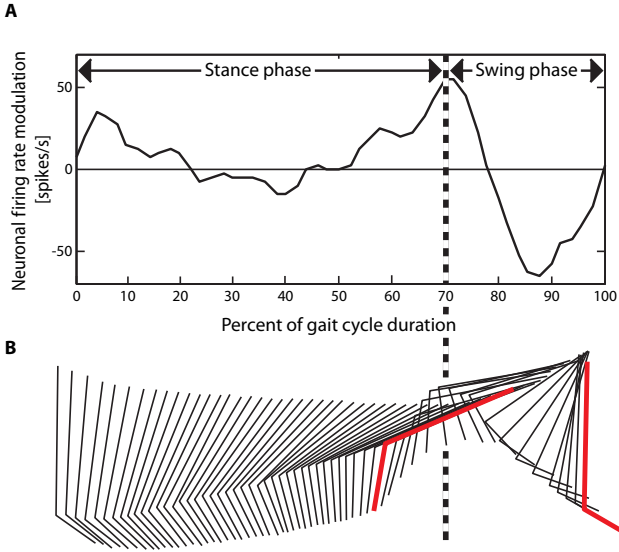


Fig. 2: **A:** The figure depicts a PSTH from data where individual gait cycles have been normalised according to the mean duration of stance-, swing-, and gait cycle- duration, resulting in the neuronal firing rate pattern being described according to percent of gait cycle duration. **B:** A matchstick figure of the lower hindlimb (knee-heel and heel-toe segment) trajectory is displayed below the PSTH. The matchstick figure is aligned according to percent of gait cycle duration, thus the first hindlimb highlighted in red represent stance-swing transition, whereas the second represent the opposite transition.

transformed from the time domain into percentage of gait cycle duration for each recording day (fig. 2). The PSTHs were rectified, and the sum of firing rates was calculated, hereby obtaining the total amount of modulation within the PSTH. Firing rate modulations were grouped according to results from IC microstimulation tests (subgroup 1: channels only related to hindlimb movement on the initial microstimulation test, subgroup 2: channels related to hindlimb movement on both microstimulation tests, and subgroup 3: channels only related to hindlimb on the terminal microstimulation test). The center of gravity (CoG) for x- and y-coordinates of the toe-, heel-, and knee-marker was calculated for each gait cycle, and averaged for each recording day.

Statistics: For all tests, except the IC microstimulation test, difference between baselines within each group was tested with one-way ANOVA, if no significant differences were seen between baselines, they were averaged. Furthermore, differences between intervention groups in baselines were tested with one-way ANOVA, if significant difference were observed, the data were normalised according to baseline. For all tests, the parameters of interest were analysed with one-way ANOVA tests, revealing if recording day was a significant main factor for the parameter, within each group, and if group was a significant main factor for the parameter between intervention groups. When a significant main factor was detected, post-hoc test was used for pair-wise comparison. Significance level was defined as p-values smaller than 0.05. In this way, * denotes recording days with significant differences

between the two intervention groups. \square and \triangle denote within group post stroke recording days with significant different results compared to baseline level. \square represents within group significance for intervention group 1, whereas \triangle represents significance for intervention group 2.

III. RESULTS

A. Intracortical microstimulation test

Within group analysis revealed that a significant increase of hindlimb related channels, from pre to post stroke, was present for intervention group 1 for row 3, row 4, and all channels. No significant differences between pre and post stroke were seen for intervention group 2. Between group analysis revealed that intervention group 2 had significantly higher amount of hindlimb related channels on row 3, row 4, and all channels compared to intervention group 1 pre stroke, whereas the opposite was seen post stroke for row 1 and row 2 (table I).

| Results from IC microstimulation tests | | | | |
|--|------------------|-------------------|-------------------|-------------------|
| Row | Pre stroke | | Post stroke | |
| | Group 1 | Group 2 | Group 1 | Group 2 |
| 1 | 75.0 \pm 7.9 % | 75.0 \pm 10.2 % | 95.0 \pm 5.0 % | 43.8 \pm 18.8 % |
| 2 | 80.0 \pm 9.4 % | 68.8 \pm 6.3 % | 95.0 \pm 5.0 % | 62.5 \pm 7.2 % |
| 3 | 20.0 \pm 9.4 % | 75.0 \pm 14.4 % | 65.0 \pm 17.0 % | 87.5 \pm 7.2 % |
| 4 | 10.0 \pm 6.1 % | 62.5 \pm 12.5 % | 60.0 \pm 20.3 % | 50.0 \pm 17.7 % |
| All | 46.3 \pm 5.8 % | 70.3 \pm 5.3 % | 78.8 \pm 10.2 % | 60.9 \pm 3.0 % |

TABLE I: Results from the IC microstimulation tests. The percents represent the amount of channels corresponding to hindlimb movement. N corresponds to the number of rats in each group.

B. Beam walking test

Results from one-way ANOVA showed that recording day was a significant main factor for intervention group 1 and 2 (fig. 3).

Foot drops per beam traversal

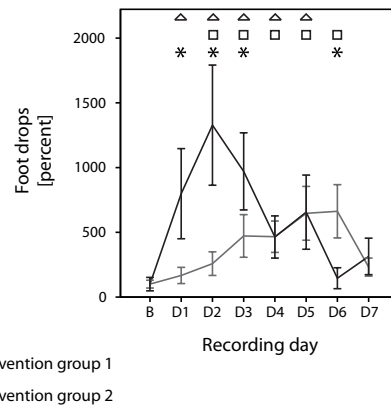


Fig. 3: Results for foot drops per beam traversal.

Examples of the firing rate patterns recorded during the course of the experiment

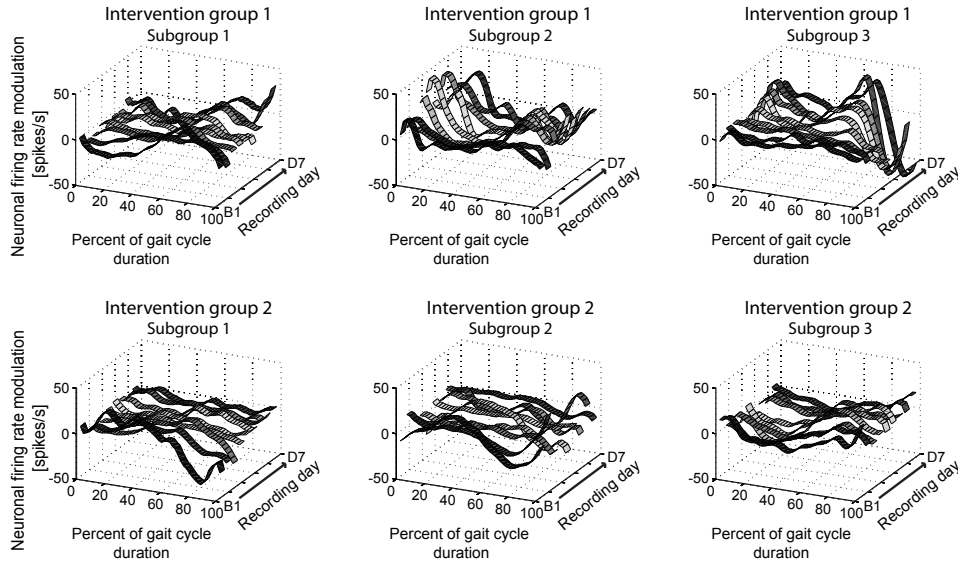


Fig. 4: Examples of the firing rate modulations recorded by individual IC electrodes during the course of the experiment. Three channels for each intervention group is represented. Each channel represent one of the three subcategories obtained from analysis of the IC microstimulation tests. Each recording day is represented within the plots, starting from the front with B1 and ending at the back with D7.

The within group analysis for intervention group 1 revealed that the number of foot drops per beam traversal was significantly increased on day D2 - D6 compared to baseline. The amount of foot drops per traversal declined to baseline level on D7. For intervention group 2, D1 - D5 were significantly increased compared to baseline. The amount of foot drops per traversal declined to baseline level on D6 and was unchanged on D7.

One-way ANOVA showed that group was a significant main factor for the number of foot drops per beam traversal post stroke. A pair-wise comparison between intervention group 1 and 2 revealed that intervention group 2 had a significantly higher number of foot drops per beam traversal, than intervention group 1, on D1 - D3, whereas the opposite was seen on D6.

C. Treadmill walking test

Neuronal firing rate modulation: An example of PSTHs for the different subgroups within each intervention group is shown on figure 4. One-way ANOVA for intervention group 1 showed that recording day was a significant main factor for all subgroups. The within group analysis for intervention group 1 revealed a significant decrease in firing rate modulation on D1 - D4 compared to baseline for subgroup 1. For subgroup 2, D5 - D7 had a significantly increased firing rate modulation compared to baseline, whereas for subgroup 3, D1 - D7 showed a significantly increased firing rate modulation compared to baseline.

One-way ANOVA for intervention group 2 showed that recording day was a significant main factor for all subgroups. The within group analysis for intervention group 2 revealed a significant decrease in firing rate modulation on D1 and

D4 compared to baseline for subgroup 1. For subgroup 2, D1 - D5 and D7 had a significantly decreased firing rate modulation compared to baseline level, whereas for subgroup 3, D1 - D2 and D4 had a significantly decreased firing rate modulation compared to baseline.

One-way ANOVA showed that group was a significant main factor for subgroup 1, 2, and 3. Pair-wise analysis between intervention group 1 and 2 revealed that intervention group 2 had a significantly higher firing rate modulation than intervention group 1 on D1 and D3 for subgroup 1. For subgroup 2, the firing rate modulation for intervention group 2 was significantly lower than for intervention group 1 on D1 - D7. For subgroup 3, the firing rate modulation for intervention group 2 was significantly lower compared to intervention group 1 on D1 - D7.

Centre of gravity for marker trajectories: One-way ANOVA for intervention group 1 showed that recording day was a significant main factor for all three markers. Within group analysis for toe-marker x-coordinates revealed a significant increase compared to baseline on D3, D6 and D7, whereas a significant decrease was seen on D1, D4, and D5. The toe-marker y-coordinate revealed a significant increase compared to baseline on D1 - D4, D6, and D7, whereas a significant decrease was seen on D5. Within group analysis for heel-marker x-coordinates revealed a significant increase compared to baseline on D3, D6 and D7, whereas a significant decrease was seen on D1, D2, D4, and D5. The heel-marker y-coordinate revealed a significant increase compared to baseline on D1 - D7.

Within group analysis for knee-marker x-coordinates revealed a significant increase compared to baseline on D2, D3,

Centre of gravity for marker trajectories

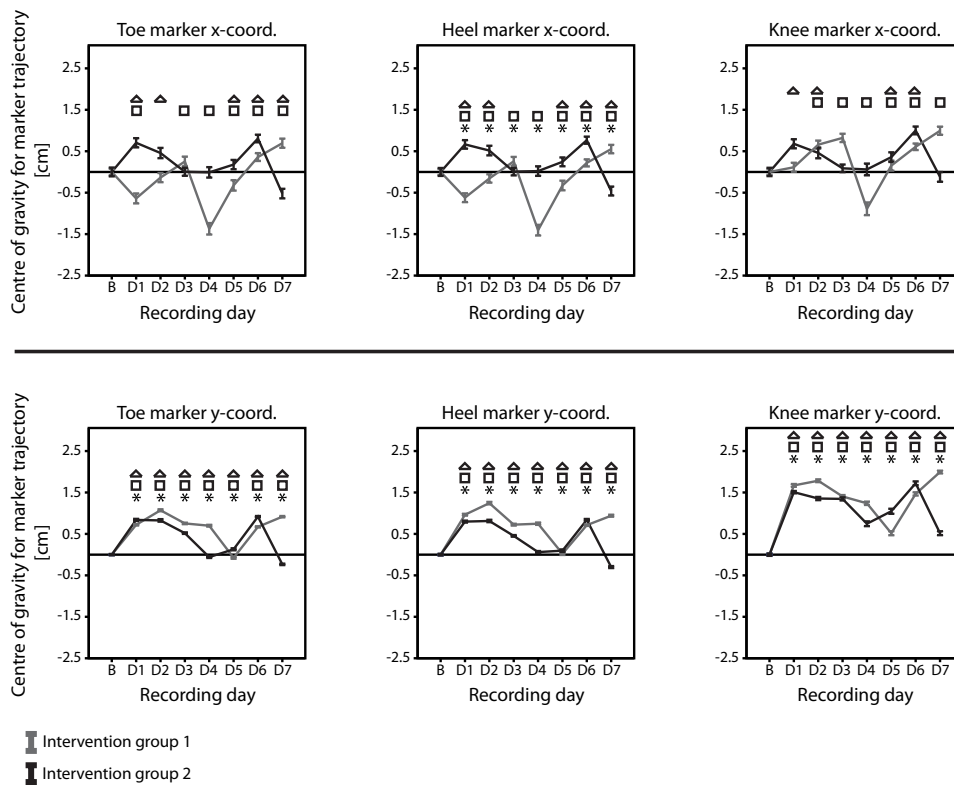


Fig. 5: Results for kinematics related to CoG for marker trajectory alterations in the horizontal and vertical plane.

and D5 - D7, whereas a significant decrease was seen on D4. The knee-marker y-coordinate revealed a significant increase compared to baseline on D1 - D7.

One-way ANOVA analysis for intervention group 2 showed that recording day was a significant main factor for all three markers. Within group analysis for toe-marker x-coordinates revealed a significant increase compared to baseline on D1, D2, D5, and D6, whereas a significant decrease was seen on D7. The toe-marker y-coordinate revealed a significant increase compared to baseline on D1 - D3, D5, and D6, whereas a significant decrease was seen on D4 and D7. Within group analysis for heel-marker x-coordinates revealed a significant increase compared to baseline on D1, D2, D5, and D6, whereas a significant decrease was seen on D7. The heel-marker y-coordinate revealed a significant increase compared to baseline on D1 - D6, whereas a significant decrease was seen on D7. Within group analysis for knee-marker x-coordinates revealed a significant increase compared to baseline on D1, D2, D5, and D6. The knee-marker y-coordinate revealed a significant increase compared to baseline on D1 - D7.

One-way ANOVA analysis showed that group was a significant main factor for the toe-marker CoG y-coordinate, heel-marker CoG x- and y-coordinate, and knee-marker CoG y-coordinate. Between group analysis for toe-marker y-coordinates revealed a significantly higher level for intervention group 2 compared to intervention group 1 on D1, D5, and D6, whereas the

opposite was seen on D2 - D4 and D7. Between group analysis for heel-marker x-coordinates revealed a significantly higher level for intervention group 2 compared to intervention group 1 on D1, D2, and D4 - D6, whereas the opposite was seen on D3 and D7. Between group analysis for heel-marker y-coordinates revealed a significantly higher level for intervention group 2 compared to intervention group 1 on D5 and D6, whereas the opposite was seen on D1 - D4 and D7. Between group analysis for knee-marker y-coordinates revealed a significantly higher level for intervention group 2 compared to intervention group 1 on D5 and D6, whereas the opposite was seen on D1 - D4 and D7.

IV. DISCUSSION

A. Intracortical measures

IC microstimulation tests, conducted upon initiation and termination of the experiment, revealed that significant remapping did occur for intervention group 1, which started rehabilitation on day one post stroke intervention. The remapping was characterised by emergence of new hindlimb related channels on row 3 and 4 at termination of the experiment. The emergence of new hindlimb related channels was not related to disappearance of hindlimb related channels on row 1 and 2. Intervention group 2, who started rehabilitation on day seven did not show any

Neuronal firing rate modulation size

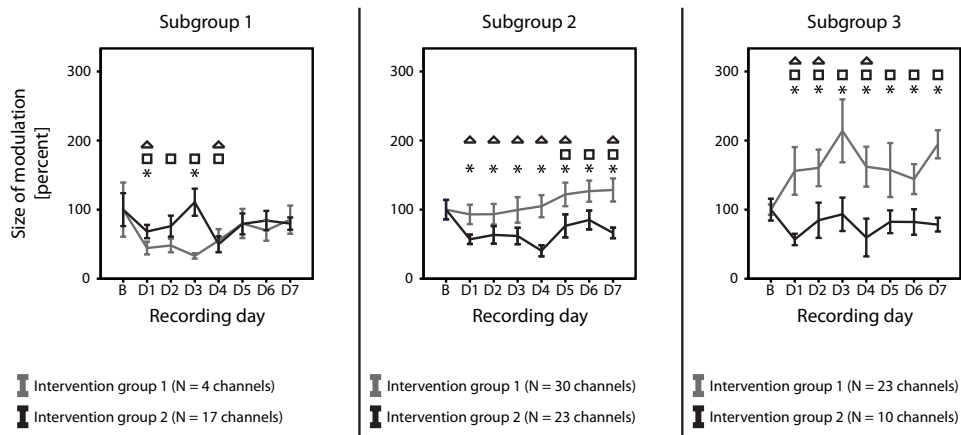


Fig. 6: Results for neuronal firing rate modulation size during treadmill walking.

significant remapping from the initial to the terminal IC microstimulation test.

Neuronal firing rate data from intervention group 2, showed that channels, which went from being correlated to hindlimb motor function on the initial IC microstimulation, to no correlation with hindlimb motor function on the terminal microstimulation test (subgroup 1), did include two recording days with significantly decreased sizes of firing rate modulation, indicating damaging effects of the stroke on a neural level. Though, on D5 - D7, sizes of firing rate modulation were similar to pre stroke levels. One, possible explanation for the re-emergence of firing rate modulation sizes lies in the result that the majority (10/17 channels) of the aforementioned channels remapped from hindlimb correlation to being correlated to forelimb motor function. Thus, alignment of individual gait cycles according to hindlimb related gait events, might possibly result in calculation of PSTHs depicting forelimb firing rate characteristics, since forelimb and hindlimb movement are phase-locked to each other [14], [15]. Intervention group 1 showed similar results to intervention group 2, though differing on D3 - D4, where firing rate modulation sizes were significantly decreased. However, the similarity cannot be explained by a remapping from hindlimb motor function to forelimb motor function, and thus the reason for the re-emergence to pre stroke levels of firing rate modulation size is unclear.

Results from channels that were correlated to hindlimb on both IC microstimulation tests, for intervention group 1, revealed that on D5 - D7, firing rate modulation sizes were significantly increased. Further, results from channels, only correlated to hindlimb on the terminal IC microstimulation test, revealed significantly increased amounts of firing rate modulation on D1 - D7. A joint interpretation of the results from subgroup 2 and 3 could indicate that a relationship

between the firing rate modulation characteristics is apparent. It might be suggested that the relationship is related to hebbian synaptic learning, where synaptic connections between affiliated neurons are strengthened as a consequence of coincidental activity, which results in increased activity, and thus remapping leading to behavioral compensation [4].

Results from channels that were correlated to hindlimb on both IC microstimulation test, for intervention group 2, revealed that firing rate modulation sizes were significantly decreased on all recording days, except on D6, which was similar to the pre stroke level. Further, results from channels, only correlated to hindlimb on the terminal IC stimulation test, revealed decreased amounts of firing rate modulation on recording D1 - D2 and D4. A joint interpretation of the results of subgroup 2 and 3 could indicate that a relationship between the firing rate modulation characteristics is apparent. Keeping in mind that no significant remapping occurred in intervention group 2, and secondly that the firing rate modulation size from subgroup 2 and 3 was significantly lower on D1 - D2, it might be suggested that homeostatic strategies are the main mechanisms for preservation of neuronal circuitries, eventually scaling neuronal activity [4]. Further, this suggestion could be supported by the fact that rehabilitation onset for intervention group 2 was delayed by seven days, resulting in a cortical environment with enhanced susceptibility for hebbian synaptic learning, through repetitive rehabilitative training.

B. Gait measures

The beam walking test documented that both intervention groups, had impaired performance levels initially post stroke, but each intervention group reached pre stroke performance levels before termination of the experiment. Even though, intervention group 2 had a higher amount of performance impairment, compared to intervention group 1, pre stroke

levels of performance were reached earlier relative to rehabilitation onset.

CoG of the marker trajectories for all x-coordinates, for intervention group 1, revealed unstable trajectory patterns across recording days. Recording days with significantly decreased CoG can be explained by difficulties in regards to the execution of transition from stance to swing (paw drag), whereby the affected hindlimb is elongated. For instance the review by [16], based on data from cortically injured cats, stated that in quadrupeds the cortex and corticospinal tract are important factors, involved in stance-swing transition. Recording days with significantly increased CoG can possibly be explained by an execution of stance-swing transition, early in the backwards extension phase of the hindlimb. For intervention group 2 it was observed that the CoG for the x-coordinates was increased on all recording days, significantly different from baseline level. CoG of the marker trajectories for all y-coordinates, for both intervention groups, revealed that on the majority of recording days, CoG was significantly increased compared to the baseline level. This observation can imply two different scenarios related to movement execution. Either, the duration of stance, relative to swing duration was decreased, or the average marker trajectory heights were increased during swing. The most likely scenario, though is that the marker trajectory heights were increased during swing, since [8] showed that stance duration in rats was unaffected post stroke intervention, and [7] described increased stance duration post brain injury in mice. In general, a significant difference, compared to baseline level, was observed for all marker trajectories for both groups. However, on D7, intervention group 2 showed CoG for marker trajectories, closer to baseline level compared to intervention group 1.

C. Comparison of intracortical and gait measures between intervention groups

Comparing results for the individual intervention groups, it is apparent that rehabilitation, initiated on D1, resulted in expansion of hindlimb related channels, and increased firing rate modulation size, within the channels correlated to hindlimb on the terminal IC microstimulation test. Similar remapping was shown by [17], in an experiment with healthy rats performing a skilled reaching task. Further, [18] utilised a monkey model of stroke, and documented expansion of the hand representation after repetitive training. Therefore, the remapping and increased firing rate modulation can possibly be explained by hebbian plasticity, since the training paradigm, utilised during the present study, focuses on repetitive movement training. This remapping, leading to behavioral compensation on a neuronal level, though indicates loss of former motor programmes. This observation is further emphasised by altered CoG of marker trajectories, documenting behavioral compensation of the walking pattern. However, the functional performance level, of the intervention groups, returned to baseline level. This rapid return to baseline performance level is in line with the transient deficits, observed in hindlimb use, post motor system lesion [19]. On the contrary, intervention

group 2 did not show any hindlimb motor area expansion or increased firing rate modulation size during rehabilitation. Similarly to intervention group 1, the functional performance level returned to pre stroke levels. Combining this with the kinematic results, it is suggested that the delayed onset of rehabilitation coincides with a neuronal environment, in which repetitive rehabilitative training, initiated within the critical period, is more effective, resulting in a higher degree of "true recovery" on both the neuronal and functional level.

V. CONCLUSION

The aim of the present study was to investigate if a higher amount of "true recovery" was obtained on both cellular level and in gait function, when rehabilitation onset is within the critical period. For both intervention groups, stroke induction was verified by performance deficits initially post stroke. However, both intervention groups returned to baseline performance levels. Further, the results revealed an expansion of the hindlimb representation within the motor cortex, and an increased firing rate modulation post stroke for intervention group 1. In contrast, for intervention group 2, these parameters were not significantly changed compared to baseline level. Kinematic data revealed a significant change pre to post stroke for both intervention groups. However, this difference was larger for intervention group 1 compared to intervention group 2. The results indicate a higher degree of "true recovery", both on cortical and peripheral level, when initiating rehabilitation on day seven compared to day one post stroke. Future studies could include continuous time recording of IC signals, hereby enabling spike-sorting and inclusion of methods for correlation between firing patterns of individual neurons.

ACKNOWLEDGMENT

Jens Soerensen, Ole Soerensen, and Torben Madsen at Pathological Institute at Aalborg Sygehus Nord for assistance during experiments.

REFERENCES

- [1] T. G. Hornby, D. D. Campbell, J. H. Kahn, T. Demott, J. L. Moore, and H. R. Roth, "Enhanced Gait-Related Improvements After Therapist-Versus Robotic-Assisted Locomotor Training in Subjects With Chronic Stroke: A Randomized Controlled Study", *Stroke*, vol. 39, p. 1786-1792, 2008.
- [2] T. G. Deliagina, G. Orlovsky, and S. Grillner. *Neuronal Control of Locomotion*, 1st ed. Oxford, UK: Oxford University Press, 1999.
- [3] G. A. Metz, I. Antonow-Schlorke, and O. W. Witte, "Motor Improvements After focal Cortical Ischemia in Adult Rats are Mediated by Compensatory Mechanisms", *Behavioral Brain Research*, vol. 162, p. 71-82, 2005.
- [4] T. H. Murphy and D. Corbett, "Plasticity During Stroke Recovery: From Synapse to Behaviour", *Nature Reviews*, vol. 10, p. 861-872, 2009.
- [5] J. B. Nielsen, "How we Walk: Central Control of Muscle Activity during Human Walking", *The Neuroscientist*, vol. 9, p. 195-204, 2003.
- [6] D. M. Armstrong, "The Supraspinal Control of Mammalian Locomotion", *Journal of Physiology*, vol. 405, p. 1-37, 1988.
- [7] M. Ueno and T. Yamashita, "Kinematic Analyses Reveal Impaired Locomotion Following Injury of the Motor Cortex in Mice", *Experimental Neurology*, vol. 230, p. 280-290, 2011.
- [8] Y. Wang, B. Bontempi, S. M. Hong, K. Mehta, P. R. Weinstein, G. M. Abrams, and J. Liu. "A comprehensive analysis of gait impairment after experimental stroke and the therapeutic effect of environmental enrichment in rats", *Journal of Cerebral Blood Flow & Metabolism*, vol. 28, p. 1936-1950, 2008.

- [9] M. Neumann, Y. Wang, S. Kim, S. M. Hong, L. Jeng, M. Bilgen, and J. Liu. "Assessing gait impairment following experimental traumatic brain injury in mice", *Journal of Neuroscience Methods*, vol. 176, p. 34-44, 2009.
- [10] W. Jensen, P. J. Rousche, and T. C. Chiganos. "A Method for Monitoring Intra-cortical Motor Cortex Responses in an Animal Model of Ischemic Stroke", *Proceedings of the 28th IEEE EMBS Annual International Conference New York City, USA, Aug 30-Sept 3, 2006*, p. 1201-1203, 2006.
- [11] E. J. Neafsey, E. L. Bold, G. Haas, K. M. Hurley-Gius, G. Quirk, C. F. Sievert, and R. R. Terreberry. "The Organization of the Rat Motor Cortex: A Microstimulation Mapping Study", *Brain Research Reviews*, vol. 11, p. 77-96, 1986.
- [12] P. Wester, B. D. Watson, R. Prado, and D. Dietrich. "A Photothrombotic Ring Model of Rat Stroke-in-Evolution Displaying Putative Penumbra Inversion", *Stroke*, vol. 26, p. 444-450, 1995.
- [13] T. Schallert, M. T. Woodlee, and S. M. Fleming. "Disentangling multiple types of recovery from brain injury", *Pharmacology of Cerebral Ischemia*, p. 201-216, 2002.
- [14] L. B. Rowell and J. T. Shephard. *Handbook of Physiology - Section 12: Exercise: Regulation and Integration of Multiple Systems*, 1st ed. United Kingdom: Oxford University Press, 1997.
- [15] C. Garnier, M. Falenpin, and M. Canu. "A 3D analysis of fore- and hindlimb motion during locomotion: Comparison of overground and ladder walking in rats", *Behavioural Brain Research*, vol. 186, p. 57-65, 2008.
- [16] T. Drew, W. Jiang, and W. Widajewicz. "Contributions of the motor cortex to the control of the hindlimbs during locomotion in the cat", *Brain Research Reviews*, vol. 40, p. 178-191, 2002.
- [17] J. A. Kleim, S. Barbay, N. R. Cooper, T. M. Hogg, C. N. Reidel, M. S. Rempel, and R. J. Nudo. "Motor Learning-Dependent Synaptogenesis Is Localized to Functionally Reorganized Motor Cortex", *Neurobiology of Learning and Memory*, vol. 77, p. 63-77, 2002.
- [18] R. J. Nudo, E. J. Plautz, and S. B. Frost. "Role of Adaptive Plasticity in Recovery of Function After Damage to Motor Cortex", *Muscle and Nerve*, vol. 24, p. 1000-1019, 2001.
- [19] G. A. Metz and I. Q. Whishaw. "Cortical and subcortical lesions impair skilled walking in the ladder rung walking test: a new task to evaluate fore- and hindlimb stepping, placing, and co-ordination", *Journal of Neuroscience Methods*, vol. 115, p. 169-179, 2002.

Background Knowledge

II

The neocortex of the rat, which is the phylogenetically youngest part of the brain, has a six layered structure, and constitutes regions, which have motor, sensory, or associative functions (fig. 4.1). The neocortex has been subdivided into several anatomical and functional subdivisions, according to areal and laminar differences such as cell packing density (cytoarchitecture), myelin density (myeloarchitecture), and distribution of neurotransmitters (neurochemical organisation), and by electrophysiological tests, e.g. microstimulation studies [Paxinos, 2004].

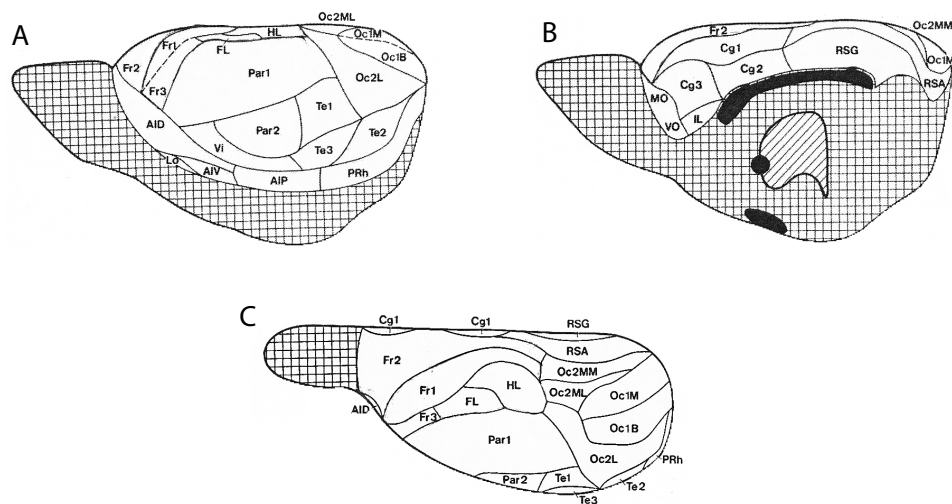


Figure 4.1: Map of the neocortex based on quantitative cytoarchitectonical and myeloarchitectonical studies. **A:** lateral view, **B:** medial view, and **C:** dorsal view. Abbreviations are according to the terminology of Zilles [1985]. Frontal cortex area 1 (Fr1), frontal cortex area 2 (Fr2), frontal cortex area 3 (Fr3), parietal cortex area 1 (Par1), and parietal cortex area 2 (Par2) [Kolb and Tees, 1990].

4.1 Cellular Composition

Studies, of the cellular composition of the neocortex, have documented a variety of neuron types, which have been classified according to the extent of dendritic spines and the proportion of cytoplasm compared with the nucleus. In general, projection neurons have a large amount of dendritic spines, whereas intrinsic neurons tend to have fewer spines. In relation to the cytoplasmic nuclear ratio, neurons with a high and low ratio have been documented in both groups [Kolb and Tees, 1990].

Pyramidal cells, which are projecting neurons and are thus spine-rich, comprise the largest amount of cells, within layers II - VI of the neocortex (71 - 97 % of the cells in the visual cortex, which has been

regarded as a model of the whole neocortex). The pyramidal cells have an oval or triangular cell body, a round nucleus, a large apical dendrite, and a long axon that leaves the cortex, in order to reach other cortical areas, subcortical regions, or the spinal circuitry (fig. 4.2.E) [Nolte, 2009]. The spiny stellate cells are most abundant in layer IV of the neocortex (fig. 4.2.A), whereas the spine-rich multiangular cells have been described in layer I (fig. 4.2.C). Both the bipolar and the double bouquet neurons have a strictly vertical orientation of dendrites and axons (spanning several layers of the neocortex), which constitutes a cylindrical space [Kolb and Tees, 1990].

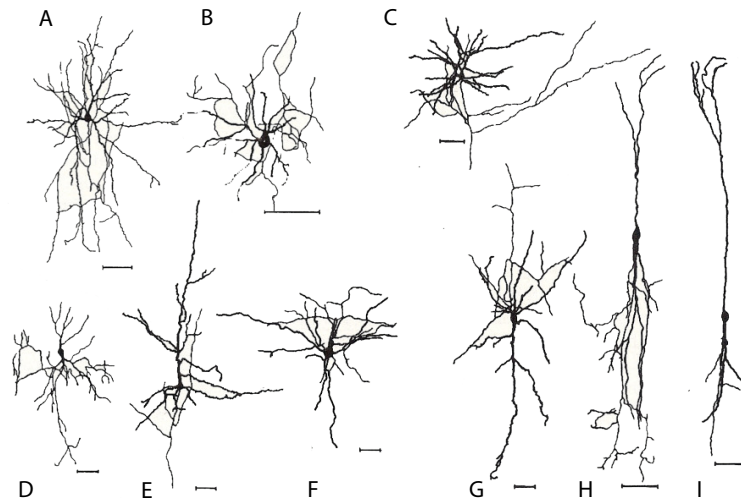


Figure 4.2: Neuron types in the neocortex of the rat. **A:** Spiny stellate cell. **B:** Neurogliform cell. **C:** Spiny multiangular cell of layer 1. **D:** Chandelier cell. **E:** Pyramidal cell. **F:** Basket cell. **G:** Martinotti cell. **H:** Double-bouquet cell. **I:** Fusiform bipolar cell. Modified from [Kolb and Tees, 1990].

4.2 Cortical Connectivity

Studies, of a variety of neocortical areas in different species, e.g. monkeys, rats, and humans, have shown a distinct laminar specificity of the neuronal cells. Hence, all cells within a neocortical circuitry, including projection neurons and intrinsic neurons, are organised according to lamina, hereby constituting an organised pattern of neuronal connections [Douglas and Martin, 2004].

4.2.1 Interhemisphere Connections

The cell bodies, of neurons that are a part of the corpus callosum, are concentrated in layer II to III and V to VI and mainly project to layer I to III and V to VI of the contralateral hemisphere. The interhemisphere connections can either be homotopic (between identical loci in both hemispheres) or heterotopic (between non-identical loci in the hemispheres). The cell body of neurons with homotopic connection tends to be situated in layer II and III and terminates in the same layer in the contralateral hemisphere, whereas heterotopic connections originate from cell bodies, within layer V and terminate in several layers, within the contralateral hemisphere. The cell bodies and terminal endings, of association interneurons that connect areas of the same hemisphere or traverse to the contralateral hemisphere, exhibit laminar patterns that are similar to those found in the case of homotopic corpus

callosum neurons [Kolb and Tees, 1990].

4.2.2 Connectivity within Sensory Areas

In sensory areas of the neocortex, it has been documented that these areas receive afferent fibres from the thalamus. In sensory regions with a highly developed layer IV, these fibres mainly terminate in layer IV and the lower layer III. In addition to these terminals, thalamocortical fibres also terminate in layer I and VI, though in a much lower density. In neocortical regions with a less pronounced layer IV, the main target of thalamic fibres is layer I and III. Reciprocal connections to the specific areas within the thalamus originate from layer VI of the neocortex, whereas non-reciprocal connections to thalamic nuclei originate from pyramidal neurons within layer V [Kolb and Tees, 1990].

4.2.3 Connectivity within Motor Areas

Efferent fibres mainly originate from cell bodies in layer V and VI. For instance, projections to the caudateputamen complex mostly originate from pyramidal cell bodies in the upper layer V. However, pyramidal cell bodies of fibres that terminate in the caudateputamen complex have also been documented in the lower layer V and layer III and VI, though at much lower densities. Similarly, long descending fibres to the spinal cord, cranial nerve nuclei, and pons originate from large pyramidal cells in the lower layer V. Cell bodies of corticotectal axons also originate from large pyramidal cells of layer V, whereas cell bodies of projections to the claustrum are situated in layer VI [Kolb and Tees, 1990].

4.3 Characteristics of the Motor Cortices

Keeping the general organisation of neocortical connectivity in mind, it is not surprising that quantitative analysis of the laminar patterns is used to define regions, having either motor or sensory function. In this way, the frontal and parietal cortex have been defined as motor and sensory regions, due to differences in the distribution of cell bodies per volume and myelin per volume within the different laminae.

4.3.1 Layer Structure

The frontal cortex encompasses Fr1, Fr2, and Fr3, all having a highly developed layer V, which mainly contains large pyramidal neurons (agranular structure), suggesting a motor function. Further, layer IV, which mainly contains sensory terminals, is indistinct (fig. 4.3) [Paxinos, 2004]. The largest proportion of myelin is found in layer V and VI. This distribution of myelin can be related to the location of the pyramidal cells and their descending axons [Kolb and Tees, 1990].

The parietal cortex encompasses Par1, Par2, FL, and HL, all having a highly developed layer IV (granular structure) (fig. 4.3.B). This layer composition suggests a somatosensory function. The areas FL and HL, situated at the mediodorsal border of Par1 (fig. 4.1), though have a peculiar cytoarchitecture, since their density distribution, within the different layers, shares characteristics with both the frontal

cortex, Par1, and Par2. Thus, having a highly granular layer IV together with large pyramidal cells in layer V. These features of HL and FL have entailed experiments to verify if motor functions can be elicited from the parietal cortex, and especially from HL and FL [Kolb and Tees, 1990].

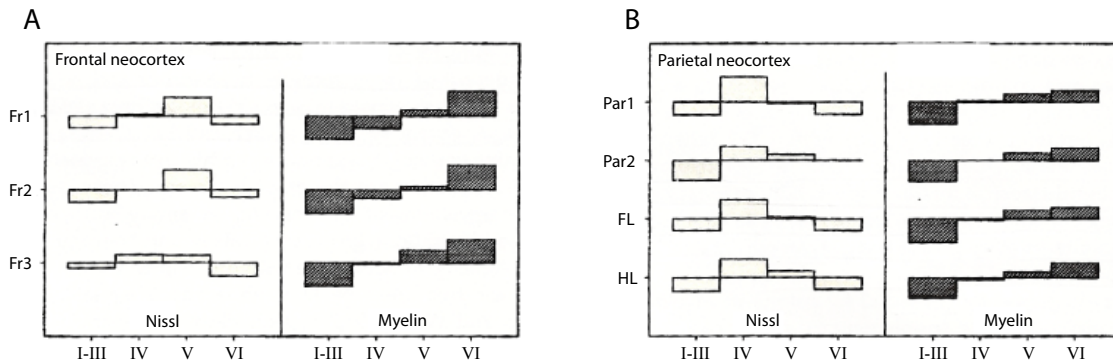


Figure 4.3: Relative density of myelinated nerve fibres and cell bodies in the six layered structure of **A:** the frontal neocortex, and **B:** the parietal neocortex. The mean density per volume over all layers is defined as 100 %, and the individual values for the layers are expressed as relative values on this basis [Kolb and Tees, 1990].

4.3.2 The Motor Ratunculus

The terminology of Donoghue and Wise [1982] is used, in order to describe the functional characteristics of the frontal and parietal cortex. Thus, Fr1 and Fr3 correspond to the lateral agranular frontal cortex (AGL), and Fr2 corresponds to the medial agranular frontal cortex (AGM) used in the terminology of Donoghue and Wise [1982]. Similarly, Par1, Par2, HL, and FL correspond to the granular primary somatosensory area (SI) and granular secondary somatosensory area (SII) used in Donoghue and Wise [1982] (fig. 4.4) [Kolb and Tees, 1990].

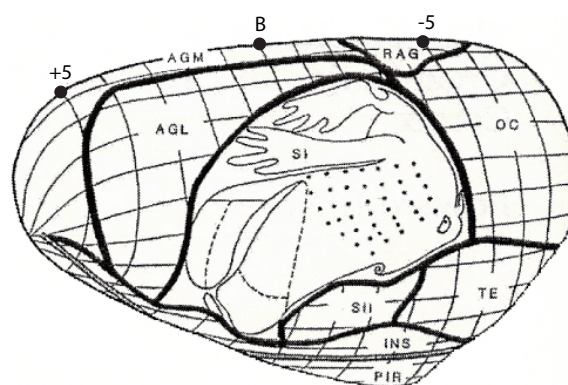


Figure 4.4: Dorsolateral view of the left hemisphere of the rat brain. A 1 mm² grid is superimposed upon the surface of the hemisphere, and the numbers +5 and -5 denote distance in mm rostral and caudal according to bregma (B), respectively. Cytoarchitectonic borders are indicated by heavy lines [Neafsey et al., 1986; Kolb and Tees, 1990].

The article Neafsey et al. [1986] summarises results from multiple mapping experiments, describing

the organisation of the motor cortex of the rat. IC microstimulations (300 ms trains, 0.25 ms pulses applied at 350 Hz, currents less than 50 μA), applied in layer V of the neocortex, were used to map the motor cortex. Rats were anaesthetised with ketamine hydrochloride (100 mg/kg). As a result of the experiments, a rostral motor area (RMA), containing both a forelimb and hindlimb area, was revealed (fig. 4.5). The RMA contains corticospinal neurons and is less responsive to afferent sensory input than the caudal motor area (CMA), which is analogous to the human primary motor cortex. These characteristics support the idea that RMA functions as a supplementary motor cortex. The CMA was located in both AGL and SI while applying low currents ($< 25 \mu\text{A}$). Low-threshold movement responses can be elicited by IC microstimulations within the CMA, since descending corticospinal and corticobulbar projections are situated within this area [Neafsey et al., 1986; Kolb and Tees, 1990].

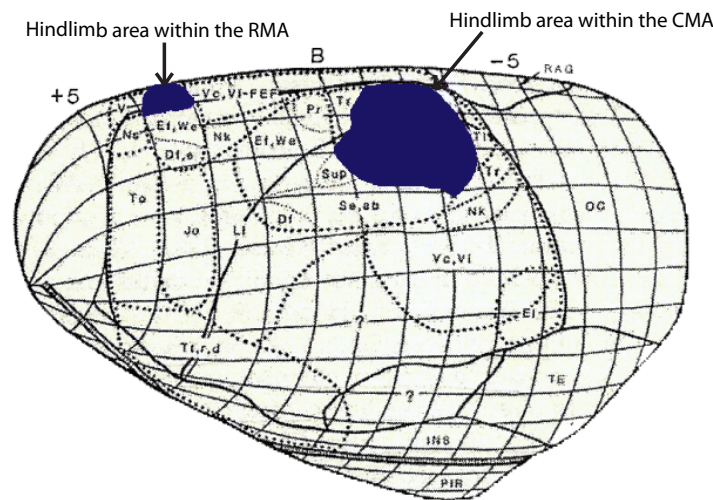


Figure 4.5: Idealised map of motor responses elicited with currents below 50 μA . A 1 mm² grid is superimposed upon the surface of the hemisphere, and the numbers +5 and -5 denote distance in mm rostral and caudal according to bregma (B), respectively. An area, located 3 - 4 mm according to bregma and 0 - 1 mm lateral to the midline indicates the hindlimb area within the RMA. An area, located (-3) - 0.5 mm according to bregma and 1 - 4 mm lateral to the midline indicates the hindlimb area within the CMA. Modified from [Neafsey et al., 1986; Kolb and Tees, 1990].

4.3.3 The Corticospinal Tract

As indicated by the results from Neafsey et al. [1986], corticospinal neurons are most apparent in the RMA and CMA regions (fig. 4.6). The majority of corticospinal tract neurons crosses the midline of the caudal medulla and propagates through the dorsal columns. The remainder of neurons propagates through the ipsilateral ventral funiculus (fig. 4.6). Collaterals of the corticospinal neurons terminate in the midbrain, trigeminal nuclei, pontine nuclei, and red nucleus. Terminations in the dorsal horn are apparent in layer III - VII, and more sparse in layer I and II and the ventral horn (fig. 4.6) [Paxinos, 2004].

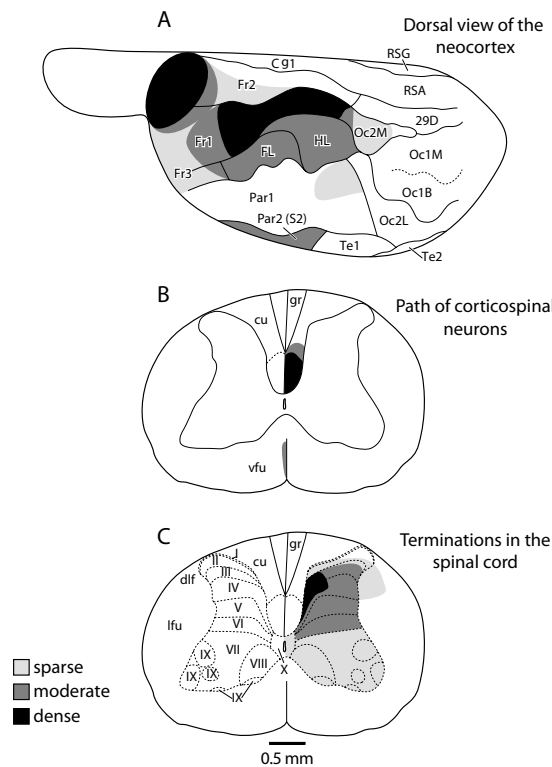


Figure 4.6: The corticospinal tract. The terminology of Zilles [1985] is used on the figure. **A:** the gray scale specifies the amount corticospinal neurons originating within a given cortical region. **B:** the amount of corticospinal projections, and **C:** the amount of corticospinal terminations within the spinal cord. Thus, black regions does contain many corticospinal neurons, dark gray regions contain a moderate amount of corticospinal neurons, and light gray specifies regions with a lower amount of corticospinal neurons. Modified from [Paxinos, 2004].

4.4 Correlations and Discrepancies between the Human and Rat Motor Cortices

Humans and other primates, similar to rats, have a neocortex with a six layered structure, and the general layered structure bears resemblance to that of the rat [Nolte, 2009; Douglas and Martin, 2004]. The motor cortex of the human is constituted by three areas; primary motor area (M1), premotor area (PMA), and supplementary motor area (SMA) [Despopoulos and Silbernagl, 2003; Nudo, 2007]. In the brain of the rat, Neafsey et al. [1986] found two cerebral regions related to motor function. The CMA is analogous to M1 in primates (e.g. human), and the RMA have resemblance to the PMA and SMA of primates, but cannot be regarded analogous to these, since RFA probably evolved independently in rodents (fig. 4.7) [Nudo, 2007; Neafsey et al., 1986; Kolb and Tees, 1990].

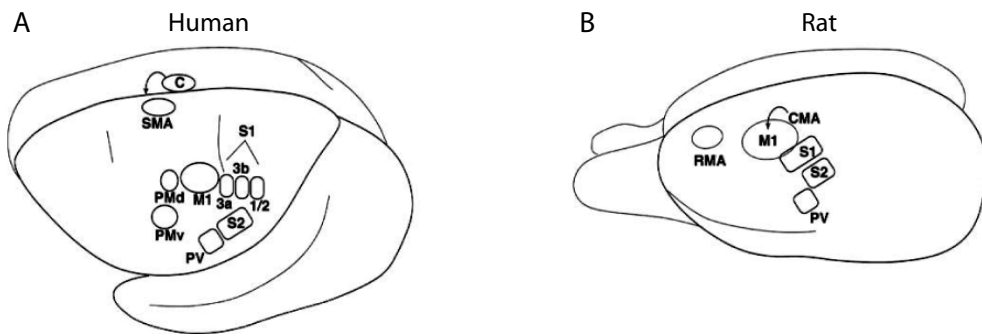


Figure 4.7: Lateral view of somatosensory and motor areas within the left hemisphere of the brain.

A: shows the distribution of the different motor areas within the human brain. *PMd* and *PMv* are subdivisions of the PMA, *C* refers to a secondary area related to the motor cortex; cingulate motor area. *S1*, *S2* and *PV* are subdivisions of the somatosensory cortex. **B:** shows the distribution of areas related to motor control within the brain of rats. Modified from [Nudo, 2007].

When focusing on the corticospinal tract, where the signals from the motor cortex mainly are propagated through, it has been documented that the tract in rats and primates have several structures in common. Both in primates and rodents, the tract originates from layer V pyramidal cells, primarily within large contiguous regions of M1 and descend to the spinal cord through the same path. One difference though, is that primates have a larger amount of corticospinal neurons per unit brain weight compared to rodents [Nudo, 2007].

If nothing else is mentioned, the studies used in this chapter concern quadrupeds, since there has not been conducted much research on rats. Further, rats are part of quadrupeds and thus they can be used as a representation for gait in rats.

Gait in quadrupeds consists of a complex sequence of contractions, which can be divided into two main phases; swing and stance. The swing phase consists of a flexion and an extension phase, whereas the stance phase consists of two extension phases (fig. 5.1). Each gait cycle is initiated with the swing phase by flexion of the hip, knee, and ankle. In the second part of the swing phase an extension is present at the knee and ankle, while the hip flexion is sustained. The stance phase is initiated upon paw-ground contact. During the first extension phase of stance the knee and ankle joint extensors are active, but the joint flexes due to paw-ground contact, while in the second phase of stance both hip, knee, and ankle joints are extending (fig. 5.1) [Kandel et al., 2000; Rowell and Shepherd, 1997].

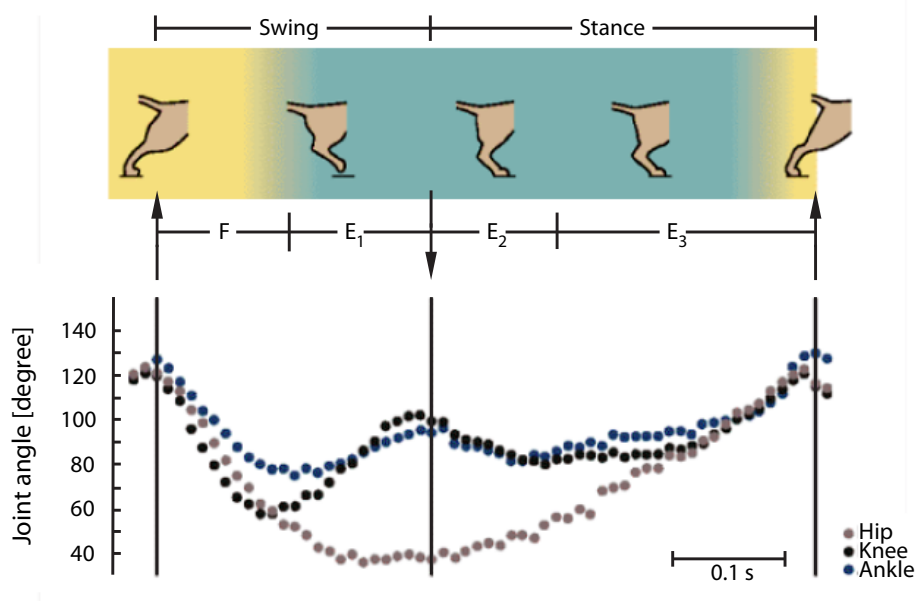


Figure 5.1: Illustration of the different phases of the gait cycle in quadrupeds. Modified from [Kandel et al., 2000].

In general, motor behavior is constituted by three components; sensory input, interneuronal processing, and motor output, which is each mediated by a single group or several groups of neurons (fig. 5.2) [Kandel et al., 2000].

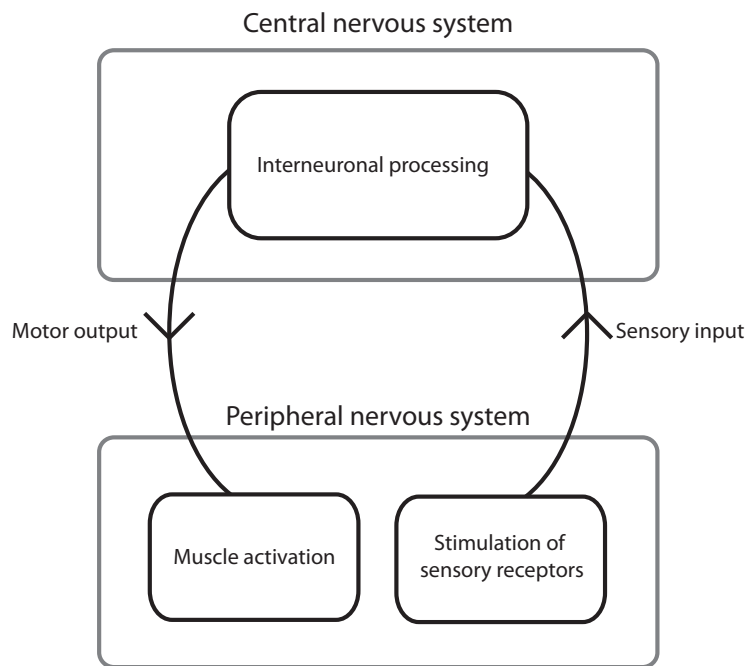


Figure 5.2: Illustration of the different components of motor behavior. Sensory input from the periphery is propagated to the central nervous system, where the incoming information is processed, and as a result, motor output is generated. Modified from [Kandel et al., 2000].

Increasing complexity of a given motor task results in a need for more sensory information, and thus a higher amount of interneuronal processing. This hierarchical organisation implies that only a small amount of sensory information is needed, when simple spinal reflexes are elicited. Whereas, when conducting a complex motor task (e.g. gait), sensory information can be integrated at multiple levels, going from the spinal cord to the motor cortex [Kandel et al., 2000].

5.1 Central Pattern Generators

Experiments on quadrupeds, initiated in the early 20th century by Graham Brown, have given rise to the half-center hypothesis, in which flexor and extensor muscle activation in the limb are controlled by two groups of neurons (flexor and extensor motor neurons) collectively called, central pattern generators (CPG), which are capable of mutually inhibiting each other. The simultaneous elicitation of muscle contractions and inhibition of the group of neurons, responsible for antagonist muscle activation, has been shown to take place in the absence of sensory input to the CPGs of the spinal cord. Thus, CPGs are able to maintain a basic firing rhythm upon initiation, by descending input from supraspinal levels. Supraspinal and sensory input can then modify the basic firing rhythm of the neural network within the spinal cord, and thus modify gait patterns e.g. gait velocity or alterations, in order to avoid hitting obstacles (fig. 5.3) [Kandel et al., 2000].

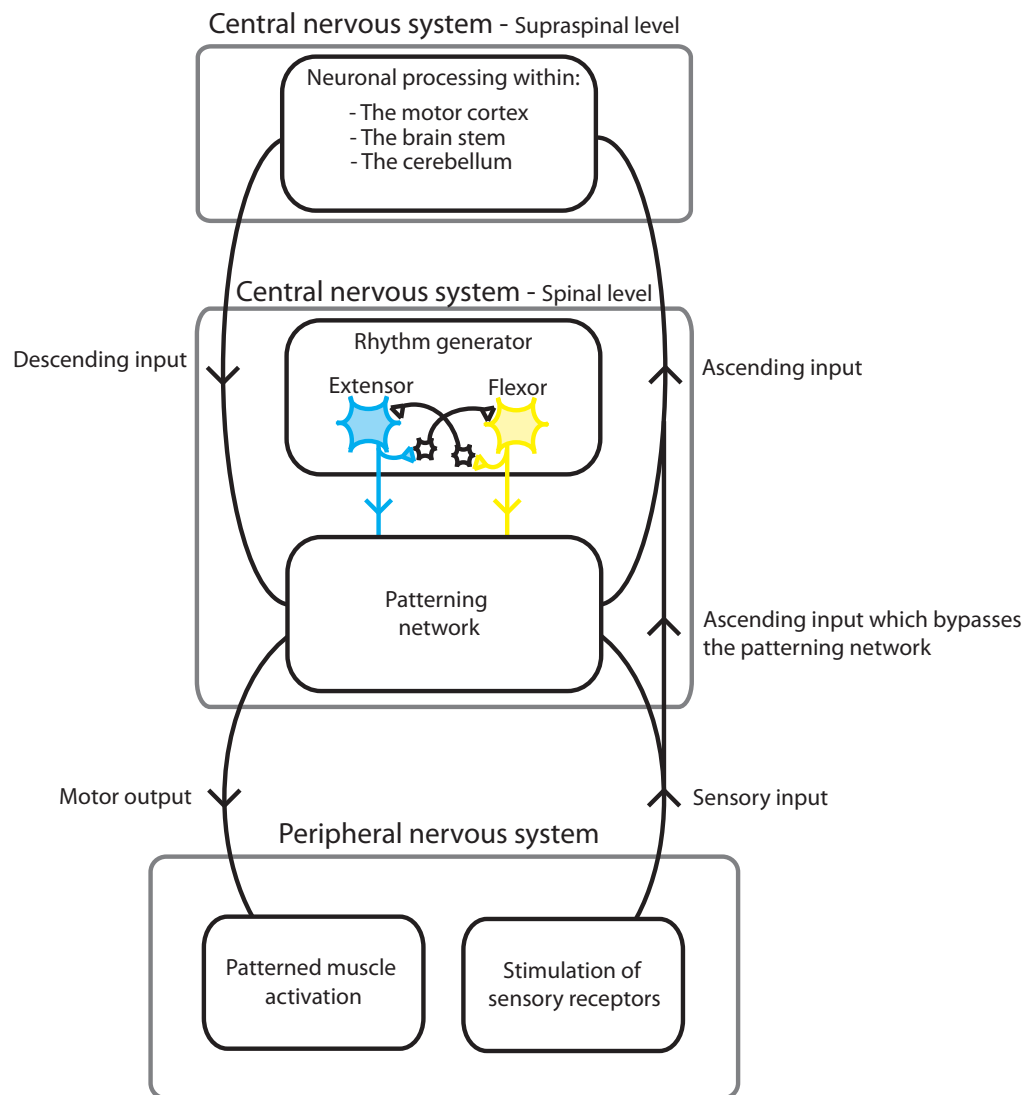


Figure 5.3: Schematic illustration of the neural networks that constitute the neuromuscular system responsible for execution and monitoring of gait. Modified from [Kandel et al., 2000].

5.2 Gait Adjustments as a Result of Peripheral Input

Peripheral inputs, aiding in the process of adjusting gait, originate from both proprioceptors and exteroceptors. In relation to proprioceptive input, it has been shown that spinal and decerebrate cats are able to adjust their gait velocity, in order to keep up to speed with the motorised treadmill, on which they are walking. Data from the experiments suggest that sensory input cues the end of the stance phase, since a reverse relationship between stance duration and treadmill velocity was observed. In contrast, no significant change in swing duration, when changing treadmill velocity, was documented [Canu and Garnier, 2009].

In relation to exteroceptors, one well-documented example is the stumbling-corrective reaction. When a light mechanical stimulation is applied to the dorsal part of the paw, two outcomes can be observed,

depending on the current phase of the affected limb. If the limb is in the swing phase, when the paw is stimulated, excitation of the flexors will occur. Meanwhile, extensor activation is inhibited resulting in a rapid flexion of the paw. On the contrary, a mechanical stimulation, being applied during the stance phase, will result in a reinforced extension of the limb [Kandel et al., 2000].

5.3 Gait Adjustments as a Result of Supraspinal Processes

Descending signals, which influence the gait pattern, originate from three different supraspinal areas; the brain stem, motor cortex, and cerebellum. The mesencephalic locomotor region, located in the brain stem, has been documented to initiate and control the velocity of gait. The gait velocity has experimentally been shown to be related to the intensity of the descending signals. Thus, the higher intensity of the mesencephalic signal the higher gait velocity [Kandel et al., 2000; Nielsen, 2003].

The motor cortex is essential in the coordination of gait, while it forwards the input from visual cortex to the spinal cord. Motor cortex activity may regulate interneurons, which are part of, or influenced by the CPGs, since many motor cortex neurons project directly to the spinal cord [Kandel et al., 2000]. Furthermore, a study by Drew [1988] found that the firing rate of motor cortex cells in cats increased, when they step over obstacles. This indicates that a progressively higher amount of cortical input is needed as a function of a more complex gait pattern. Another study, by Ueno and Yamashita [2011], showed that the joint angles were changed, following cortical injury. This suggesting that the motor cortex is responsible for the control of fine motor movements.

The cerebellum is responsible for fine-tuning of the gait pattern. Sensory information from the hindlimbs is propagated through two ascending pathways to the cerebellum; the dorsal and ventral spinocerebellar tracts. Neurons, within the dorsal tract, are activated by proprioceptors, whereas the neurons in the ventral tract are activated mainly by interneurons, associated with the CPGs. It is believed that the cerebellum compares the information that is received from the two tracts, hereby comparing information about the actual movement (proprioceptive input), with information about the intended movement (input from CPGs). The output from this comparison is a corrective signal, which is sent to different regions, within the brain stem, whereby adjustments, of the input from the brain stem to the CPGs, occur [Kandel et al., 2000].

5.4 Correlations and Discrepancies between Human and Rat Gait

The general neuronal organisation of walking is the same for humans and quadrupeds. The walking pattern is controlled by a combination of three parameters; CPGs in the spinal cord, sensory feedback, and descending motor commands. The difference between control of human walking and control of quadrupedal walking lies in the weighting of the three parameters [Nielsen, 2003]. One of the largest differences between human walking and quadrupedal walking is that humans have a bipedal walking pattern. Thus, having a higher need for supraspinal inputs to the spinal cord, in order to maintain an upright position [Kandel et al., 2000]. Humans are more affected by motor cortex lesions than quadrupeds. This leads to the conclusion that it is crucial, for humans to have an intact motor

cortex, in order to maintain walking ability. However, humans are able to recover from lesions in the pyramidal tract, since the transmission from motor cortex to spinal cord does not necessarily have to happen through the corticospinal tract, but can be sustained by other pathways [Nielsen, 2003]. It has been shown that patients with incomplete spinal cord injury performed involuntary movements, although they were not able to perform voluntary movements. Furthermore, rhythmic patterns have been elicited, by using electrical stimulation, in patients with complete spinal cord injury. These studies lead to the conclusion that CPGs are partly controlling the generation of rhythmic movements as in quadrupeds [Nielsen, 2003].

Ischemic Stroke Induction and Recovery

6

In this chapter the photothrombosis method for induction of stroke, which is a part of the rat ischemic stroke model being used in this project, is analysed. Further, the physiological processes, following ischemic stroke, and how these can be affected are described. Studies are based on rats unless anything else is stated.

6.1 Ischemic Stroke Induced by the Photothrombosis Method

The photothrombosis method for induction of ischemic stroke was developed by Watson et al. [1985]. The method requires injection of a photosensitive dye, e.g. rose bengal, into the blood circulation of the rat. Following injection of the dye, the target area for stroke is irradiated with a light beam to activate the photosensitive dye, whereby an occlusion is formed. Several parameters can be adjusted in the photothrombosis method, in order to determine the infarct size. These parameters include the diameter of the light beam, exposure time, and concentration of the photosensitive dye.

6.1.1 Analysis of the Variable Parameters in the Photothrombosis Method

In a photothrombosis study by Grome et al. [1988], 1 ml rose bengal dye with a concentration of 5 mg/ml saline was injected into the femoral vein of rats (300 - 350 g). The skull was exposed and illuminated with a light probe ($\lambda = 570$ nm) for a duration of 15 min. The diameter of the illuminated area on the skull was 3 mm. The ischemic area reached a maximum of ≈ 50 mm³, 24 hours post photothrombosis intervention.

Lanens et al. [1995] injected 0.133 ml/100 g bodyweight of rose bengal dye with a concentration of 10 mg/ml saline into the blood circulation of rats (250 - 300 g). The skull was exposed to light, emitted from a lamp through a fiber-optic cable without any special filter, for 20 min. The diameter of the illuminated area on the skull was 1 mm. Assessment of the ischemic area showed a maximum of ≈ 10 mm², 24 hours post photothrombosis intervention.

Lee et al. [1996] injected 0.1 ml/100 g bodyweight of rose bengal dye with a concentration of 20 mg/ml saline into the circulation of rats, to induce stroke. Subsequently, the skull was illuminated, by a lamp connected to a light probe ($\phi = 3.2$ mm, $\lambda = 400 - 1200$ nm) for 5 min. Histology of the lesions revealed that the size reached a maximum of ≈ 110 mm³ after 24 hours.

Comparing the three studies, it can be suggested that the concentration of the photosensitive dye is positively correlated with the size of the infarcted area post stroke. This is further supported by the

difference in the size of the illuminated area, in Grome et al. [1988] and Lanens et al. [1995], which might not be as decisive in the size of the stroke as the concentration of the dye.

6.2 Plasticity post Ischemic Stroke

Peri stroke, function of neurons in the ischemic core is lost. Further, function of tissue in the penumbral area, and eventually remote tissue, even including the contralesional hemisphere, are damaged by the stroke, e.g. due to edema (fig. 6.1). However, in the period following stroke, affected tissue will try to recover, possibly leading to return of specific neurological functions [Wieloch and Nikolich, 2006]. The functional recovery rate is largest for the initial 30 days post stroke, but has been shown to continue for at least six months [Duncan et al., 2000]. Recovery post stroke is affected by the amount of tissue lost due to the stroke, and activation of remaining neuronal networks through rehabilitation [Wieloch and Nikolich, 2006].

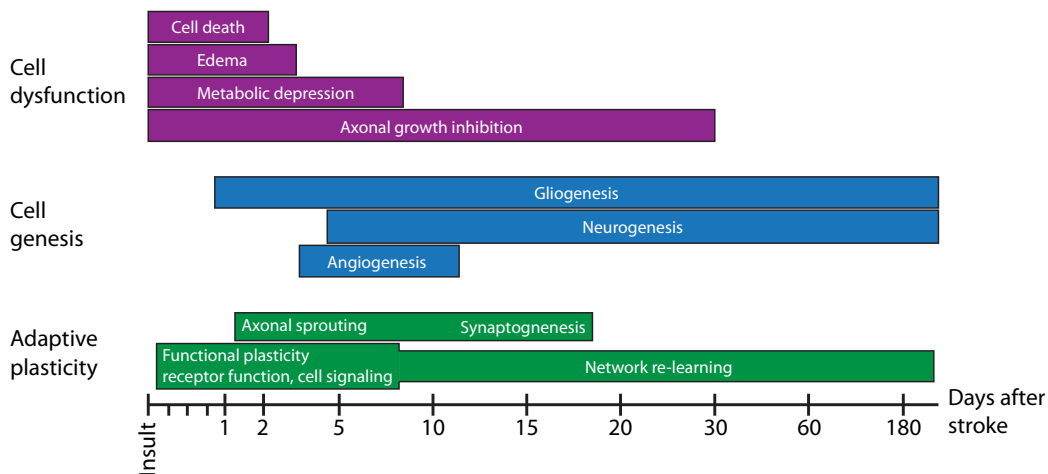


Figure 6.1: The physiological processes post stroke include cell dysfunction, cell genesis, and adaptive plasticity. Modified from [Wieloch and Nikolich, 2006].

6.2.1 Acute Patophysiological Events post Stroke

Immediately following stroke onset, where a thrombus is formed, the cerebral blood flow (CBF) is decreased from the normal level of approximately 50 - 60 ml/100 g tissue/min to a lower level, dependant on the relative distance to the ischemic core. At the site of the occlusion, the CBF is decreased to less than 10 ml/100 g tissue/min resulting in immediate irreversible neuronal damage, or neuronal death. In the penumbra, CBF is decreased to approximately 20 ml/100 g tissue/min, which causes synaptic activity to be lowered to a minimum. However, at this site, the neuronal damage is reversible, and thus is a possible target for therapeutic interventions. As a further consequence of the decreased CBF, excitotoxicity is initiated, which triggers peri infarct depolarisations, inflammation, and apoptosis in the surrounding tissues [Woodruff et al., 2011].

6.2.2 Spontaneous Repair Mechanisms

Repair and Growth of Existing Cells post Stroke

On a short-term scale post stroke, the extent of cellular stress, originating from peri infarct depolarisations, edema, and inflammation, imposed on the surviving tissue of the penumbra, is a main factor, determining the recovery rate. Even though damaged neurons recover from the stroke, they might have collapsed spines due to the ischemia, causing the neuron to exhibit aberrant neurotransmission. In time though, also the collapsed spines will recover. However, recovered spines have changed their position on the dendrites of the neuron, and have an altered morphology, which might be partly responsible for the dysfunction post stroke [Wieloch and Nikolich, 2006].

Together with the non-ischemic tissue, the recovered parts of the penumbra are main sites for further recovery processes. This is due to the release of growth-promoting factors within the tissue. Release of genes, related to the recovery process (survival, repair, and plasticity genes), is occurring in two phases post stroke; just following stroke and 9 - 24 hours post stroke. In addition to this, a further release of growth-promoting genes occurs during the first week post stroke, followed by a release of growth-inhibitory genes. During this period, tissue of the peri infarct region and corresponding contralesional hemisphere initially become hyperexcitable. In these hyperexcitable tissues, LTP is enhanced, the number of gamma-aminobutyric acid (GABA_A) receptors is lowered, and the number of N-methyl-D-aspartic acid (NMDA) receptors is increased. As a consequence of these processes axonal sprouting occurs [Witte et al., 2006; Wieloch and Nikolich, 2006; Murphy and Corbett, 2009]. Though, one mechanism, homeostatic plasticity, aims at restricting the synaptic activity, within the neuronal circuitry, to a certain level, thus acting as a negative feedback loop. The role of homeostatic plasticity in recovery post stroke is to stabilise the interrupted synaptic activity originating from the infarcted tissue. It is suggested that homeostatic plasticity performs this stabilisation of synaptic activity, either by resetting activity levels of specific neurons, by formation of new connections, or changes in the activity at the already existing synapses, hereby possibly unmasking silent pathways and preventing the neurological network from becoming hypo or hyperactive [Metz et al., 2005; Murphy and Corbett, 2009].

Cell Genesis Post Stroke

Several studies have shown that the adult brain is continuously generating new neurons. This cell genesis mainly has its base in the subventricular zone, and the subgranular zone of the dentate gyrus. Post stroke, neuronal death leads to an increase in the ongoing cell genesis in the subventricular zone and the subgranular zone of the dentate gyrus [Arvidsson et al., 2002]. The neurogenesis is sustained for up to four months, and the new neurons are recruited to damaged regions [Thored et al., 2006]. The recruited neurons are suggested to contribute to the recovery process on a long-term scale. This is also supported by Raber et al. [2004], who ruled out that angiogenesis, giving rise to enhanced vascularisation of the damaged tissue, was responsible for the improved functional outcome. However, it is unclear, whether the new neurons also contribute to the early phases of recovery, since these processes are too fast for the neurons to be integrated in the existing neural circuits [Arvidsson et al., 2002].

Within two days post stroke, a dual astrocytic response occurs. One part of this gliosis, occurring in the penumbral zone, starts within two days of stroke and persists for 10 weeks. The second part, occurring remotely from the ischemic lesion, starts on day three post stroke, but ceases around day 14 post stroke. In contrast to the gliosis occurring in the penumbral zone, the gliosis occurring remote from the ischemic lesion affects the whole ipsilateral hemisphere during its active period. This dual response is fundamental to CNS injury, since it has been seen in a variety of different CNS injuries, including global cerebral ischemia, laser irradiation injury, and stab wounds [Schroeter et al., 1995].

6.2.3 Experience Dependant Plasticity

Several studies have investigated the effects of rehabilitative training on plasticity post brain injury. Experience dependant plasticity is dependant on several principles related to the rehabilitative training itself, the timing of it, and the age of the experimental subject undergoing rehabilitation [Kleim and Jones, 2008]. One major mechanism, related to repetitive rehabilitative training, is hebbian plasticity, which acts as a positive, activity-dependent feedback loop. Thus, this mechanism causes a strengthening of synapses between presynaptic and postsynaptic connections that are coincidentally activated, e.g. due to a specific motor task. In this way, circuits that are behaviorally relevant are strengthened and as a consequence of this non-relevant connections are weakened. Post stroke, this mechanism is important, since it can detect surviving structures and strengthen them [Murphy and Corbett, 2009].

Role of Training Intensity Repetition and Specificity

Neural circuits, related to motor function, must be engaged in motor performance, in order to avoid degradation. Thus, in order to limit the negative effects on motor performance post stroke, rehabilitative training of the lost motor functions must be carried out. Rehabilitation is also important to restore motor functions through reprogramming of motor programmes into different neural circuits compared to pre stroke [Kleim and Jones, 2008]. In practice, this has been shown in several experiments on rehabilitation of skilled movements [Nudo, 2007; Kleim et al., 2002]. In the study by Kleim et al. [2002], rats undergoing rehabilitation, through a skilled forelimb reaching task, were compared to a control group, in order to describe changes in synaptogenesis and its relation to reorganisation of the motor cortex. Compared to the control group, rats undergoing the skilled reaching task, exhibited expansion of wrist and digit representations in the motor cortex. This reorganisation of the motor cortex occurred simultaneously with a significant increase in the number of synapses per neuron. Similarly, Jones et al. [1996] found an increase of synapses post sensorimotor cortex injury, and an increase in the volume and surface area of dendritic processes per neuron. However, these observations were in rats, not encouraged to perform any specific training tasks. It is also suggested by Jones et al. [1996] that these findings might be related to behavioral compensation, implying that the lesion has caused changes in the use of the non-impaired forelimb.

6.2.3.1 Role of Training Onset

Plasticity post stroke is not a single event, but is composed of several physiological processes. Some occur in parallel, whereas others are interdependant. Thus, timing is crucial, when investigating plas-

tivity or interventions affecting plasticity [Kleim and Jones, 2008]. A study by Murphy and Corbett [2009] suggests that there might be a critical period of post stroke rehabilitation, extending from 5 to 14 days following stroke onset (fig. 6.2). This critical period, where neuroplasticity is assumed to be more affective, is based on the up and down regulation of growth-inhibitory and excitatory genes. At the beginning of the critical period the amount of growth promoting genes is higher and maintained at a specific level, compared to the growth-inhibitory genes. However, this ratio, between present excitatory and inhibitory genes, is altered during the critical period, since the growth-inhibitory genes are upregulated gradually.

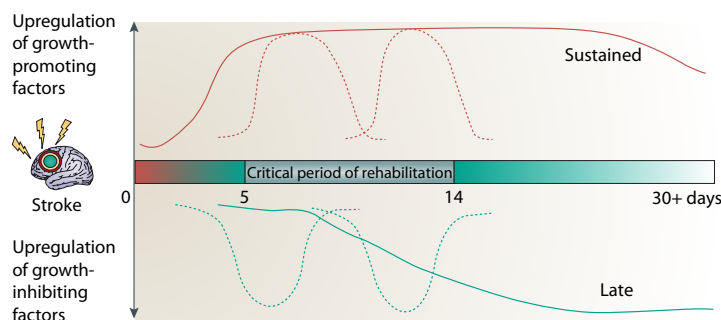


Figure 6.2: Following ischemic stroke in the brain, there might exist a critical period for onset of rehabilitation. In this period, ranging from around 5 to 14 days post stroke, the amount of growth-promoting factors is high compared to the amount of growth-inhibiting factors [Murphy and Corbett, 2009].

Several different studies have been carried out to investigate the effect of different rehabilitation onset times post brain injury. Among these studies is Biernaskie et al. [2004], who investigated the effect of three different onset times of rehabilitation, utilising enriched environment techniques. Rats, who underwent enriched rehabilitation, initiated 5 and 14 days post stroke, showed improvements in skilled reaching ability, ladder and beam walking tests, compared to controls, whereas rats, who were subjected to rehabilitation, initiated on day 30 post stroke, did not differ from controls. Further, the rats, who started enriched rehabilitation five days post stroke, showed the largest improvements. In the same study, the dendritic morphology within the motor cortex of the contralesional hemisphere was assessed. When comparing the rehabilitated animals to the controls, the group of rats with the earliest onset of rehabilitation were the only one showing increased dendritic growth [Biernaskie et al., 2004]. Further, results from a study, conducted on humans, by Dromerick et al. [2009] support the existence of a critical period, since very early onset of rehabilitation (three days post stroke) resulted in less motor improvement, compared to later onset.

A study by Metz et al. [2005], investigated the effect of minor stroke lesions in the forelimb area of the sensorimotor cortex of female rats. The rats were trained for four weeks to perform a skilled reaching test. Each rat was tested daily from the second day post stroke. The movements of the rat during the test were video recorded to allow for qualitative analysis. Post stroke induction, no significant differences were seen in the skilled reaching test compared to baseline tests. The minor size of the stroke lesions induced is suggested to be responsible for the lack of deficits post stroke. Some rats even improved significantly for the first four days post stroke in the skilled reaching test, and this improvement was maintained during the remaining period of the experiment. Even though no deficits

were seen post stroke in the quantitative analysis of the results from the skilled reaching test, significant changes compared to baseline level were seen in several parameters of the qualitative analysis. Thus, behavioral compensation had occurred and caused changes, in some cases even improvement, in the movement strategies employed during the skilled reaching test.

Barbay et al. [2006] investigated the behavioral and neurophysiological effects of late rehabilitation onset. The study of late rehabilitation onset was carried out using an established ischemic stroke model, developed from experiments in squirrel monkeys. The animals were trained to perform a reaching task both pre and post ischemic stroke in M1. However, the rehabilitative training post stroke was delayed by one month. Movement representations of the hand within M1 were obtained through IC microstimulations, conducted pre ischemic stroke, one, and two months after. The results from the experiment documented that the number of flexions per retrieval, in the reaching task, were significantly higher during the four weeks without rehabilitative training. However, after delayed rehabilitation there was no longer any significant difference compared to baseline results [Barbay et al., 2006].

Role of Age

An important factor in neural plasticity is the plasticity of synapses. Synaptic plasticity is at its highest levels during development. In this phase, synapses are constantly formed and degraded according to time and environmental conditions. In adulthood, the plastic abilities of synapses are maintained, but to a lesser extent than during the development phase. During synaptic plasticity glia is often actively involved, and this part of synaptic plasticity is dependant on age [Nieto-Sampedro and Nieto-Diaz, 2005]. Further, potentiation of synapses and reorganisation of cortical maps are reduced according to increased age. Contributing to the degradation of the basis for synaptic plasticity is atrophy of neurons and synapses [Kleim and Jones, 2008]. In order to assess the relationship between recovery of motor function and age, Kolb et al. [2000] applied bilateral lesions to the motor cortex in rats of three different ages. The three cases were at the day of birth (P1), 10th post-natal day (P10), and adulthood (90 days of age). It was observed that the P10 group was less impaired than the other two groups in a skilled reaching test. In other behavioral tasks, including beam walking, locomotor activity, and tongue extension, the P10 group did not show significant difference from the control group, whereas the other groups did [Kolb et al., 2000].

6.3 Correlations and Discrepancies between Human and Rat Stroke

Induction of stroke by the photothrombosis method in experimental animals might not fully represent human stroke. This is due to the possible development of a penumbral area, which is located inside a developing vasogenic edema [Carmichael, 2005]. However, the photothrombosis allows for determination of the stroke lesion size. By adjusting the different parameters of the method it is possible to produce stroke lesions with a size of 5 - 15 %, which is close to the size of survivable human stroke [Murphy and Corbett, 2009]. The integration, of knowledge from animal studies into strategies of clinical treatment of stroke in humans, is challenging. Several factors might cause inconsistency in the translation process. Among these factors are the differences between the brain of humans and dif-

ferent animals, both on a functional and morphological level. Also the relatively homogeneous nature of stroke in experimental animals compared to the heterogeneity of human stroke can challenge the translation. Generally, several physiological variables can be controlled in animal studies, whereas they cannot be controlled in clinical trials of human stroke [Woodruff et al., 2011].

Intervention Study

III

7.1 Aim of Pilot Experiment

The pilot experiment was conducted in order to test, if all aspects of the experimental protocol were appropriate for reaching the aim of the project, and to refine the practical skills of the research group. The main issues to be solved, during the pilot experiment, were:

- **Verification of the optimal implementation site of the IC electrode array**
- **Choosing the appropriate concentration of rose bengal dye to be injected during photothrombosis intervention**
- **Selection of the appropriate diameter of the light probe, used for induction of stroke**

The pilot experiment was conducted, as described in the experimental protocol (ch. 8). The only discrepancies from the experimental protocol were related to the parameters that were to be tested and the duration of the experiment. Four rats were included in the pilot experiment and were assigned into two groups, each including a different setup of the parameters, needed to be tested:

| Parameter specifications related to the experimental groups | | |
|--|---|---|
| | Group 1 (Rat 1 and 2) | Group 2 (Rat 3 and 4) |
| Implementation coordinates | 1 - 3 mm lateral, 1 - 3 mm caudally to bregma | 1 - 3 mm lateral, 0 - 2 mm caudally to bregma |
| Light probe diameter | 0.3 mm | 0.12 mm |

Table 7.1: Parameter specifications that were tested during the pilot experiment.

Both groups were exposed to identical injections of rose bengal dye (concentration = 10 mg dye/ml saline, injection dose = 0.3 ml/100 g body weight). Depending on the effect of the photothrombosis intervention, the dose was either chosen for the intervention study, or if no effect was observed for both groups, a higher concentration was tested. The beam walking test was used, in order to verify if an ischemic stroke, resulting in gait dysfunction, had been induced during the photothrombosis intervention. The time schedule for the experiment included; an IC microstimulation test upon initiation of the experiment, two baseline recordings (both a treadmill walking test and a beam walking test per recording) prior to photothrombosis intervention, and three post stroke recordings (identical to the baseline tests) conducted on day one, four, and six post stroke induction.

7.2 Results

Intracortical Microstimulations

The IC microstimulations were conducted using a current range of 100 μA - 600 μA (stimulus train = 100 Hz, pulse duration = 200 ms). Results were obtained from rat 1, 2, and 3 (fig. 7.1), whereas results could not be obtained from rat 4, due to malfunction of ground wires. The malfunction was related to a dissociation between the bonescrew and the ground wire, resulting in loss of the grounding.

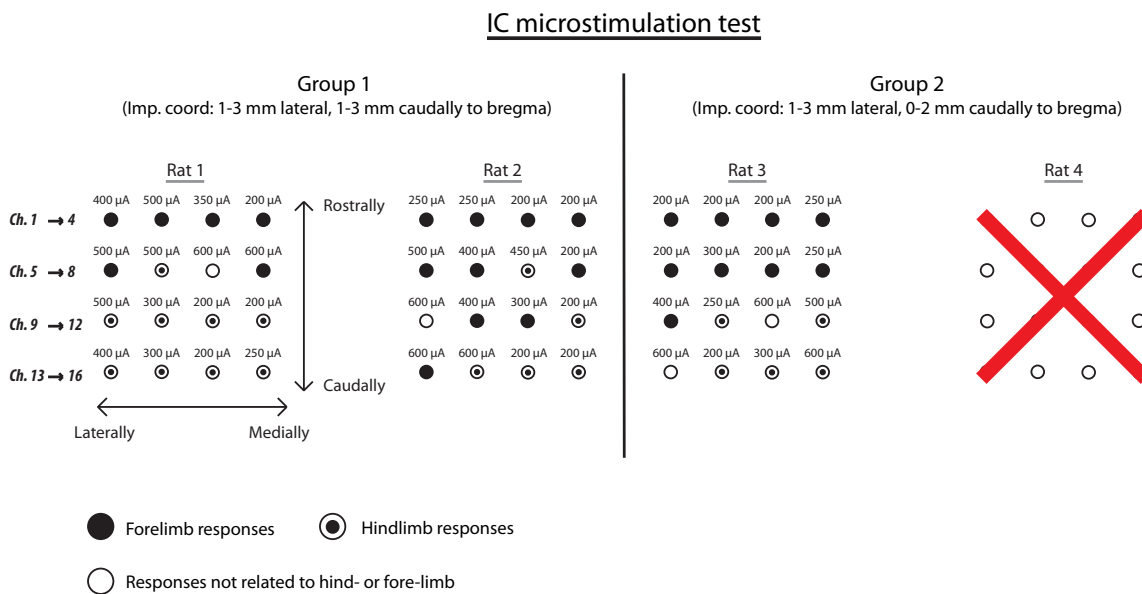


Figure 7.1: Results from IC microstimulation test conducted on the pilot rats. No microstimulation test was conducted on rat 4 since the ground wires did separate from the bones screws post surgery.

Results from the IC microstimulation test revealed that the rats from group 1 in general had more channels, through which, hindlimb responses could be elicited, compared to rat 3 (group 2). Further, rats from group 1 had hindlimb evoked responses on channels located more rostrally, within the IC electrode array, compared to rat 3. This indicates that group 1, where the more caudally implementation coordinates were used, had a higher success rate, targeting cortical regions, related to hindlimb motor function.

7.2.1 Photothrombosis Intervention

When utilising a rose bengal dye injection dose of 0.3 ml/100 g body weight, with a concentration of 10 mg dye/ml saline, no alterations of the gait pattern could be visually observed on the day following intervention. Therefore, the concentration was changed to 20 mg dye/ml saline and the injection dose was left unchanged. Following a second photothrombosis intervention, where the new concentration was used, alterations of the gait pattern were visually observed.

7.2.2 Treadmill Walking Test

At the initiation of baseline recording, only one rat was able to walk on the treadmill. Unfortunately, this was the rat from whom it was not possible to conduct an IC microstimulation test due to separation of the ground wire. Despite the lack of possibility for recording of IC signals, the treadmill walking tests post stroke were conducted, in order to visually assess if the rat was still able to walk on the treadmill. Though, the post stroke treadmill walking tests were delayed until day five and six, due to wounds emerging on the tail of the rat, making the conduction of the early post stroke recordings too inconvenient for the animals to complete. The cause of the wounds was most likely related to rose bengal dye being spilt on the skin of the rats tail. This suggestion is also supported by Sigma-Aldrich [2006], stating that the dye may be harmful if absorbed through the skin, and can cause irritation. Due to the aforementioned problems, no indications concerning alterations of the IC signals could be extrapolated from the treadmill walking test.

7.2.3 Beam Walking Test

Baseline recordings on the ledged beam were conducted according to plan. Though, post stroke intervention one of the four rats (rat 2) was no longer able to walk on the ledged beam. Therefore, results from the beam walking test only include three rats (fig. 7.2). It is believed that the lack of ability to walk on the beam, was not caused by the stroke, since no visual deficits could be observed, when comparing rat 1 and 2 in their housing environments.

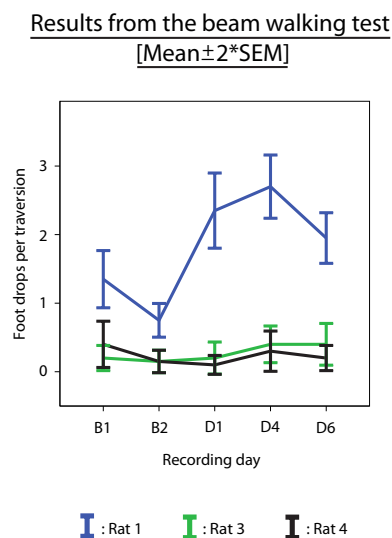


Figure 7.2: Results from the beam walking test conducted during the pilot experiment. B1 and B2 refers to baseline one and two, respectively. D1, D4, and D6 refers to recording day one, four, and six post stroke.

From visual inspection, of the results from the beam walking test, there was indications of differences between the two experimental groups. Baseline recordings from the two groups showed that rat 1 (group 1) had a higher baseline level of foot drops per traversal compared to rat 3 and rat 4 (group 2). Post stroke recordings showed an increase in number of foot drops per traversal for both rat 1 and

rat 3, whereas rat 4 appeared to exhibit approximately the same amount of foot drops per traversal, post stroke as compared to baseline recordings. Taking into account the higher baseline level for rat 1 compared to rat 3, it appears as if rat 1 and rat 3 exhibited a similar degree of change in relation to beam performance level post stroke, whereas rat 4 did not show any effect of the stroke.

7.3 Experiences from the Pilot Experiment

7.3.1 Selection of Experimental Parameters

The two different electrode placements were assessed by applying microstimulations to all channels of the electrode in each rat. The resulting responses revealed that the electrode position used in rat 1 and 2 resulted in the highest number of channels related to movement of the right hindlimb.

- **IC electrode implementation coordinates: 1-3 mm lateral, 1-3 mm caudally to bregma was selected for the intervention study**

Two concentrations of the rose bengal dye solution were tested; 10 mg dye/ml saline and 20 mg dye/ml saline. The effect of the two concentrations was verified, on the day following intervention, through visual observation of the results from the rats walking on the ledged beam. No effect was observed, for either of the experimental groups, using the low concentration of rose bengal dye. On the contrary, rats exhibited some degree of gait dysfunction upon intervention, using the higher concentration of rose bengal dye.

- **A rose bengal dye concentration of 20 mg dye/ml saline was selected for the intervention study**

The beam walking test was used to clarify if different light probe diameters would result in different degrees of performance alterations. Two different sizes of light probe diameters were tested, and it was found that rat 1 (group 1) and rat 3 (group 2) exhibited similar performance level alterations, whereas rat 4 (group 2) did not exhibit any decreased performance as a result of stroke intervention. Therefore, the larger light probe diameter was chosen, in order to assure that an ischemic stroke, sufficient to inflict gait alterations, would be induced.

- **A light probe diameter of 3 mm was selected for the intervention study**

7.3.2 Practical Learnings

Through the pilot experiment, the practical skills in regards to conduction of tests, IC electrode fabrication, and surgery were improved due to practical experience. Further, a couple of noteworthy experiences were learned. Thus, a better method for bonescrew fabrication was developed, in order to avoid breakage of ground wires, and a larger degree of precaution was taken during photothrombosis intervention, in order to avoid spill of rose bengal dye onto the tail of the rat.

All experimental procedures were approved by the Animal Experiments Inspectorate under the Danish Ministry of Justice. 24 male Sprague-Dawley rats were initially enrolled in the experiment. At delivery, the rats were 13 weeks old and weighed 350 - 400 g. The first three weeks of the experiment solely featured training, in order to familiarise the rats with the experimental settings. The training consisted of beam walking training, treadmill walking training, and handtraining. At the conclusion of week three, the performance level of the rats was evaluated, and 16 out of 24 rats were chosen to continue in the experiment. During week four and five the rats were instrumented with IC electrode arrays, and microstimulation tests were conducted, in order to verify electrode placement, within the area of the left CMA related to hindlimb innervation.

The rats were randomly divided into two groups of eight rats, which were subjected to identical rehabilitations, only differing in the time of intervention onset. The two groups of eight rats were further subdivided into two groups consisting of six rats (intervention group) and two rats (control group), respectively. The subgroup of two rats served as control for the remaining six rats, and thus did not undergo photothrombosis intervention, but otherwise did undergo the same experimental procedures as their respective intervention group. Intervention group 1 started rehabilitation on day one post photothrombosis intervention, whereas intervention group 2 started rehabilitation on day seven post photothrombosis intervention (fig. 8.1).

Timeline of the experiment

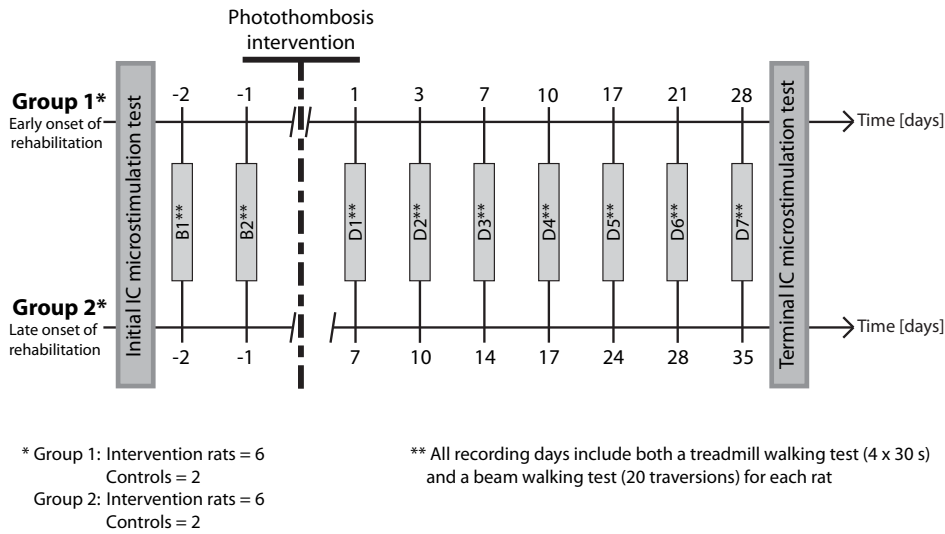


Figure 8.1: Timeline of the experiment. Both experimental groups consisted of eight rats (six intervention rats and two controls per group). Rehabilitative training was initiated on D1, corresponding to day one post stroke for group 1, and day seven for group 2. The remaining recording days relative to stroke induction are displayed above the time axes for group 1 and below for group 2.

Upon initiation of the experiment, the rats were submitted to a IC microstimulation test. Two inter-related beam walking and treadmill walking sessions were conducted pre stroke (B1 and B2). Post stroke, seven recording days were conducted for each group (D1 - D7). Each recording day contained both a treadmill walking test and a beam walking test. Following the last recording day, the rats were subjected to an additional IC microstimulation test.

The IC microstimulation tests were performed, in order to produce an estimate of the cortical mapping, within the implementation site of the IC electrode array, hereby verifying correct electrode placement, and assessing if plastic remapping had occurred, during the course of the experiment. Beam walking tests were conducted, in order to assess functional performance changes as a result of stroke and the subsequent rehabilitation. Treadmill walking tests were conducted, in order to obtain IC signals and hindlimb kinematics related to walking, hereby assessing if these parameters were affected by stroke intervention and subsequent rehabilitation. Finally, by comparing the different test results, obtained over the timespan of the experiment, correlations between neuronal modulation patterns, functional performance level, and marker trajectory characteristics, related to gait could be assessed.

8.1 Setup

8.1.1 Intracortical Microstimulation Test

| List of materials for IC microstimulation test | |
|--|--|
| PC: | • PC running Windows XP 32-bit SP3 • MC Stimulus II software |
| Stimulator: | • Multichannel Systems STG2008 stimulus generator |

Table 8.1: List of materials that were utilised for the IC microstimulation setup.

The MC Stimulus II software was used to set up the stimulation parameters and trigger the Multichannel Systems stimulus generator (STG2008). Control signals to the STG2008 were transmitted through a USB cable. Once triggered, the STG2008 emitted the pre-specified patterned stimulus signal to the IC electrode array. Stimulation specifications were as follows; stimulus train = 100 Hz, pulse duration = 200 μ s, pulse amplitude 100 - 500 μ A, pulse amplitude increment = 100 μ A.

8.1.2 Treadmill Walking Test

The setup, associated with the treadmill walking test, consisted of four different subsystems; Treadmill setup, PC setup, TDT setup, and camera setup. A list of the materials used for the treadmill setup can be seen in table 8.2.

| List of materials for treadmill walking test | |
|--|---|
| Treadmill: | • Treadmill incl. perspex cage (running surface: width = 0.1 m, length = 0.4 m (Letica Scientific Instruments)) • Veroboard • 30.9 Ω resistor • 12 V Battery (MFD. by YUASA corp. for ENERSYS inc.) |
| PC: | • DT340 card (PCI bus digital I/O and counter/timer board) • PC running Windows XP 32-bit SP3 • Vicon Motus 9.2 (video acquisition software) • Real-time Processor Visual Design Studio (RPvdsEx) software |
| TDT: | • RA16CH (16-channel chronic headstage) • RA16PA (16-channel pre-amplifier) • IC electrode array • RA4LI (4-channel headstage) • RA4PA (4-channel pre-amplifier) • RX5 (Pentusa Base Station) |
| Camera: | • Basler A602fc-2 color machine vision camera • 2 x 400W telescope work lamp (SARTANO) |
| Others: | • Shaver • Tape • Black self-adhesive semispheric markers • 2 x rulers |

Table 8.2: List of materials that were utilised for the treadmill walking test setup.

Treadmill Setup

The treadmill was powered by a 12 V battery. To control the velocity of the treadmill, the input power to the treadmill was altered by a voltage divider, consisting of a resistor (30.9 Ω) and the internal resistance of the treadmill (10.6 Ω) (fig. 8.2).

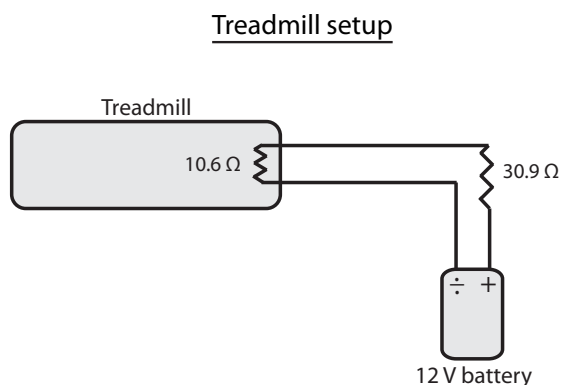


Figure 8.2: Schematic overview of the treadmill setup.

PC Setup

The main function of the PC setup (fig. 8.3) was to store and process both IC data and video data, and maintain synchronisation between the camera and the TDT. RPvdsEx was used, in order to set up the TDT and transfer IC data from the TDT to the PC. Vicon Motus 9.2 software was used for synchronisation by transmitting a 5 V square triggering signal from a DT340 card to the camera and TDT. Hereby, the frame rate of the camera was equal to the frequency of the 5 V signal. In addition, the trigger signal was recorded by the TDT, whereby a timestamp for every single videoframe was obtained. Further, Vicon Motus 9.2 controls the data transfer from the camera through the IEEE 1394 firewire card to the PC.

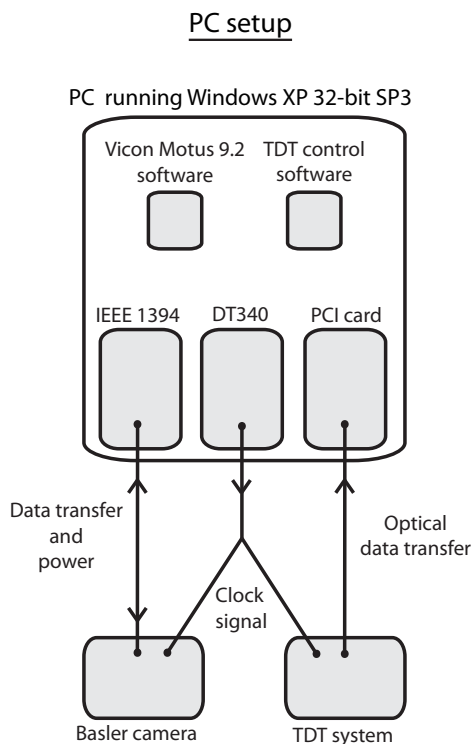


Figure 8.3: Schematic overview of the PC setup.

TDT Setup

A TDT recording system was used for IC recordings from the hindlimb area of the left CMA of the rats. The full setup for recording of IC signals consisted of a 16-channel chronic headstage (RA16CH), connecting the implanted electrode to a 16-channel pre-amplifier (RA16PA). The pre-amplifier was connected to the base station of the TDT system (RX5 Pentusa Base Station) through an optical cable (fig. 8.4).

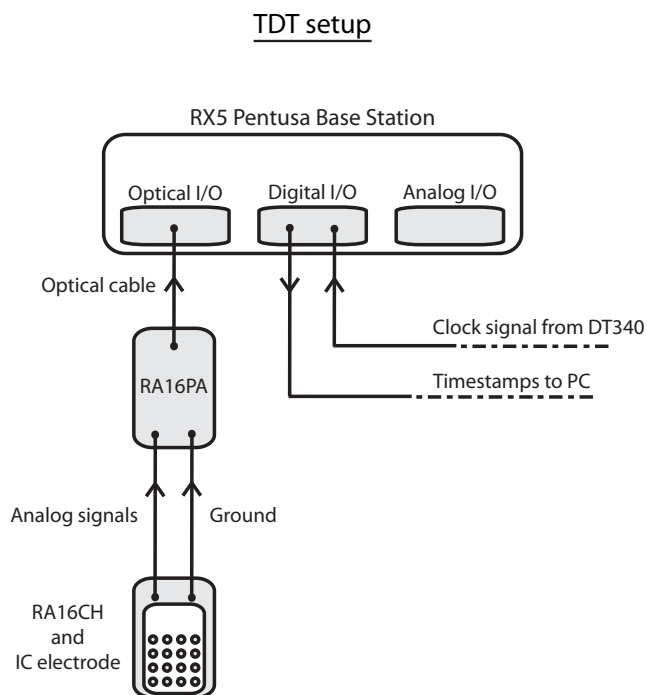


Figure 8.4: Schematic overview of TDT setup.

RA16CH - 16-Channel Chronic Headstage

A 16 pin board-to-board socket was connected to the RA16CH headstage, hereby enabling connection to the interface of the implanted electrode. The headstage has unity gain and serves to wire the IC signals to the RA16PA pre-amplifier [Tucker-Davis Technologies Inc., 2011].

RA16PA - 16-Channel Pre-amplifier

A 16-channel battery driven pre-amplifier, with a bandwidth ranging from 2.2 Hz to 7.5 kHz, was used to amplify and sample the analog IC signal. The sampling rate was set to 24.414 kHz. The pre-amplifier was connected to the Pentusa base station with a optic fiber connector [Tucker-Davis Technologies Inc., 2011].

RX5 Pentusa Base Station

Within the Pentusa base station, the spike data was bandpass filtered (800 Hz - 8 kHz). Online spike detection was performed, using an approach, where a lower threshold of $\approx 1.5 \times$ RMS of the raw data was automatically set, and subsequently adjusted manually by the TDT operator. Whenever a spike was detected, due to exceeding the threshold, the corresponding timestamp for onset was saved for

off-line analysis.

Camera Setup

For detection of the kinematics, a Basler A602fc-2 camera were used. The camera was mounted on a customised frame, hereby obtaining a lateral view of the affected hindlimb of the rat and keeping consistency in the view that the camera captures, since the camera was secured in this position. Two rulers were fixated to the perspex cage of the treadmill (one horizontally and one vertically) in a position, within the view captured by the camera. Two black self-adhesive semispheric markers were positioned with a 0.1 m span on both rulers, hereby obtaining a calibration frame, which could be captured by the camera, simultaneously with capturing the rat walking on the treadmill. The digitised calibration frame coordinates were used during post-processing for alignment of data related to the gait pattern and unit transformation (pixels to m). Vicon Motus 9.2 was used to record and process the data, i.e. digitise marker trajectories. To optimise the light conditions in the experimental setup, two telescope work lamps were placed behind the camera and lateral to the treadmill, in order to illuminate the experimental setting (fig. 8.5).

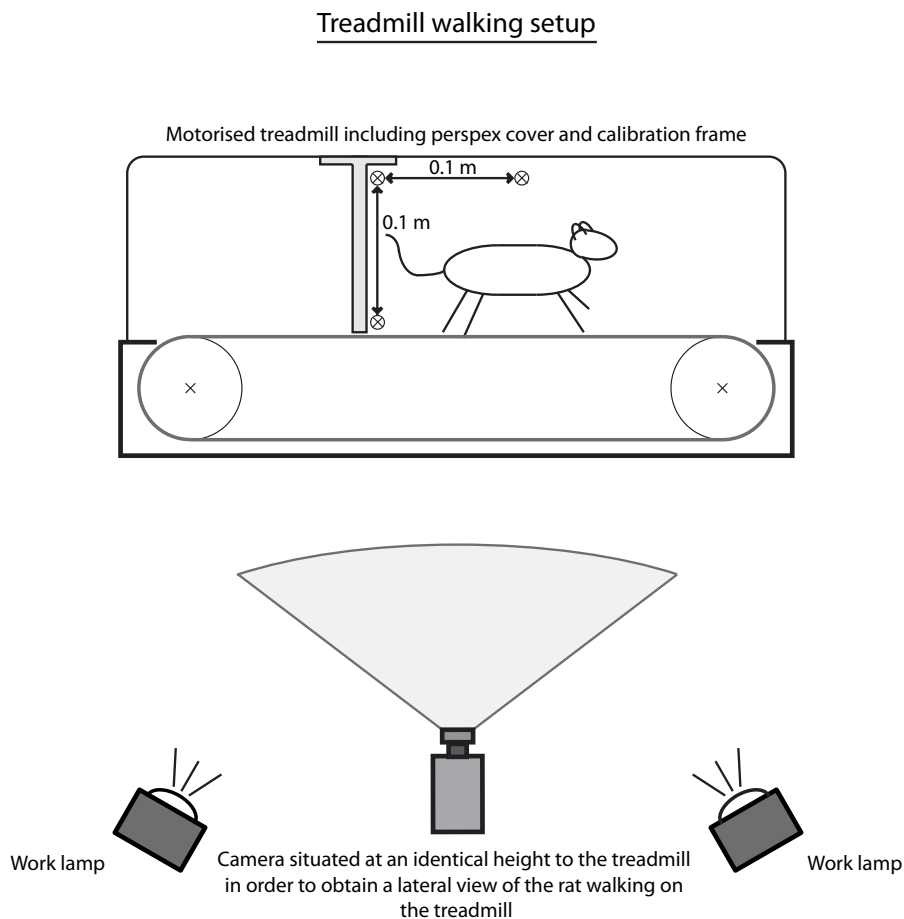


Figure 8.5: Position of the different components related to the treadmill walking test.

The camera was connected to the computer through a 10 pin RJ-45 jack and an IEEE 1394 socket,

located on the back of the camera. A cable from the computer to the IEEE 1394 socket on the camera was used for transferring video data from the camera to the computer for off-line analysis. Another connection cable, between the RJ-45 jack and a DT340 card in the computer, was used to externally clock the camera, in order to obtain a frame rate of 100 Hz (fig. 8.3) [Basler Inc., 2005].

8.1.3 Beam Walking Test

| List of materials for beam walking test | |
|--|--|
| Ledged beam: | • Ledged beam (length = 1.65 m) |
| PC: | • DT340 card (PCI bus digital I/O and counter/timer board) • PC running Windows XP 32-bit SP3 • Vicon Motus 9.2 (video acquisition software) |
| Camera: | • Basler A602fc-2 color machine vision camera • 400W telescope work lamp (SARTANO) |

Table 8.3: List of materials that were utilised for the beam walking test setup.

Ledged Beam Setup

In the beam walking test, each rat was placed on a horizontal ledged beam, based on the one described by Schallert et al. [2002] (fig. 8.6). It has a total length of 1.65 m, and is equipped with a ledge on each side. The ledges are situated 0.02 m below the beam. Two intervals, of 0.45 m each, used for quantification of foot drops, are indicated along the beam.

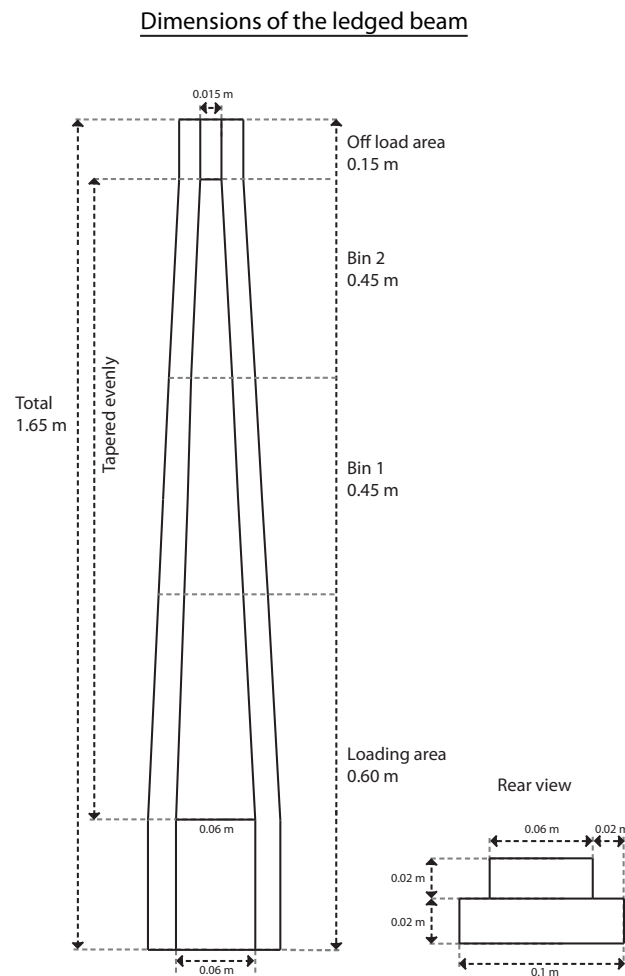


Figure 8.6: Illustration of the ledged beam. Modified from [Schallert et al., 2002].

Every session was video recorded with a Basler A602fc-2 camera, in order to enable off-line quantification of the performance of the rats, when traversing the beam. The camera was situated in an elevated position behind the beam, hereby the hindlimbs could be observed during the test (fig. 8.7). The Basler camera was externally triggered by the DT340 card within the PC, and data were transmitted from the camera to the IEEE 1394 firewire card situated in the PC. Vicon Motus 9.2 was used to handle triggering and data transferring.

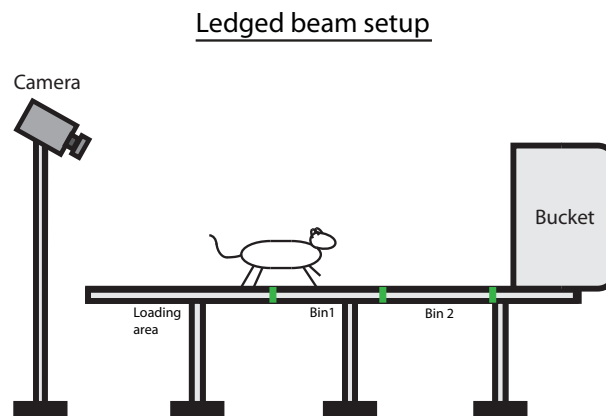


Figure 8.7: Schematic overview of ledged beam setup.

8.2 Experimental Procedures

8.2.1 Training

All 24 Sprague-Dawley rats were subjected to an identical training paradigm. The focus in week one was to familiarise the rats with being handled and introduced to the treadmill and ledged beam, whereas the main focus of week two and week three was to obtain a desirable performance level on the treadmill and ledged beam (tab. 8.4).

| | | Training paradigm | | | | |
|---------------------|--|--------------------------|-----------------------|-----------------------|-----------------------|-----------------------|
| | | Monday | Tuesday | Wednesday | Thursday | Friday |
| Week 1 | Hand training (10 min) | <input type="radio"/> | <input type="radio"/> | <input type="radio"/> | <input type="radio"/> | <input type="radio"/> |
| | Beam walking training (5 traversions) | <input type="radio"/> | <input type="radio"/> | <input type="radio"/> | <input type="radio"/> | <input type="radio"/> |
| | Treadmill walking training (3 x 1 min) | <input type="radio"/> | <input type="radio"/> | <input type="radio"/> | <input type="radio"/> | <input type="radio"/> |
| Week 2 and 3 | Hand training (10 min) | <input type="radio"/> | <input type="radio"/> | <input type="radio"/> | <input type="radio"/> | <input type="radio"/> |
| | Beam walking training (5 traversions) | <input type="radio"/> | <input type="radio"/> | <input type="radio"/> | <input type="radio"/> | <input type="radio"/> |
| | Treadmill walking training (3 x 1 min) | <input type="radio"/> | <input type="radio"/> | <input type="radio"/> | <input type="radio"/> | <input type="radio"/> |

Table 8.4: Training schedule prior to experimental onset.

During each beam and treadmill walking training session the rats were rated, according to three parameters, ranked in descending order according to priority; average continuous walking time on the treadmill, stops per traversal on the ledged beam, and foot drops per traversal on the ledged beam. The 16 rats, which performed best according to the ranked parameters, were included in the experiment and randomly assigned to the two experimental groups and further divided into intervention and control rats. Prior to initiation of the experiment, all 16 rats were instrumented with a 16-channel IC electrode array, within the hindlimb area of the left CMA.

8.2.2 Surgical Procedure

Before conduction of surgery, equipment had to be sterilised. The electrode had to be sterilised by radiation, whereas all other equipment was submitted to a steam sterilisation in an autoclave. A list of equipment used during preparation and conduction of surgery is illustrated below:

- 16 channel IC electrode array
- Shaver
- 1 % iodine solution sponge
- Hypnorm-Dormicum (anaesthesia)
- Syringe (1 ml) + hypodermic needle
- Stereotactic frame
- Scalpel (size 11)
- 4 x clamps
- Drill + 2 drill heads
- 2 x rongeurs
- Needle (G25)
- Microscissor
- Phillips screwdriver
- Dental acrylic (Heraeus Kulzer Paladur)
- SN-758 (Monosof suture)
- Forceps and tissue forceps
- 3 scissors
- Forceps and tissue forceps
- Scissor
- 6 - 10 aluminium trays
- 3 x screws with ground wires
- T-shirt
- 3 - 4 towels
- Spongostan
- Cotton buds
- Saline
- Gauze

Prior to the surgical procedure, rats were anaesthetised with a subcutaneous injection of 0.2 ml/100 g body weight of Hypnorm-Dormicum (Hypnorm: fentanyl = 0.315 mg/ml; fluanisone = 10 mg/ml, and Dormicum: midazolam = 5 mg/ml). A dose of approximately 0.05 ml/100 g body weight was administered every 30 min to maintain an appropriate level of anaesthesia. When the rat was fully anaesthetised, its head was shaved, and sterilised with a 1 % iodine solution sponge. Afterwards, it was placed in a stereotactic frame, and vaseline was applied on the eyes of the rat, in order to avoid damaging the eyes, due to drying out. An incision along the midline, extending from a point just behind the eyes of the rat and 2 - 3 cm caudally was made, hereby exposing the skull. A craniectomy was performed over the hindlimb area, within the left CMA. The initial perforation was made with a drill, and enlarged by use of a rongeur. Three additional holes (two located caudally and one rostrally, with respect to the electrode) were drilled, once the initial opening in the skull was enlarged to a size suitable for implementation of the 2 x 2 mm electrode array. The dura was removed from the cortical exposure, by use of a needle and a microscissor, prior to insertion of the 16-channel IC electrode array. The IC electrode array, including a guiding tube (array dimension: width = 2 mm, length = 2 mm, electrode: = 100 μ m, spacing = homogeneous, guiding tube: ϕ = 4 mm), was quickly lowered 1.8 mm into the cortex at position; 1:3 mm caudally to bregma, and 1:3 mm laterally to the midline (fig. 8.8). Three stainless steel bone screws, serving as mechanical stabilisation and grounding, were inserted in the three screw holes in the skull.

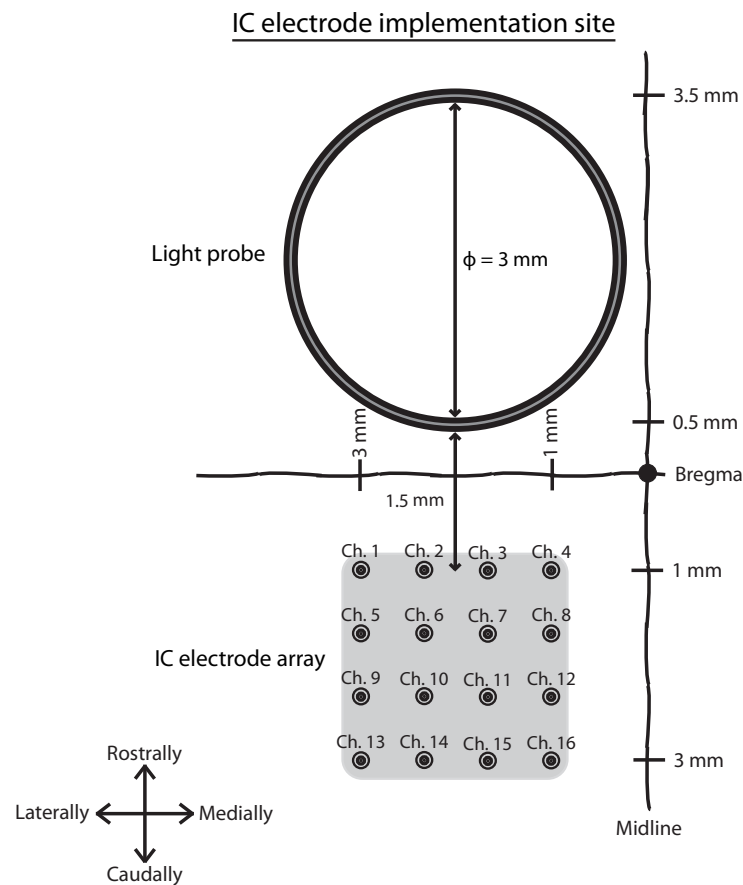


Figure 8.8: Illustration depicting the implementation site of the IC electrode array and the position, rostrally to the electrode, where the light probe is lowered down through the guiding tube, in order to illuminate the tissue upon rose bengal dye injection.

Following, insertion of the electrode, the space between the electrode and the cortex was covered with Spongostan. Subsequently, dental acrylic was applied, in order to secure the electrode array and bonescrews. Finally, the surgical incision was closed caudally and rostrally to the electrode array, by a suture.

8.2.3 Applying Stroke using Photothrombosis

Prior to the photothrombosis intervention, rats were anaesthetised with a subcutaneous injection of 0.2 ml/100 g body weight of Hypnorm-Dormicum and fixated in the stereotactic frame. A light probe ($\phi = 3 \text{ mm}$, $\lambda = 560 \text{ nm}$) was lowered into the guiding tube, until it was located 0.5 mm above the lower boundary of the guiding tube at a position rostrally to the electrode array (fig. 8.8). A rubber band was fixed around the root of the tail of the rat, in order to dilate the blood vessel before infusion. Next, a venflon catheter ($\phi = 0.7 \text{ mm}$, length = 19 mm) was inserted into the tail vein of the rat, and the ambient lights were turned off for the remainder of the photothrombosis procedure. A dose of 0.3 ml/100 g body weight (concentration = 20 mg dye/ml saline) was injected through the venflon catheter, over a two minutes timespan. The light source was turned on upon initiation of rose bengal

injection and remained on for a total of 30 min, hereby illuminating the dye, circulating through the blood vessel, supplying the cortical region situated just beneath the light probe.

8.2.4 Rehabilitative Training

Post photothrombosis intervention, the two experimental groups were submitted to identical training paradigms, only differing in the time of rehabilitation onset. Group 1 started rehabilitation on day one post stroke, whereas group 2 started rehabilitation on day seven post stroke (fig. 8.1). Training consisted of 25 beam traversions and 3 x 1 min of treadmill walking per day, five days a week.

8.2.5 Intracortical Microstimulation Test

Identical IC microstimulation tests were conducted upon initiation and termination of the experiment. The microstimulations were performed, by consecutively stimulating each channel of the electrode array (stimulation ground = groundwire on IC electrode). Motor responses were visually observed and grouped into hindlimb and forelimb motor responses, or no-motor-responses. Upon observation of a motor response, the pulse amplitude was lowered 50 μA , in order to verify if a similar response could be elicited with only half pulse amplitude increment added to the non-response pulse amplitude level. Precautions were taken by the study member handling the rat, in order to assure that the rat was relaxed prior to each stimulation, and thus the observed motor activity was related to the elicited IC microstimulation.

8.2.6 Treadmill Walking Test

The treadmill walking test consisted of 4 x 30 s sessions per recording day. The total recording duration per recording day (2 min) was chosen, in order to assure that an amount of gait cycles (> 100 gait cycles), sufficient for calculation of peri-stimulus time histograms (PSTH), were obtained. The total recording time was split into 4 x 30 s sessions, since it was discovered during pilot experiments, that the Vicon Motus 9.2 software did encounter problems, when handling data files exceeding 30 s of duration. The four sessions were conducted with a pause of one min between each session, hereby attaining a total duration of five minutes per rat per recording day. Additional training on the treadmill was conducted after end of treadmill walking test, in order to reach the rehabilitation level of three minutes per day. Four black self-adhesive semispheric markers were used to obtain kinematic data, related to the right hindlimb of the rat. Marker positions were marked with a permanent felt-tip pen, at the end of every recording day, in order to keep consistency in the marker positions. The markers were positioned at the following bony landmarks on the hindlimb and on the abdomen (fig. 8.9):

- The abdomen
- The knee joint
- The ankle joint
- The toe

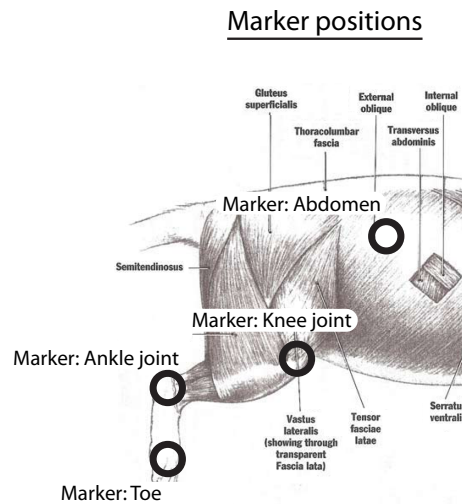


Figure 8.9: Lateral view of the distribution of muscles on the rat. The black circles indicate marker positions. Modified from [Walker Jr and Homberger, 1997].

After the markers were fixed on the rat, the IC electrode array was connected to the TDT recording system. Next, the rat was placed outside the treadmill, while thresholds for the IC signals were set. During thresholding, precautions were taken, in order to assure that the rat was sitting still, and thus the threshold adjustments were based on observation related to spontaneous motor cortex firing activity. The rat was then placed on the treadmill, in order to conduct the recordings. Firstly, the treadmill was turned on for a while (< 5 s), hereby enabling the rat to obtain a stable walking pattern before initiating data collection. Recording of IC signals, through the use of the TDT recording system, were initiated as soon as a stable walking pattern was achieved. Next, the transmission of the clock signal from the DT340 card was initiated through Vicon Motus 9.2, hereby starting the video recording and synchronisation signal to the TDT recording system. When 30 s of video data had been recorded, Vicon Motus 9.2 automatically, terminated the clock signal from the DT340, and the video recording and synchronisation signal was terminated. The IC recording by the TDT system was then also terminated. Finally, Vicon Motus 9.2 was used to post-process the video data, by tracking of the four markers on the rat, together with the markers situated on the calibration frame throughout the 30 s of video.

8.2.7 Beam Walking Test

The beam walking test consisted of 20 traversions per recording day. Additional beam traversions were conducted after end of beam walking test, in order to reach the rehabilitation level of 25 traversions per day. In the beginning of each traversion the rat was placed at the base (broad end of beam). The task for the rat was to traverse from the base to the home cage (black bucket with towel) situated at the opposite end of the beam (fig. 8.7). Each trial was video recorded, by use of Vicon Motus 9.2 and the Basler A602fc-2 camera, in order to count the number of foot drops made by the rat during traversion of the beam. Foot drops were defined as the rat touching one of the ledges located on each side of the beam with one of its hindlimbs.

9.1 Intracortical Microstimulation Test

The data from the IC microstimulation tests were grouped into five categories (row 1: channel 1 - 4, row 2: channel 5 - 8, row 3: channel 9 - 12, row 4: channel 13 - 16, and all channels). The percentage of hindlimb related channels, within each category, was quantified, and each category was subjected to one-way ANOVA, in order to assess, if the distribution of hindlimb related channels had changed within or between groups during the experiment.

9.2 Treadmill Walking Test

Video data from the treadmill walking test were processed, in order to obtain timestamps for different events within the gait cycle. The timestamps of these events were used in data processing tasks, related to quantification of IC signals. Further, the timestamps were also used in data processing, aiming at assessing kinematic alterations during the course of the experiment.

9.2.1 Gait Cycle Event Detection

Prior to analysis of the kinematics, the recorded data were pre-processed. A part of this pre-processing was detection of two different events in each gait cycle. The two events were initial and terminal stance. The events were defined as, the time when the toe is first put to the treadmill belt, and the time when the toe is leaving the treadmill belt, respectively.

The first step, in the algorithm for detection of gait cycle events, was a smoothening of the toe-marker x-coordinates, in order to attenuate high frequency noise oscillations in the data. Following smoothening, the local extrema of the toe-marker x-coordinates were detected and saved as the initial (maxima) and terminal stance (minima) events. The second step in the algorithm was calculation of the paw-ground, ankle joint, and knee-ground angle from the x-, and y-coordinates of the three markers on the hindlimb (fig. 9.1). Next, the angle data was smoothed in case that the angle difference between two consecutive samples exceeds a threshold of 5 times the mean difference between consecutive samples. Similarly, if the angle difference between two consecutive event was below a lower threshold of 0.5 times the mean difference between consecutive initial stance events, the initial and terminal stance events of the the specific gait cycle were removed.

Angles used for sorting of gait cycles

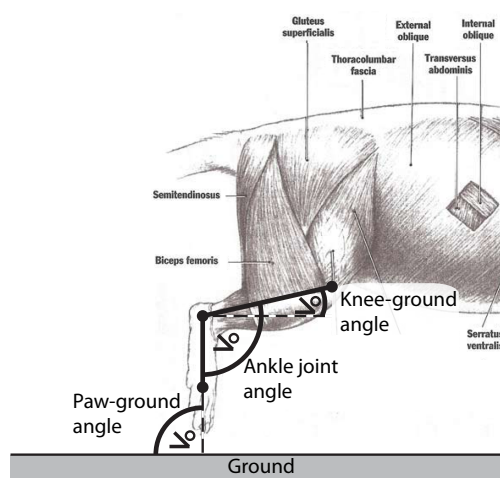


Figure 9.1: Three angles were calculated from the coordinates, obtained from the treadmill walking test. The three angles; paw-ground, ankle joint, and knee-ground angle are shown on a hindlimb sketch.

9.2.2 Analysis of Intracortical Signals

The first step in the analysis of the IC signals was to generate PSTH plots of the neuronal firing pattern during the gait cycle, on the basis of the gait cycle events. The firing pattern during several gait cycles was averaged, in order to depress random fluctuations, since cortical neurons tend to have some degree of spontaneous firing. In order to successfully calculate mean firing rates across individual gait cycles, it was thus needed to obtain a certain degree of homogeneity in the duration of the individual gait cycles. Thus, on the basis of the detected gait cycle events, the gait cycle, swing, and stance phase duration were calculated for the individual gait cycles (fig. 9.2).

Normalisation and calculation of PSTHs

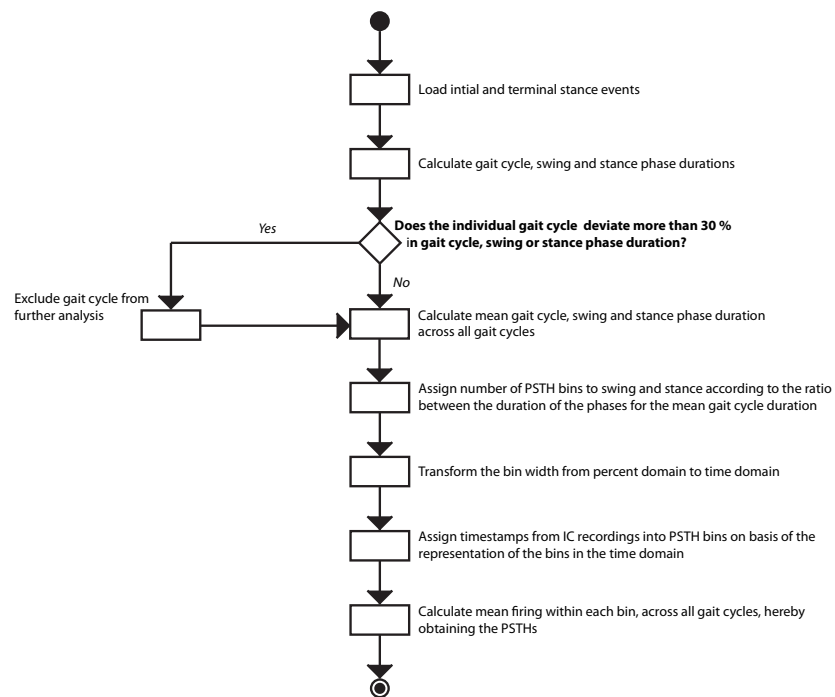


Figure 9.2: Flowchart of the normalisation and calculation of PSTH data.

Next, all gait cycles were subjected to an inclusion criteria, which stated that if the individual gait cycles deviated less than 30 %, in either gait cycle duration, swing, or stance phase duration from a pre-specified gait cycle, swing, and stance phase duration, they were included in further analysis. The pre-specified set of gait cycle parameters were in turn assigned the value of the individual gait cycles, and the amount of included gait cycles was determined. The densest cluster of gait cycles, obtained by this procedure was chosen for further analysis (fig. 9.3).

Gait cycle cluster analysis

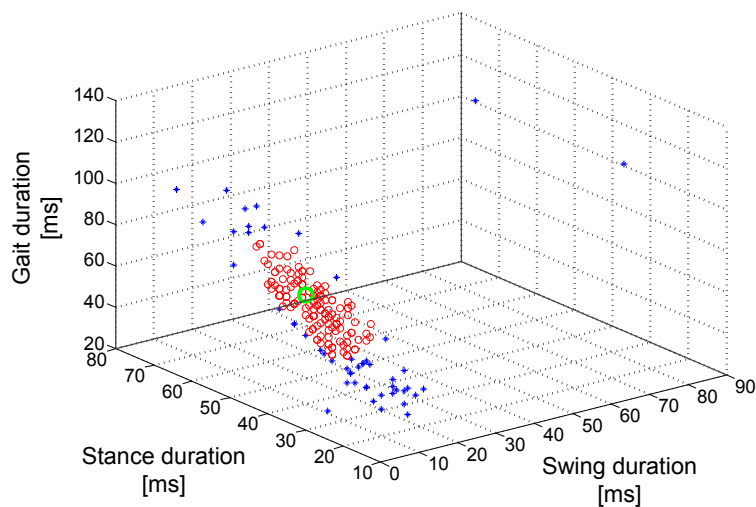


Figure 9.3: Plot of gait cycle, stance, and swing duration for the individual gait cycles. Blue asterisks indicate gait cycles, which fall outside the $< 30\%$ deviation inclusion criteria. Red circles indicate individual gait cycles, which are included in further analysis. The large green circle indicates the gait cycle, according to which the most dense cluster of gait cycles could be obtained, when its parameters were used for calculation of the $< 30\%$ deviation inclusion criteria.

After specifying gait cycles, suited for further analysis, a second procedure, where data were transformed from a time representation into percent of gait cycle duration, was conducted, in order to obtain a homegenous data set in regards to the gait cycle duration. Hence, the mean duration of the gait cycle, swing, and stance phase, across all gait cycles were calculated and used, in order to determine the ratio between PSTH bins (each bin represented 2% of the gait cycles), assigned to describe the firing characteristics of the swing and stance phase. Next, the time domain width of bins for each phase was calculated, so that the time domain width corresponded to 2% of the gait cycle duration. Finally, the PSTH for the individual gait cycle was calculated by assigning counts to the bin, which represented the timespan enclosing the timestamps. The mean firing within each bin, across all gait cycles was calculated, once all the individual firing representations were obtained, hereby achieving the final PSTHs (fig. 9.4).

Normalisation of gait cycle duration

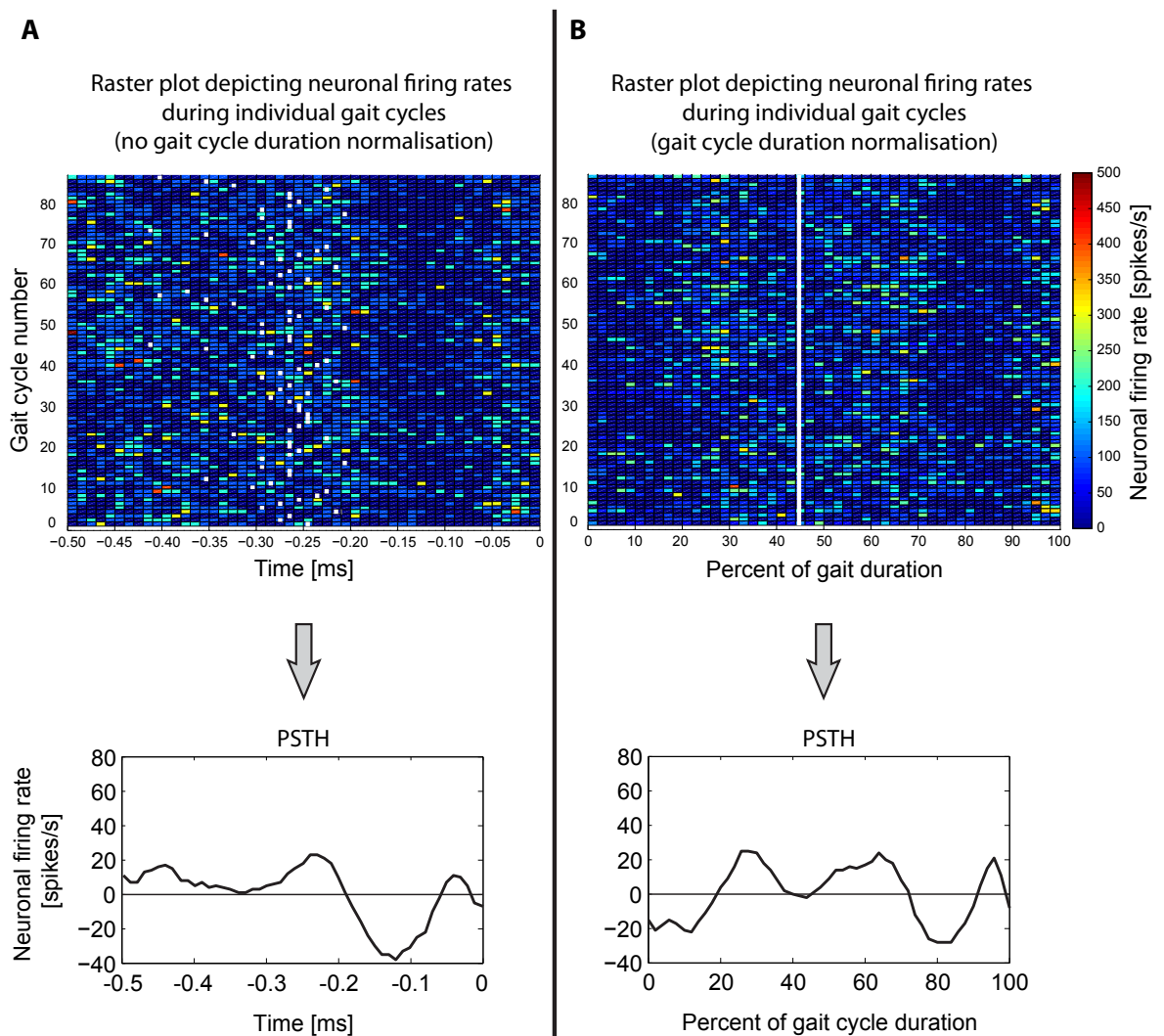


Figure 9.4: Figure depicting the result of normalisation of neuronal activity according to gait cycle, swing, and stance duration, hereby transforming timing of neuronal firing from the time domain into percentage of gait cycle duration. White dots on the raster plots indicate the timing of the stance-swing transition. **A:** stance-swing transition is not aligned, when timing of neuronal activity, within individual gait cycles, is represented in the time domain on raster plots. **B:** on the contrary, stance-swing transition is aligned across all gait cycles, when represented as percentage of the gait cycle duration. A plot of the resulting PSTHs are situated below each raster plot.

Next, PSTHs from the 16-channel IC electrode array were grouped, according to the results from the IC microstimulation tests:

- **Subgroup 1:** Channels, through which hindlimb movement could only be elicited on the initial IC microstimulation test.
- **Subgroup 2:** Channels, through which hindlimb movement could be elicited on both IC mi-

crostimulation tests.

- **Subgroup 3:** Channels, through which hindlimb movement could only be elicited on the terminal IC microstimulation test.

Finally, the amount of firing rate modulation was calculated as the area of the rectified PSTH. As such, both inhibitory and excitatory firing rates were included in the quantification of firing rate modulations.

9.2.3 Analysis of Kinematic Data

Centre of Gravity for Marker Trajectories

For each individual gait cycle the centre of gravity (CoG) for each marker trajectory was calculated. Each CoG was calculated as the mean of x-coordinates and the mean of y-coordinates for the trajectory of the individual markers during the gait cycles.

Residuals

The initial step for the algorithm was to verify, whether the input data were baseline data or post stroke data (fig. 9.5). Assuming that the input data were baseline data, the algorithm would adjust the coordinates, and rescale these. This was necessary in case that the camera had moved in the vertical dimension. Scaling was performed to convert pixel values to units of centimetres. Subsequently, all gait cycles were downsampled, in order to prepare the data for principal component analysis (PCA). The first part of the gait cycle downsampling was calculation of the grand mean (μX) across all the abdomen marker x-coordinates in each gait cycle (fig. 9.6).

Calculation of residuals

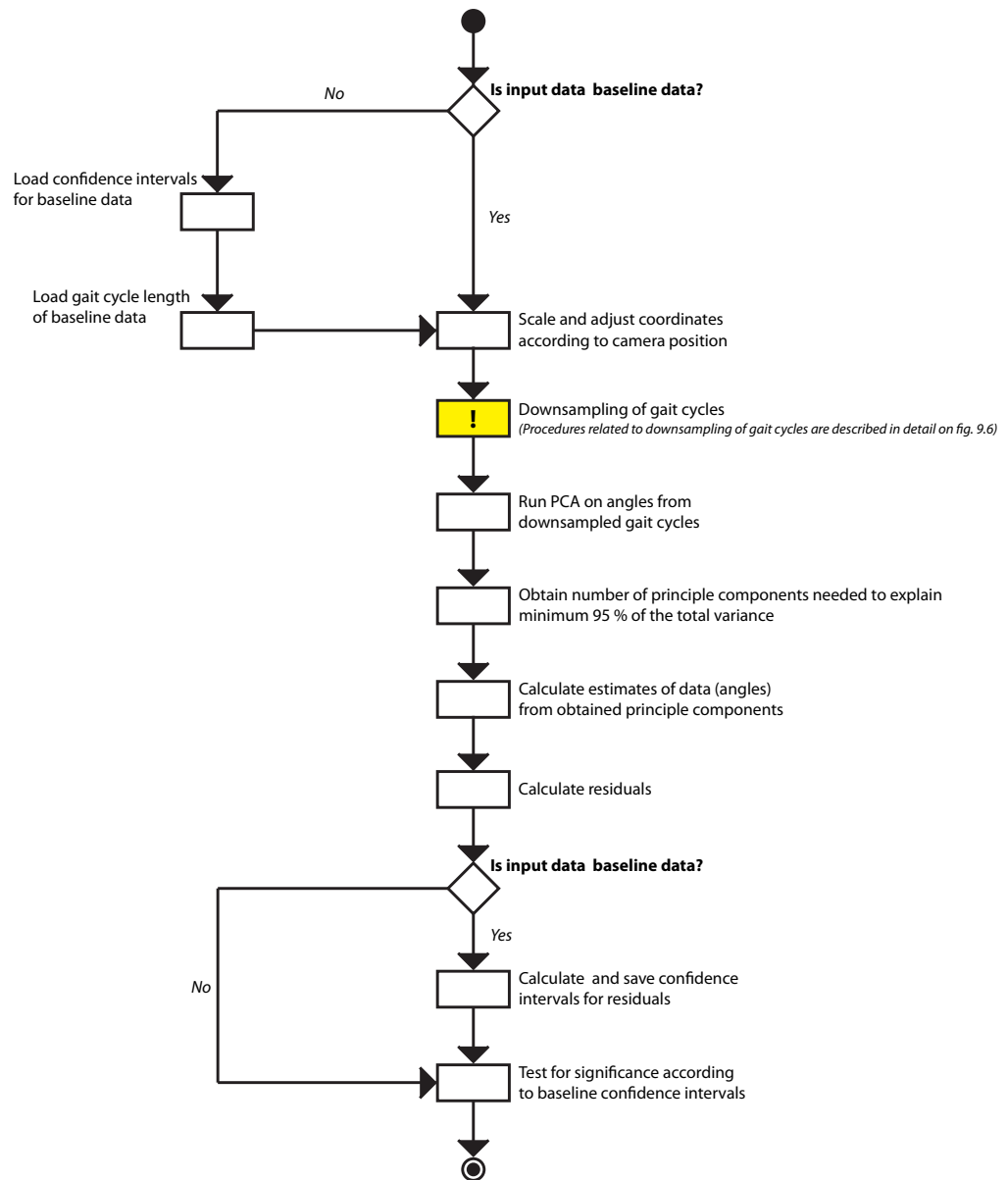


Figure 9.5: The flowchart illustrates how coordinates are processed, in order to obtain residuals.

Gait cycle downsampling

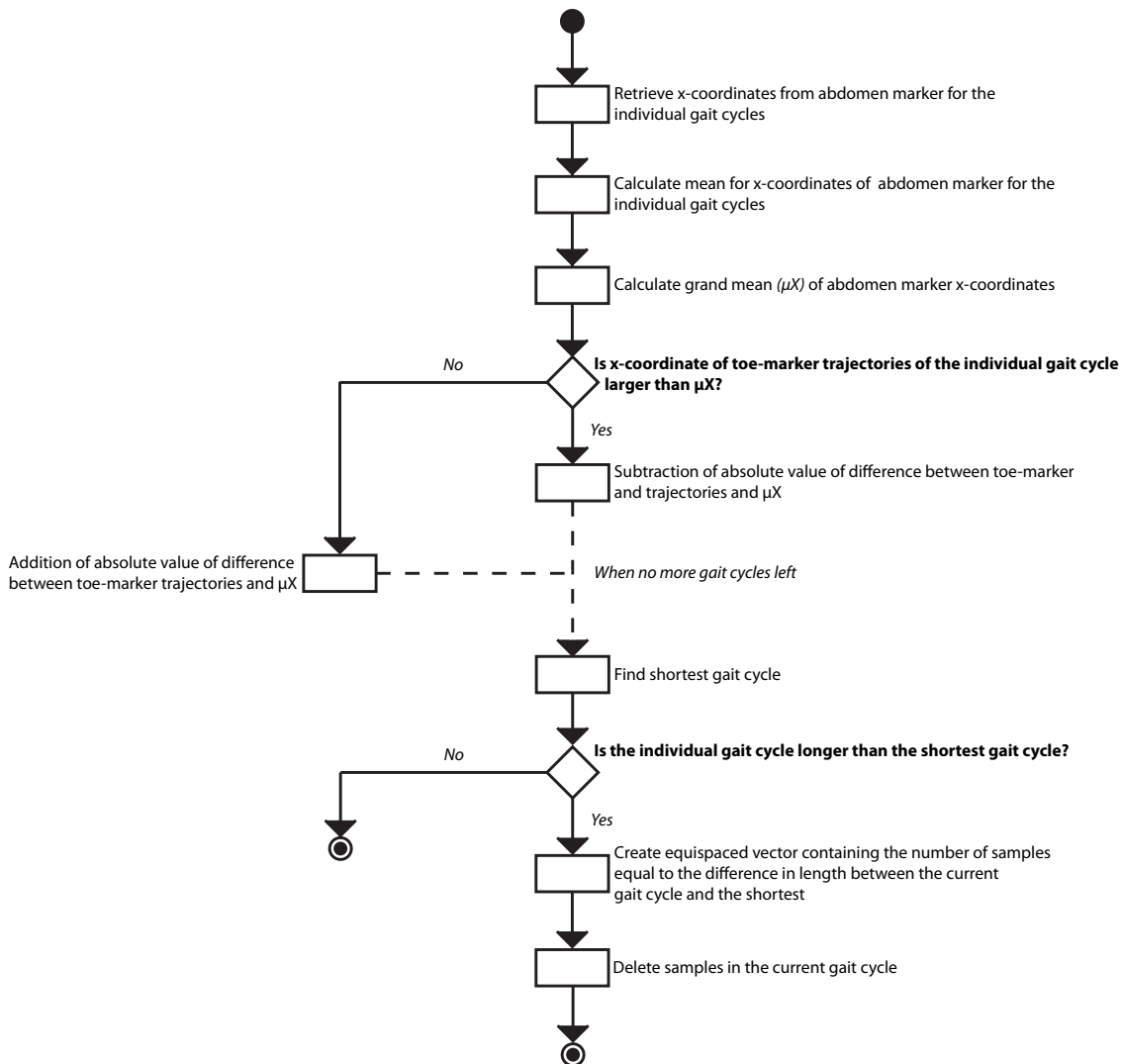


Figure 9.6: The flowchart shows how individual gait cycles are scaled to the same length, in order to prepare them for PCA.

The μX was used as reference point, to compare the individual toe-marker x-coordinates of each gait cycle, and determine, if these were larger than μX . The absolute value of the difference between the x-coordinate and μX , was subtracted from the x-coordinate if it was larger than μX , else this difference was added to the x-coordinate. When there were no more gait cycles left to adjust, the length of the shortest gait cycle was determined. In the final two steps of the downsampling algorithm, all gait cycles were downsampled to the length of the shortest gait cycle. An equispaced vector, containing the number of samples equal to the difference in length between the current gait cycle and the shortest was created, if the current gait cycle was longer than the length of the shortest gait cycle. The samples contained in the vector were then removed from the gait cycle.

After gait cycle downsampling, PCA was performed, and the number of components needed to ex-

plain minimum 95 % of the total variance was determined (fig. 9.5). From these components, an estimate of the gait cycle angles was created. Residuals were then obtained by calculating the sum of squared error between the estimate of the angles and the raw angles (fig. 9.7).

PCA estimated angle vs. actual angle

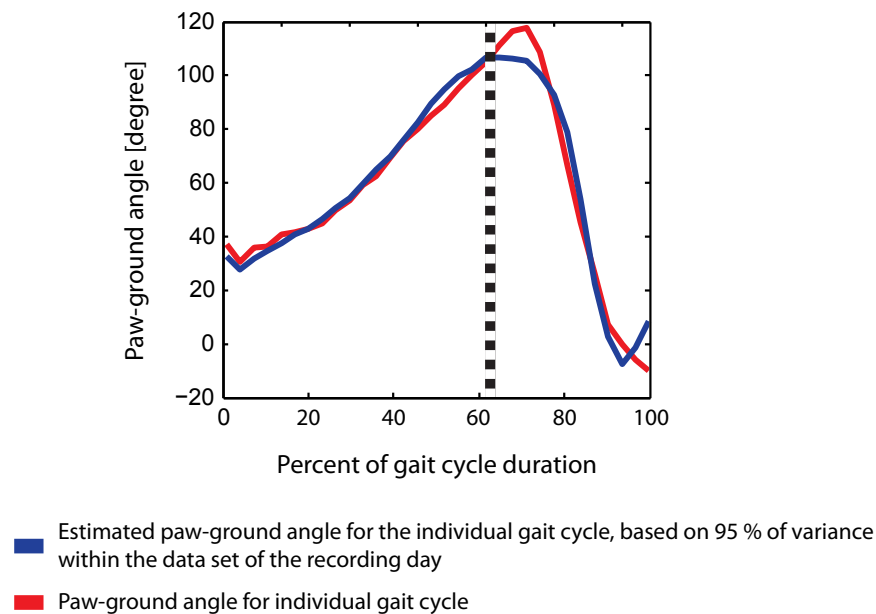


Figure 9.7: The plot shows the paw-ground angle during one gait cycle. The red graph is composed of the raw angles, while the blue is the PCA estimate, calculated from 95 % of the specific data set. The stance-swing transition is indicated by the dashed line. In this case, the gait cycle exceeds the 95 % confidence limits of the baseline residual values. It can also be seen that the main site of change during this gait cycle is located early in the swing phase.

Following calculation of residuals, the algorithm once again verified if the input data were baseline data. In case, the data were from the baseline recordings, confidence limits were calculated for the residual values. Finally, the percentage of residuals of the current data exceeding the lower or higher confidence limit, was determined.

9.3 Beam Walking Test

The data processing of the beam walking test was related to the foot drop parameter, and was conducted, in order to obtain data that were more representative of the increasing difficulty for the rat to avoid foot drops, while traversing the narrowest part of the beam. The correction concerned, multiplying the counted foot drops on the broad end of the ledged beam by two, whereas foot drops on the narrow end of the ledged beam were weighted by a factor of one.

9.4 Statistics

For all tests, except the IC microstimulation test, difference between baselines within each intervention group was tested with one-way ANOVA, if no significant difference was seen between baselines, they were averaged. Furthermore, differences between groups in baselines were tested with the one-way ANOVA, if significant differences were observed, the data were normalised according to their respective baseline level.

Each variable, obtained from the data processing of the individual tests, was analysed both within and between group. The within group differences were tested by use of a one-way ANOVA, with recording day as a possible main factor, in order to test for significant differences. Furthermore, post-hoc test was conducted, if recording day was found to be a significant main factor, in order to verify, which days that were significantly different from the baseline level. The between group differences was tested for all variables except residuals, by use of a one-way ANOVA, with group as a possible main factor. Furthermore, post-hoc test was performed, if group was a significant main factor, in order to verify, at which recording days, the two intervention groups were significantly different.

During the experiment, six rats were lost, and one rat was excluded. One rat died shortly after injection of anaesthetics prior to surgery. The injection might have caused an allergic reaction, leading to death of the rat. A second rat was lost shortly after surgery, since it was observed that the rat was not able to eat or drink, and was as a consequence put down. Two rats died after induction of stroke. It can be suggested that one of the rats died due to an allergic reaction to anaesthetics, since it died within a couple of hours after injection of anaesthetics. However, as a more likely possibility, the rat might have died due to an unintended occlusion of the large middle cerebral artery, since differences in the blood vessel distribution is apparent between rats, thus the artery might have been located within the illuminated area [Wang-Fischer, 2008]. The second rat, lost as a consequence of photothrombosis, might also have been exposed to occlusion of the same artery, since serious deficits were observed on day one post stroke induction (the rat was severely paralysed in three limbs), and was therefore put down. A fifth rat was also put down, since it was not possible to elicit any responses by applying IC microstimulations. It was observed that the base of the IC electrode array contained fluid or blood, most likely originating from the guiding tube. This observation gave rise to measuring the resistance between the channels of the IC electrode array and compare it to the IC electrode arrays of other rats, from which it was possible to elicit motor responses by IC microstimulations. The measurements showed that the resistance in the affected IC electrode array was lower compared to other implanted IC electrode arrays. The sixth rat had to be put down halfway through the experiment, since it lost its electrode. This rat was much harder to handle than any of the other rats, and therefore the IC electrode array was also exposed to more stress. Moreover, it was also observed that, the rat did hit its head into the front wall of the treadmill during recordings in a far greater extent than any of the other rats. This behavior might explain the loss of the IC electrode array.

The loss of rats resulted in intervention group 1 including five rats, intervention group 2 including four rats, and control group 1 including one rat, which all completed the experiment. Though, the rat from control group 1 was excluded from the results, since statistical calculations were not possible, when only one rat comprised the control group.

10.1 Intracortical Microstimulation Test

| Results from IC microstimulation tests | | | | |
|--|------------------|-------------------|-------------------|-------------------|
| | Pre stroke | | Post stroke | |
| | Group 1 | Group 2 | Group 1 | Group 2 |
| Row 1 | 75.00 % ± 7.91 % | 75.00 % ± 10.21 % | 95.00 % ± 5.00 % | 43.75 % ± 18.75 % |
| Row 2 | 80.00 % ± 9.36 % | 68.75 % ± 6.25 % | 95.00 % ± 5.00 % | 62.50 % ± 7.22 % |
| Row 3 | 20.00 % ± 9.36 % | 75.00 % ± 14.44 % | 65.00 % ± 16.95 % | 87.50 % ± 7.22 % |
| Row 4 | 10.00 % ± 6.12 % | 62.50 % ± 12.50 % | 60.00 % ± 20.31 % | 50.00 % ± 17.68 % |
| All channels | 46.25 % ± 5.80 % | 70.31 % ± 5.34 % | 78.75 % ± 10.19 % | 60.94 % ± 2.99 % |

Table 10.1: Results from the IC microstimulation tests. The percents represent the average amount of channels corresponding to hindlimb movement. N corresponds to the number of rats in each intervention group. Average percents are represented with ± standard error of mean (SEM).

Within group analyses revealed that a significant increase of hindlimb related channels, pre to post stroke, was present for intervention group 1 on row 3, row 4, and all channels. No significant differences between pre and post stroke were seen for intervention group 2. Between group analysis revealed that intervention group 2 had a significantly higher amount of hindlimb related channels, compared to intervention group 1, pre stroke on row 3, row 4, and all channels, whereas the opposite was seen post stroke on row 1 and row 2 (tab. 10.2).

| P-values for IC microstimulation tests | | | | |
|--|--------------|---------|---------------|--------------|
| | Within Group | | Between Group | |
| | Group 1 | Group 2 | Pre stroke | Post stroke |
| Row 1 | 0.065 | 0.194 | 1.000 | 0.022 |
| Row 2 | 0.195 | 0.537 | 0.378 | 0.007 |
| Row 3 | 0.049 | 0.468 | 0.013 | 0.303 |
| Row 4 | 0.046 | 0.585 | 0.005 | 0.729 |
| All channels | 0.003 | 0.176 | 0.02 | 0.177 |

Table 10.2: P-values for within group and between group statistical tests. Numbers in bold indicate tests, at which, significant difference was seen.

Results from the individual rats in each intervention group are shown on figure 10.1 and 10.2.

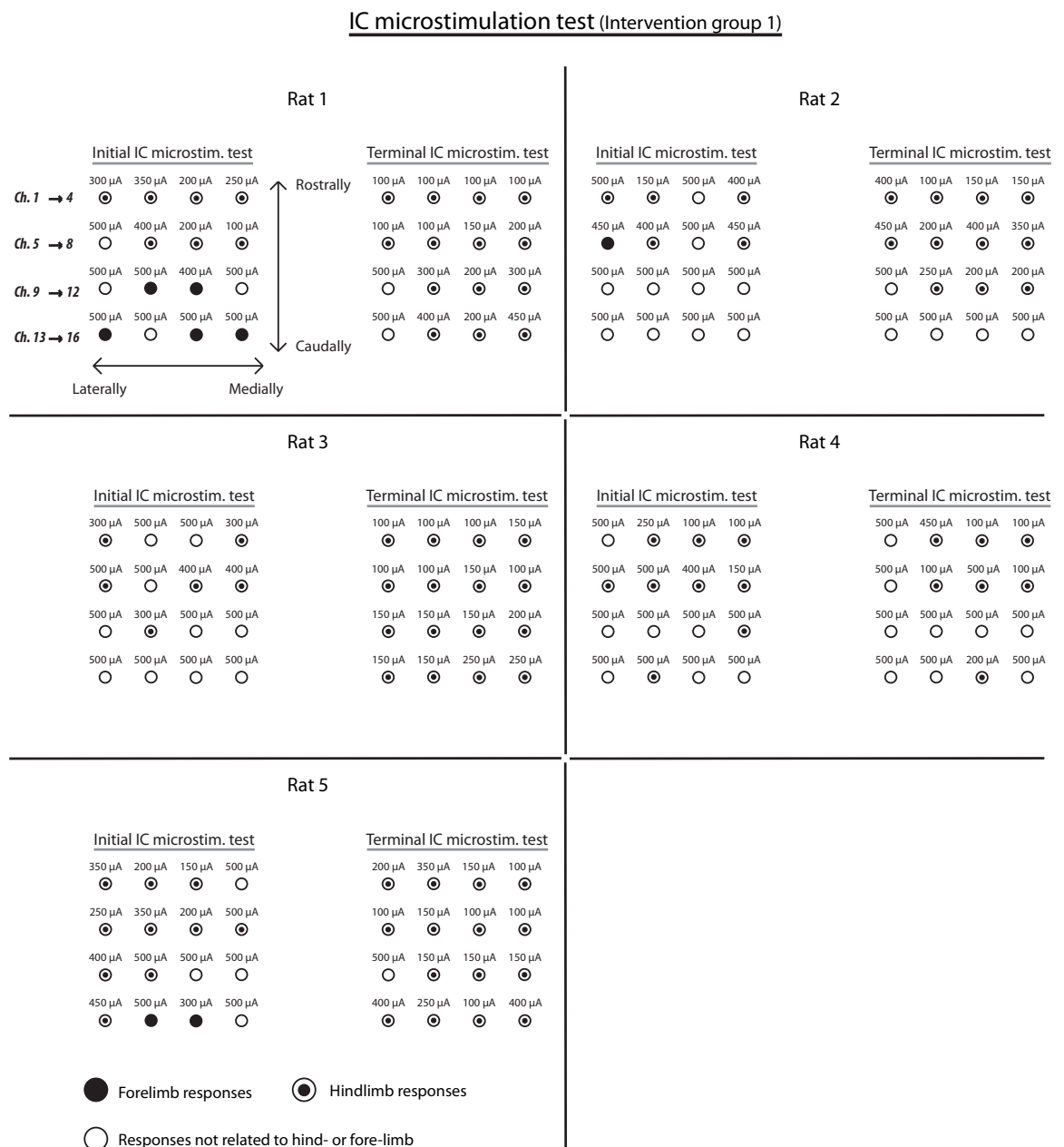


Figure 10.1: Results from the initial and terminal IC microstimulation tests conducted on intervention group 1.

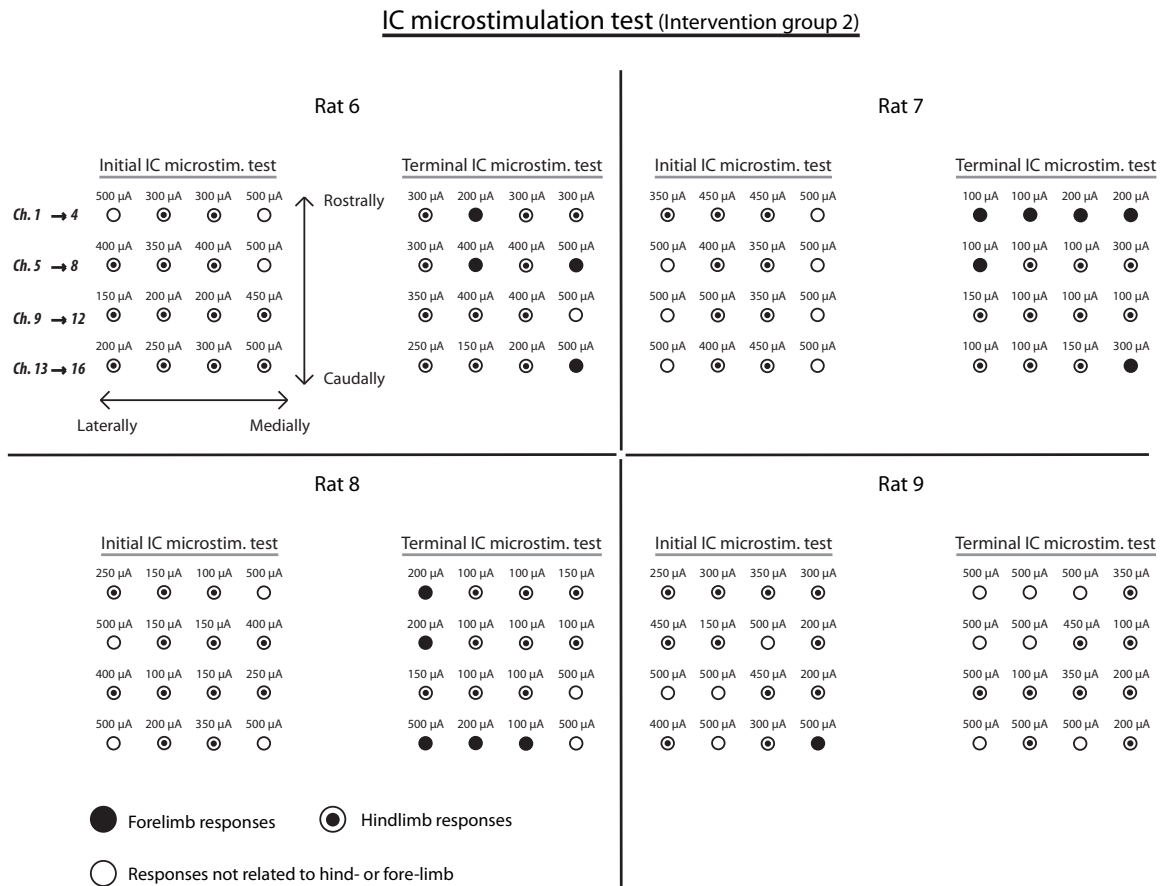


Figure 10.2: Results from the initial and terminal IC microstimulation tests conducted on intervention group 2.

10.2 Treadmill Walking Test - Intracortical Signals

An example of PSTHs for the different subgroups within each intervention group is shown on figure 10.3.

Examples of the firing rate patterns recorded during
the course of the experiment

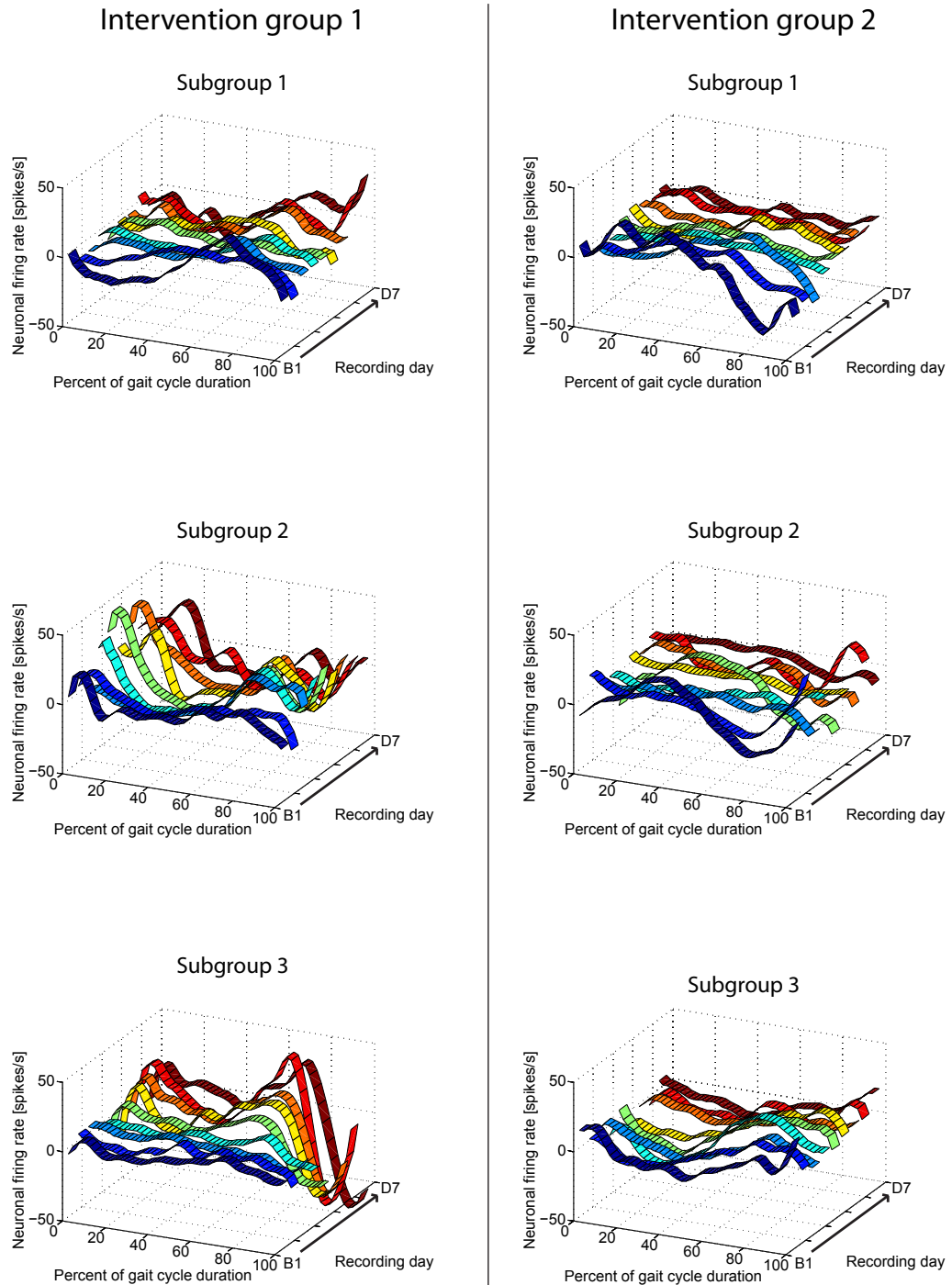


Figure 10.3: Examples of the firing rate modulations, recorded by individual IC electrodes array, during the course of the experiment. Three channels for each intervention group are represented. Each channel represents one of the three subgroups obtained from analysis of the IC microstimulation tests. The colouring on each graph, going from a dark blue (B1) to a dark red (D7) represent the different recording days.

10.2.1 Within Group

One-way ANOVA for intervention group 1 showed that recording day was a significant main factor for subgroup 1 ($p = 0.007$), subgroup 2 ($p = 0.003$), and subgroup 3 ($p < 0.001$). The within group analysis for intervention group 1 revealed a significant decrease in firing rate modulation size on D1 ($p = 0.003$), D2 ($p = 0.006$), D3 ($p = 0.001$), and D4 ($p = 0.017$) compared to baseline for subgroup 1. For subgroup 2, D5 ($p = 0.037$), D6 ($p = 0.011$), and D7 ($p = 0.009$) had a significantly increased firing rate modulation size compared to baseline, whereas for subgroup 3, all days post stroke showed a significantly increased firing rate modulation size compared to baseline; D1 ($p = 0.002$), D2 ($p = 0.001$), D3 ($p < 0.001$), D4 ($p < 0.001$), D5 ($p = 0.001$), D6 ($p = 0.012$), and D7 ($p < 0.001$) (fig. 10.4).

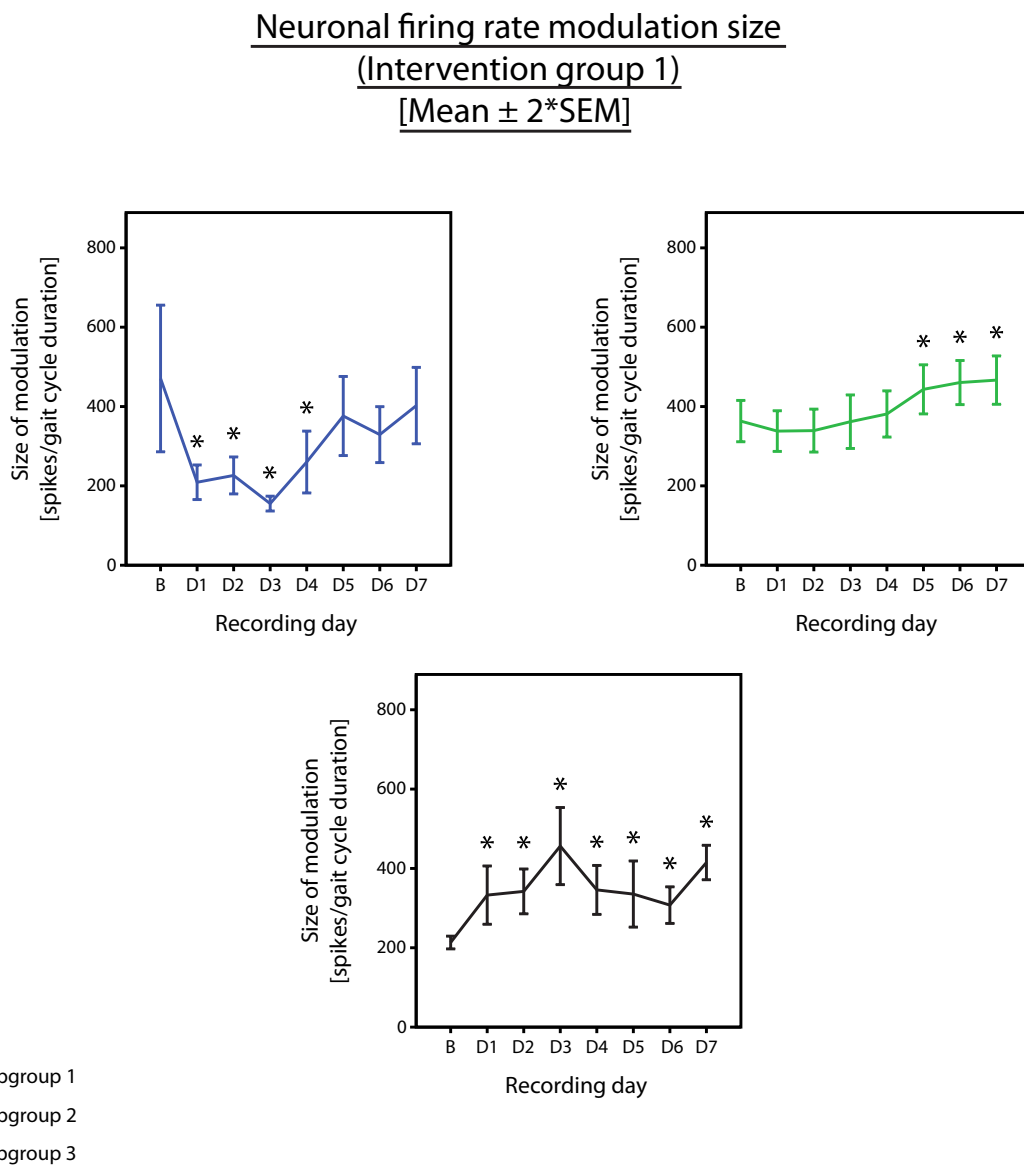


Figure 10.4: Within group results from intervention group 1. * denotes recording days with significant different firing rate modulation size throughout the gait cycles, compared to baseline level.

One-way ANOVA for intervention group 2 showed that recording day was a significant main factor for subgroup 1 ($p = 0.001$), subgroup 2 ($p < 0.001$), and subgroup 3 ($p = 0.002$). The within group analysis for intervention group 2 revealed a significant decrease in firing rate modulation size on D1 ($p = 0.009$) and D4 ($p < 0.001$) compared to baseline for subgroup 1. For subgroup 2, D1 ($p < 0.001$), D2 ($p < 0.001$), D3 ($p < 0.001$), D4 ($p < 0.001$), D5 ($p = 0.006$), and D7 ($p < 0.001$) had significantly decreased firing rate modulation size compared to baseline, whereas for subgroup 3, D1 ($p = 0.001$), D2 ($p = 0.046$), and D4 ($p < 0.001$) had significantly decreased firing rate modulation size compared to baseline (fig. 10.5).

Neuronal firing rate modulation size
(Intervention group 2)
[Mean \pm 2*SEM]

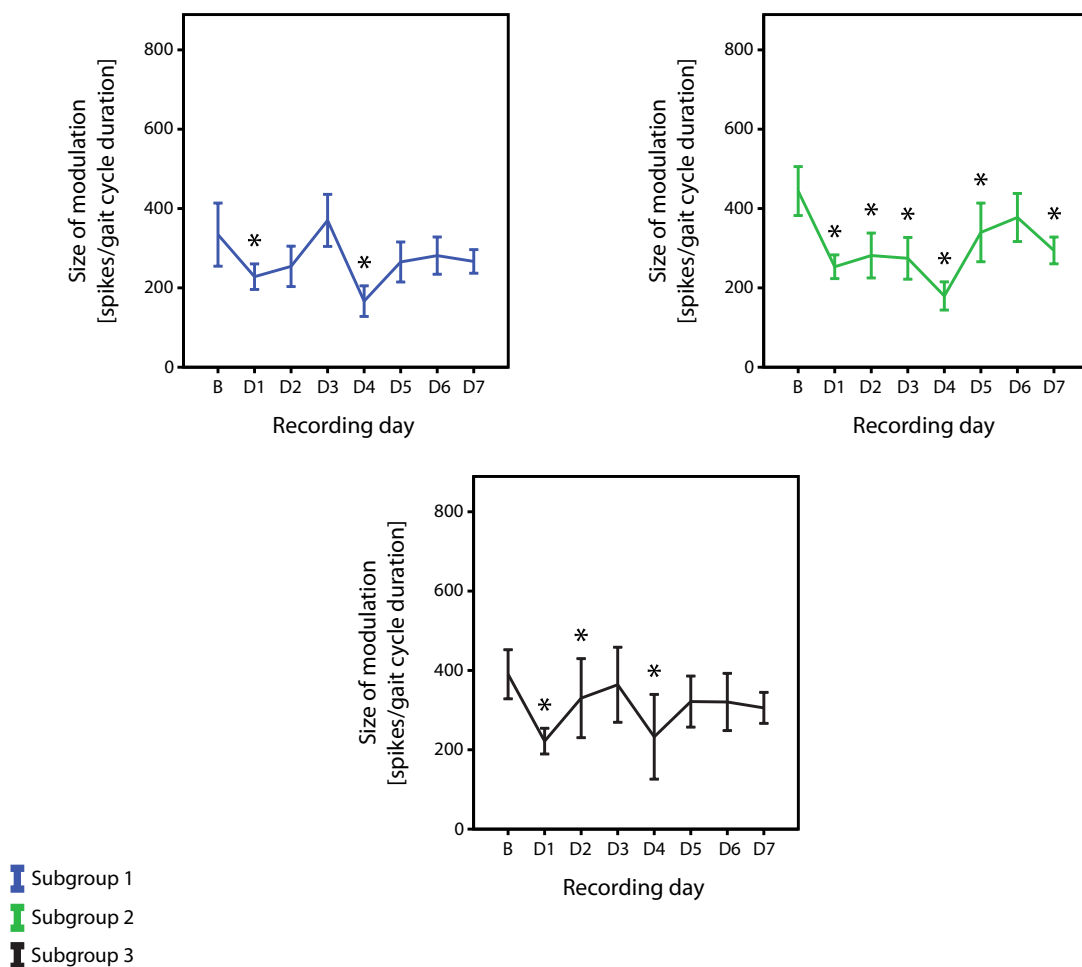


Figure 10.5: Within group results from intervention group 2. * denotes recording days with significant different firing rate modulation size throughout the gait cycles, compared to baseline level.

10.2.2 Between Groups

One-way ANOVA showed that group was a significant main factor for subgroup 1 ($p = 0.001$), subgroup 2 ($p < 0.001$), and subgroup 3 ($p < 0.001$) (fig. 10.6). Pair-wise analysis between intervention group 1 and 2 revealed that intervention group 2 had significant higher firing rate modulation size than intervention group 1 on D1 ($p = 0.025$) and D3 ($p < 0.001$) for subgroup 1. For subgroup 2, the firing rate modulation size for intervention group 2 was significantly lower than for intervention group 1 on D1 ($p < 0.001$), D2 ($p = 0.005$), D3 ($p = 0.003$), D4 ($p < 0.001$), D5 ($p < 0.001$), D6 ($p < 0.001$), and D7 ($p < 0.001$). For subgroup 3, the firing rate modulation size for intervention group 2 was significantly lower compared to intervention group 1 on D1 ($p < 0.001$), D2 ($p = 0.001$), D3 ($p = 0.001$), D4 ($p < 0.001$), D5 ($p = 0.016$), D6 ($p = 0.001$), and D7 ($p < 0.001$).

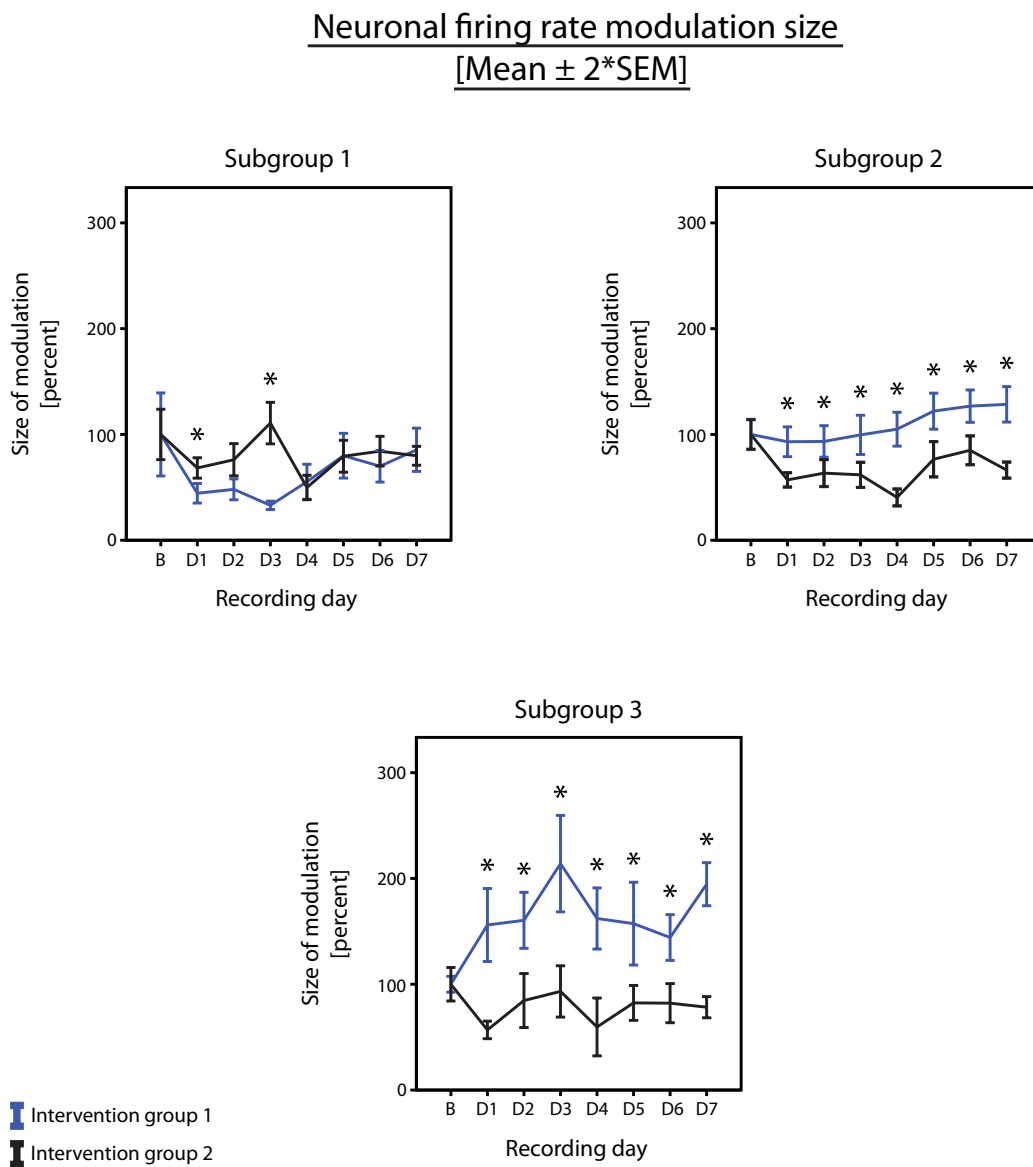


Figure 10.6: Between groups results from the different subgroups specified on the basis of the IC microstimulation results. * denotes recording days with significant different firing rate modulation size throughout the gait cycles, between the two intervention groups.

10.3 Treadmill Walking Test - Kinematics

10.3.1 Centre of Gravity for Marker Trajectories

Within Group

One-way ANOVA for intervention group 1 showed that recording day was a significant main factor for CoG of all three markers ($p < 0.001$) (fig. 10.7). The x-coordinate of the CoG for the toe-marker was significant different, compared to baseline level on D1 ($p < 0.001$) and D3 - D7 ($p < 0.001$). The y-coordinate of the CoG for the toe-marker was significant different, compared to baseline level on D1 - D7 ($p < 0.001$). The x-coordinate of the CoG for the heel-marker was significant different, compared to baseline level on D1 ($p < 0.001$), D2 ($p = 0.018$), D3 - D7 ($p < 0.001$). The y-coordinate of the CoG for the heel-marker was significant different, compared to baseline level on D1 - D4 ($p < 0.001$), D5 ($p = 0.001$), and D6 - D7 ($p < 0.001$). The x-coordinate of the CoG for the knee-marker was significant different, compared to baseline level on D2 - D4 ($p < 0.001$), D5 ($p = 0.001$), and D6 - D7 ($p < 0.001$). The y-coordinate of the CoG for the knee-marker was significant different, compared to baseline level on D1 - D7 ($p < 0.001$).

One-way ANOVA for intervention group 2 showed that recording day was a significant main factor for CoG of all three markers ($p < 0.001$) (fig. 10.8). The x-coordinate of the CoG for the toe-marker was significant different, compared to baseline level on D1 - D2 ($p < 0.001$), D5 ($p = 0.016$), and D6 - D7 ($p < 0.001$). The y-coordinate of the CoG for the toe-marker was significant different, compared to baseline level on D1 - D7 ($p < 0.001$). The x-coordinate of the CoG for the heel-marker was significant different, compared to baseline level on D1 - D2 ($p < 0.001$), D5 - D7 ($p < 0.001$). The y-coordinate of the CoG for the heel-marker was significant different, compared to baseline level on D1 - D7 ($p < 0.001$). The x-coordinate of the CoG for the knee-marker was significant different, compared to baseline level on D1 - D2 ($p < 0.001$) and D5 - D6 ($p < 0.001$). The y-coordinate of the CoG for the knee-marker was significant different, compared to baseline level on D1 - D7 ($p < 0.001$).

Centre of gravity for marker trajectories
(Intervention group 1)
[Mean \pm 2*SEM]

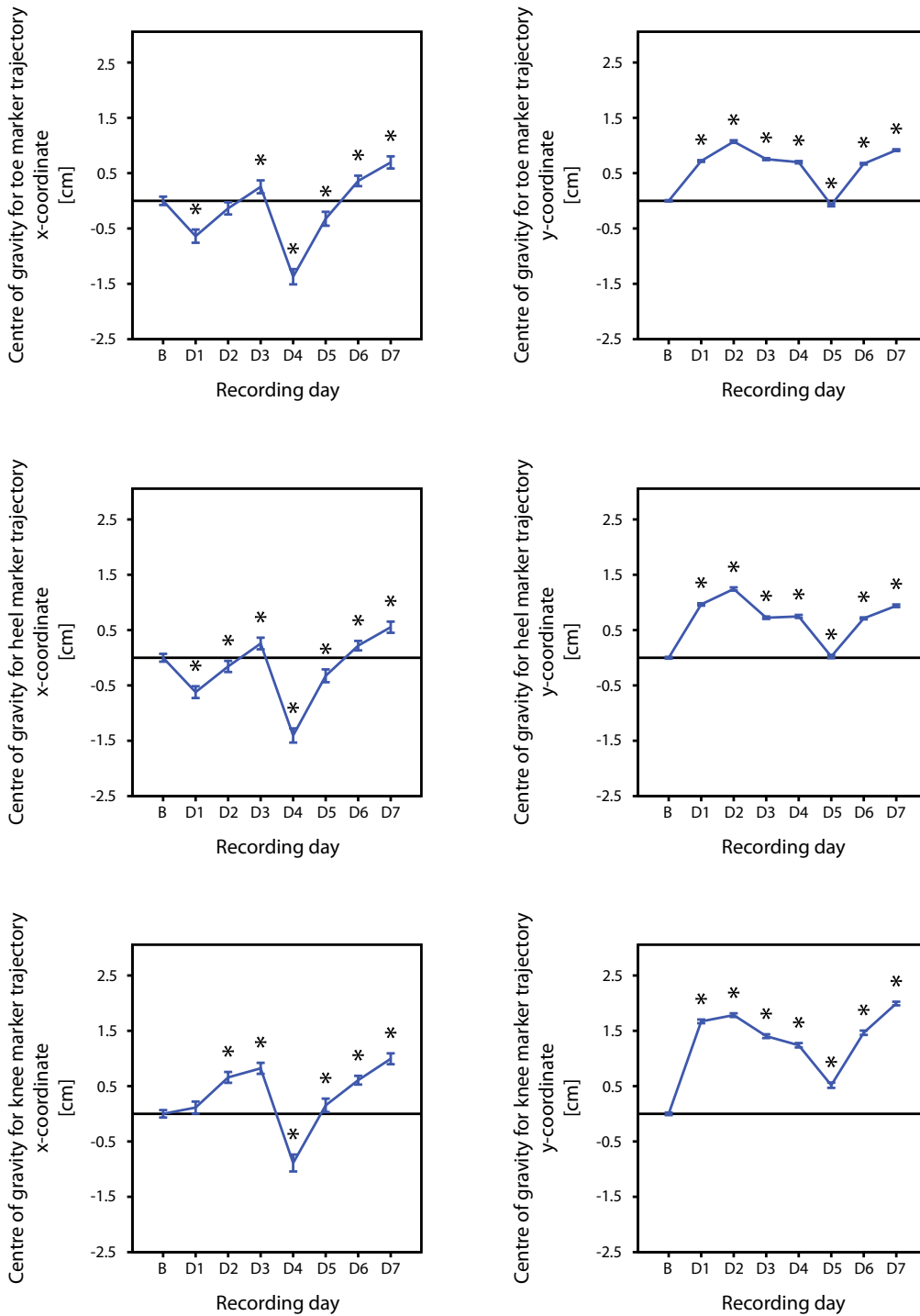


Figure 10.7: Within group results for CoG for marker trajectories during treadmill walking for intervention group 1. * denotes recording days with CoG value, significant different from baseline level.

Centre of gravity for marker trajectories
(Intervention group 2)
[Mean \pm 2*SEM]

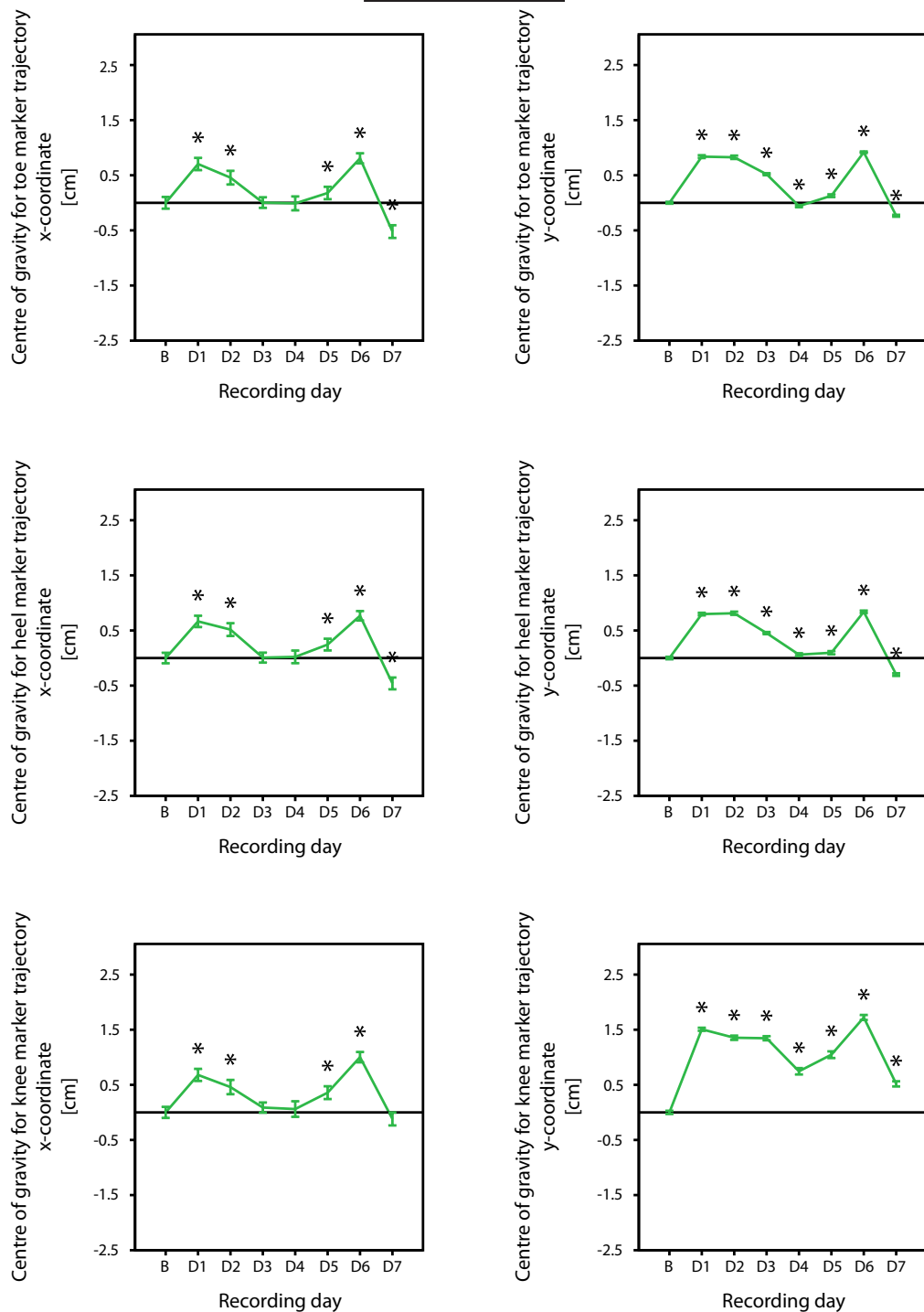
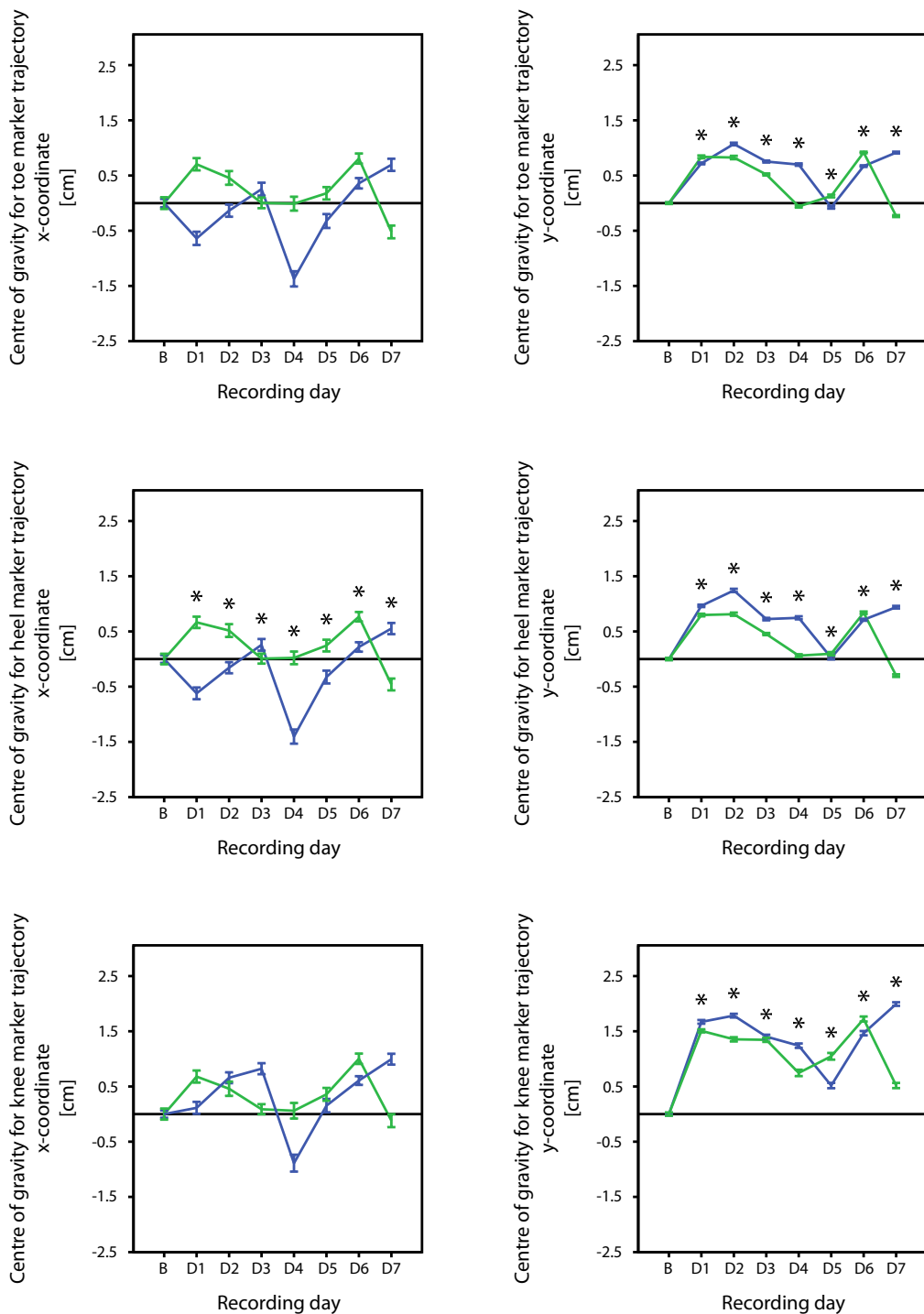


Figure 10.8: Within group results for CoG for marker trajectories during treadmill walking for intervention group 2. * denotes recording days with CoG value, significant different from baseline level.

Between Groups

One-way ANOVA showed that group was a significant main factor for the y-coordinate of the CoG for the toe-marker ($p < 0.001$), x- and y-coordinate of the CoG for the heel-marker ($p < 0.001$), and y-coordinate of the CoG for the knee-marker ($p < 0.001$) (fig. 10.9). The y-coordinate of the CoG for the toe-marker is significantly higher for intervention group 2 than intervention group 1 on D1 ($p < 0.001$) and D5 - D6 ($p < 0.001$). On the contrary, D2 - D4 ($p < 0.001$) and D7 ($p < 0.001$) showed that intervention group 2 was significantly lower compared to intervention group 1. The x-coordinate of the CoG for the heel-marker is significantly higher for intervention group 2 than intervention group 1 on D1 - D2 ($p < 0.001$) and D4 - D6 ($p < 0.001$). On the contrary, D3 ($p < 0.001$) and D7 ($p < 0.001$) showed that intervention group 2 was significantly lower compared to intervention group 1. The y-coordinate of the CoG for the heel-marker was significantly higher for intervention group 2 than intervention group 1 on D5 - D6 ($p < 0.001$). On the contrary, D1 - D4 ($p < 0.001$) and D7 ($p < 0.001$) showed that intervention group 2 was significantly lower compared to intervention group 1. The y-coordinate of the CoG for the knee-marker was significantly higher for intervention group 2 than intervention group 1 on D5 - D6 ($p < 0.001$). On the contrary, D1 - D4 ($p < 0.001$) and D7 ($p < 0.001$) showed that intervention group 2 was significantly lower compared to intervention group 1.

Centre of gravity for marker trajectories
[Mean \pm 2*SEM]



■ Intervention group 1
 ■ Intervention group 2

Figure 10.9: Between groups results for CoG for marker trajectories during treadmill walking. * denotes recording days with significant difference between the two intervention groups.

10.3.2 Residuals

Within Group

One-way ANOVA for intervention group 1 showed that recording day was a significant main factor for the knee-ground angle ($p = 0.029$) (fig. 10.10). The residuals for the knee-ground angle showed significant differences from baseline level to D1 ($p = 0.004$), D2 ($p = 0.003$), D3 ($p = 0.013$), D4 ($p = 0.003$), D5 - D7 ($p = 0.002$).

Classification of residuals
(Intervention group 1)
[Mean \pm 2*SEM]

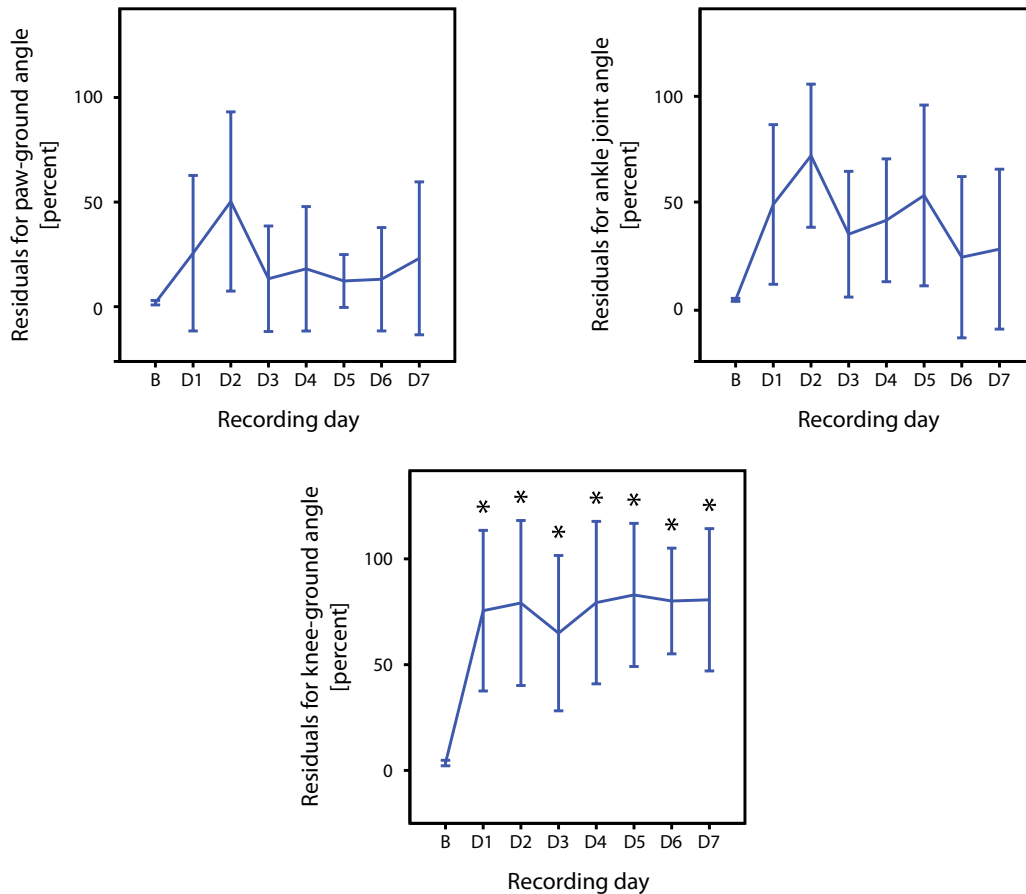


Figure 10.10: Results for residual classification for intervention group 1. * denotes recording days with significant different amounts of abnormal gait cycles, compared to baseline level.

One-way ANOVA for intervention group 2 showed that recording day was a significant main factor for the knee-ground angle ($p = 0.046$) (fig. 10.11). The residuals for the knee-ground angle showed significant differences from baseline level to D1 ($p = 0.016$), D3 ($p = 0.002$), D4 ($p = 0.005$), D5 ($p =$

0.007), and D6 ($p = 0.016$).

Classification of residuals
(Intervention group 2)
[Mean \pm 2*SEM]

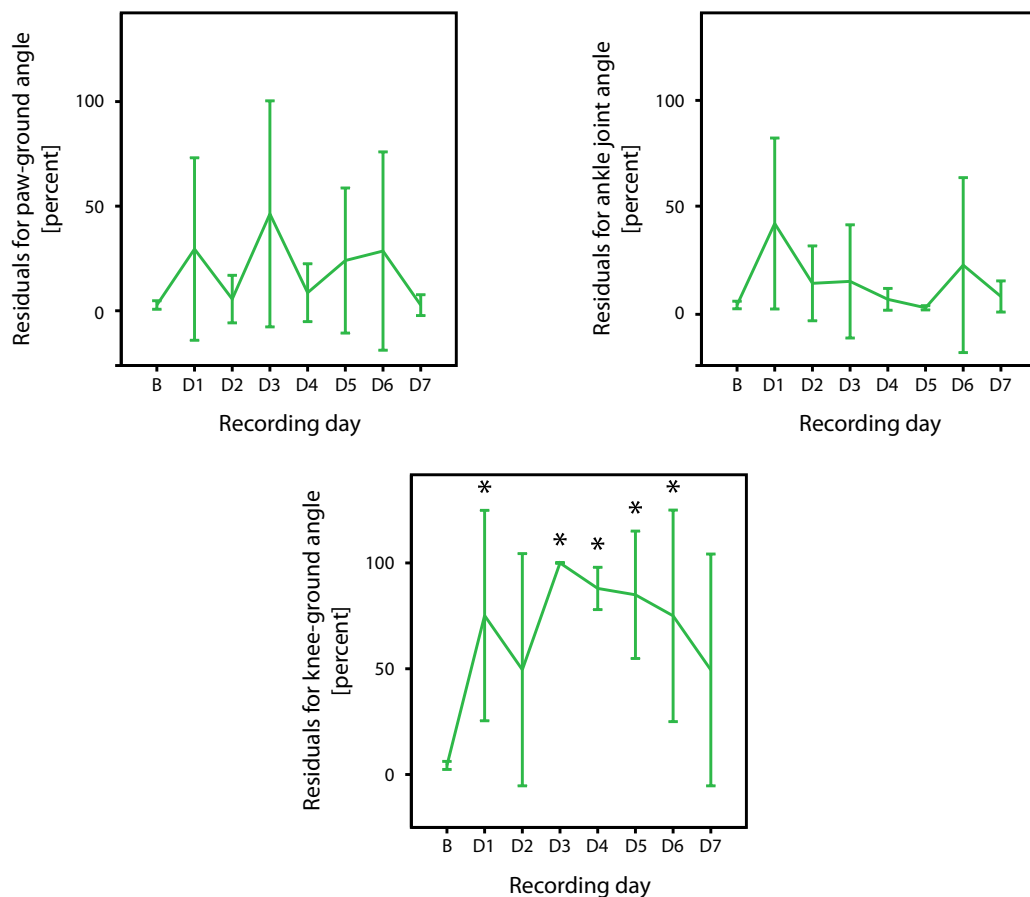


Figure 10.11: Results for residual classification for intervention group 2. * denotes recording days with significant different amounts of abnormal gait cycles, compared to baseline level.

Between Groups

One-way ANOVA between intervention group 1 and 2 showed that group was a significant main factor for ankle joint angle ($p = 0.002$) (fig. 10.12). The residuals for the ankle joint angle revealed a significant difference between intervention groups on D2 ($p = 0.026$). On this recording day, intervention group 2 had a significantly lower percentage of residuals for the ankle joint angle than intervention group 1.

Classification of residuals
[Mean \pm 2*SEM]

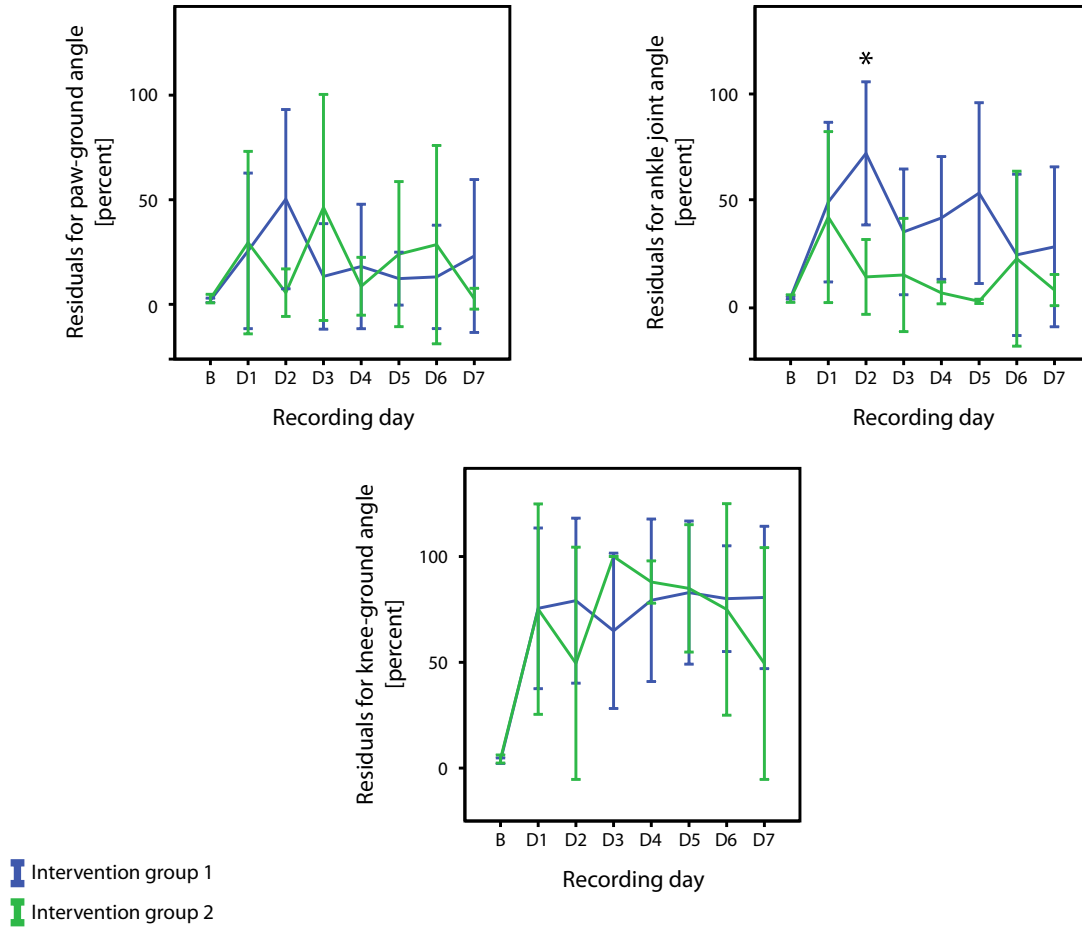


Figure 10.12: Results for residual classification of gait cycles recorded during treadmill walking. * denotes recording days with significant difference between the two intervention groups.

10.4 Beam Walking Test

10.4.1 Within Group

A one-way ANOVA showed that recording day was a significant main factor for intervention group 1 ($p < 0.001$) and intervention group 2 ($p < 0.001$) (fig. 10.13). The within group analysis, of the beam walking test for intervention group 1, revealed that the number of foot drops per beam traversal was significantly increased on D2 ($p = 0.044$) and D3 - D6 ($p < 0.001$) compared to baseline. For intervention group 2, D1 - D3 ($p < 0.001$), D4 ($p = 0.019$), and D5 ($p < 0.001$) were significantly increased from baseline.

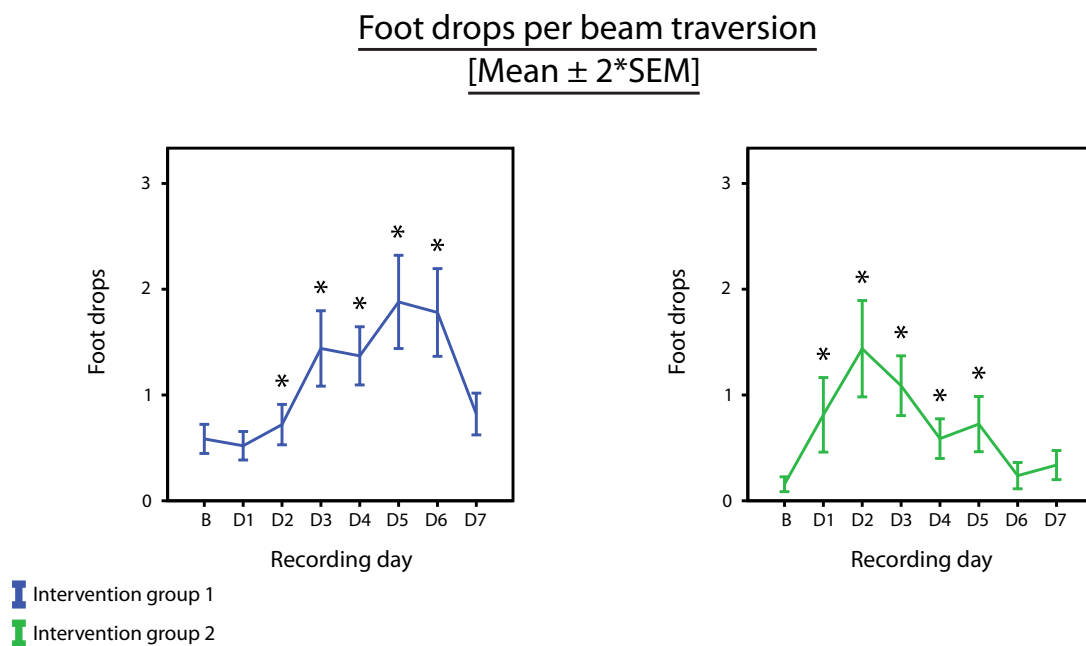


Figure 10.13: Within group results for foot drops during beam traversal for the intervention groups. * denotes recording days with significant different foot drop rates during beam traversal, compared to baseline level.

10.4.2 Between Group

One-way ANOVA showed that group was a significant main factor for the number of foot drops per beam traversal post stroke ($p < 0.001$) (fig. 10.14). A pair-wise comparison, between intervention group 1 and 2, revealed that intervention group 2 had a significantly higher number of foot drops per beam traversal, than intervention group 1, on D1 - D2 ($p < 0.001$) and D3 ($p = 0.002$), whereas the number of foot drops per beam traversal was significantly lower for intervention group 2 compared to intervention group 1 on D6 ($p < 0.001$).

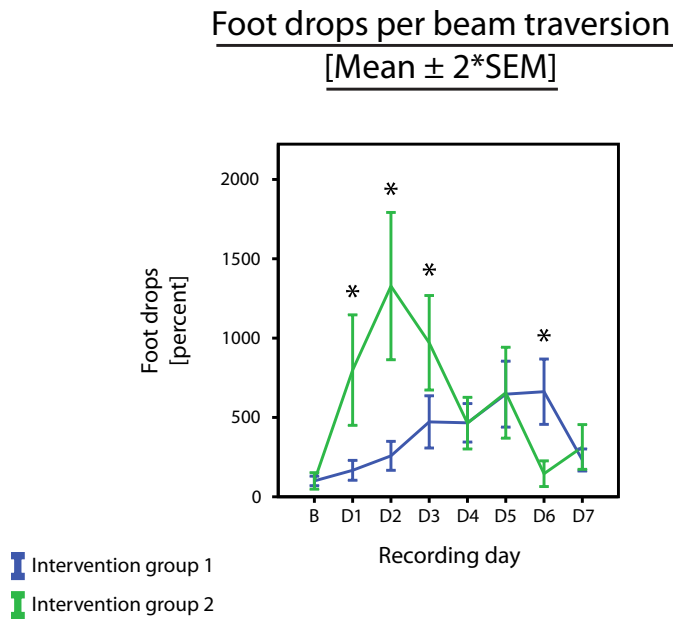


Figure 10.14: Between group results for foot drops per beam traversal. * denotes recording days with significant difference between the two intervention groups.

10.5 Summary of Results

In the following sections, tables comparing results from all tests within and between group, are illustrated, in order to summaries on the obtained results, hereby providing a base for an overall comparison within and between intervention groups.

10.5.1 Intervention Group 1

Within group IC microstimulation test results for intervention group 1 (tab. 10.3), in relations to IC measures, revealed an expansion of the hindlimb area within CMA, since the amount of hindlimb related channels did increase pre to post stroke. This result correlates with increased firing rate modulation of hindlimb related channels, which emerged post stroke across all recording days. For subgroup 1 however, firing rate modulation initially decreased, whereafter it returned to baseline level. The reason, for the re-emergence to baseline level of firing rate modulation size, is unclear, but might be related to the low amount of channels within the subgroup. Subgroup 2 initially did exhibit in firing rate modulation size similar to baseline level. However, on the terminal three days, the firing rate modulation increased. Concerning gait measures, the CoG of marker trajectories and knee-ground residual revealed altered gait patterns across all recording days post stroke. This is in correlation with remapping and altered firing rate modulation, indicating rewiring of the neuronal network within the CMA, and resulting in behavioral compensation, observed as the altered gait pattern [Kleim et al., 2002]. Though, in relations to foot drops during beam traversal, a temporary increase in amount of foot drops was observed. However, the amount of foot drops returned to baseline level at termination of the experiment.

| Comparison of results within intervention group 1 | | | | | | | | | | | | | | |
|---|---|-------------------------------------|-------------------------------------|-------------------------------------|---------------|--------------------|--------------------|---------------------|---------------------|---------------------|---------------------|------------------------|-------------------------|-------------------------|
| | Intracortical measures | | | | Gait measures | | | | | | | | | |
| | IC microstimulation (hindlimb channels) | Firing rate modulation (subgroup 1) | Firing rate modulation (subgroup 2) | Firing rate modulation (subgroup 3) | Foot drops | CoG (toe x-coord.) | CoG (toe y-coord.) | CoG (heel x-coord.) | CoG (heel y-coord.) | CoG (knee x-coord.) | CoG (knee y-coord.) | Residuals (paw-ground) | Residuals (ankle joint) | Residuals (knee-ground) |
| D1 | N/A | ↓ | - | ↑ | - | ↓ | ↑ | ↓ | ↑ | - | ↑ | - | - | ↑ |
| D2 | N/A | ↓ | - | ↑ | - | - | ↑ | ↓ | ↑ | ↑ | ↑ | ↑ | ↑ | ↑ |
| D3 | N/A | ↓ | - | ↑ | ↑ | ↑ | ↑ | ↑ | ↑ | ↑ | ↑ | - | - | ↑ |
| D4 | N/A | ↓ | - | ↑ | ↑ | ↓ | ↑ | ↓ | ↑ | ↓ | ↑ | - | - | ↑ |
| D5 | N/A | - | ↑ | ↑ | ↑ | ↓ | ↑ | ↓ | ↑ | ↑ | ↑ | - | ↑ | ↑ |
| D6 | N/A | - | ↑ | ↑ | ↑ | ↑ | ↑ | ↑ | ↑ | ↑ | ↑ | - | - | ↑ |
| D7 | ↑ | - | ↑ | ↑ | - | ↑ | ↑ | ↑ | ↑ | ↑ | ↑ | - | - | ↑ |

Table 10.3: Comparison of all results within intervention group 1. ↑ indicates variables, which were significantly increased compared to baseline level. ↓ indicates variables, which were significantly decreased compared to baseline level. - indicates variables, which were unchanged compared to baseline level.

10.5.2 Intervention Group 2

Within group IC microstimulation test results for intervention group 2 (tab. 10.4), in relations to IC measures, revealed no expansion of the hindlimb area within CMA, since the amount of hindlimb related channels did not change pre to post stroke. For subgroup 1 and 3, firing rate modulation across all recording days did in general remain unchanged. Though, on a couple of days, a minor decrease in the firing rate modulation size was observed. In relations to subgroup 1, the lack of significant decrease of firing rate modulation size could be explained by the observation that the majority (10/17 channel) of the channels within the subgroup did remap from hindlimb to forelimb correlation on the terminal IC microstimulation test. Thus, alignment of individual gait cycles according to hindlimb related gait events, might possibly result in calculation of a PSTH depicting forelimb firing rate modulations, since forelimb and hindlimb movement is phase-locked to each other. Subgroup 2 did exhibit a decreased firing rate modulation size across all recording days. Concerning gait measures, the CoG of marker trajectories and knee-ground residual revealed altered gait patterns across all recording days post stroke. Though, at termination of the experiment the differences from baseline level were smaller, than for intervention group 1. This observation indicates a less degree of altered gait pattern, which is in correlation with the lack of remapping and thus possible absence of neuronal rewiring within the CMA [Murphy and Corbett, 2009]. Though, in relations to foot drops during beam traversal a temporary increase in the amount of foot drops was initially observed. However, the amount of foot drops returned to baseline level at termination of the experiment.

10.5.3 Comparison of Intervention Groups

Comparing results for the individual interventions group, it is apparent that rehabilitation, initiated on day one post stroke, resulted in expansion of hindlimb related channels, and increased firing modu-

| Comparison of results within intervention group 2 | | | | | | | | | | | | | | |
|---|---|-------------------------------------|-------------------------------------|-------------------------------------|---------------|--------------------|--------------------|---------------------|---------------------|---------------------|---------------------|------------------------|-------------------------|-------------------------|
| | Intracortical measures | | | | Gait measures | | | | | | | | | |
| | IC microstimulation (hindlimb channels) | Firing rate modulation (subgroup 1) | Firing rate modulation (subgroup 2) | Firing rate modulation (subgroup 3) | Foot drops | CoG (toe x-coord.) | CoG (toe y-coord.) | CoG (heel x-coord.) | CoG (heel y-coord.) | CoG (knee x-coord.) | CoG (knee y-coord.) | Residuals (paw-ground) | Residuals (ankle joint) | Residuals (knee-ground) |
| D1 | N/A | ↓ | ↓ | ↓ | ↑ | ↑ | ↑ | ↑ | ↑ | ↑ | ↑ | - | - | ↑ |
| D2 | N/A | - | ↓ | ↓ | ↑ | ↑ | ↑ | ↑ | ↑ | ↑ | ↑ | - | ↑ | - |
| D3 | N/A | - | ↓ | - | ↑ | - | ↑ | - | ↑ | - | ↑ | - | - | ↑ |
| D4 | N/A | ↓ | ↓ | ↓ | ↑ | - | ↓ | - | ↑ | - | ↑ | - | - | ↑ |
| D5 | N/A | - | ↓ | - | ↑ | ↑ | ↑ | ↑ | ↑ | ↑ | ↑ | - | - | ↑ |
| D6 | N/A | - | - | - | - | ↑ | ↑ | ↑ | ↑ | ↑ | ↑ | - | - | ↑ |
| D7 | - | - | ↓ | - | - | ↓ | ↓ | ↓ | ↓ | - | ↑ | - | - | - |

Table 10.4: Comparison of all results within intervention group 2. ↑ indicates variables, which were significant increased compared to baseline level. ↓ indicates variables, which were significant decreased compared to baseline level. - indicates variables, which were unchanged compared to baseline level.

lation size within the channels correlated to hindlimb on the terminal IC microstimulation test. The remapping and increased firing rate modulation can possible be explained by hebbian plasticity, since the training paradigm, utilised during the present study, focuses on repetitive movement training. This remapping on the neuronal level, indicates loss of former motor programmes, which is further emphasised by altered CoG for marker trajectories and results from residuals, describing general behavioral compensation. However, the functional performance level returned to baseline level. On the contrary, intervention group 2 did not show any hindlimb motor area expansion or increased firing rate modulation size during rehabilitation. Combining this with the less degree of alterations related to CoG for marker trajectories and results from residuals, it might be suggested that the delayed onset of rehabilitation coincides with a neuronal environment, in which repetitive training is more effective, resulting in a less degree of behavioral compensation on both neuronal and functional level.

11.1 Methodological Considerations

16 out of 24 rats, enrolled in the training paradigm prior to experimental onset, did successfully meet the experimental inclusion criteria. Out of these 16, six rats died and one was excluded after termination of the experiment. As a consequence the results only reflects on data from nine rats, of which none were within the control groups. However, the lack of control groups was not crucial, since each rat served as its own control on the basis of the baseline recordings. While the baseline recordings were not significantly different, indicating stable physiological conditions, these were assumed to be sufficient as control. The rats died of several different reasons, of which most are uncontrollable, and the deaths could therefore not be avoided. Thus, it is necessary to have a larger group of rats, enrolled in the training paradigm, prior to experimental onset, in order to assure a sufficiently large experimental group.

The concentration of rose bengal dye, used in the experiment, was 20 mg/ml saline, and a dose of 0.3 ml/100 g body weight were used. In this way the total amount of rose bengal dye, which is injected, is higher than the ones used in the experiments represented in sec. 6.1. The choice of dose size was based on experiences from the pilot experiment, where lower doses did not induce visible motor deficits during gait. One possible explanation, for the lack of visible deficits, is the difference in the injury site in the pilot experiment, compared to previous studies, since different blood vessel distribution is apparent across cortical regions [Wang-Fischer, 2008]. Another possible explanation is related to the low degree of motor cortical control of gait in quadrupeds, which might result in the need of inducing a larger stroke, in order to produce visible gait deficits [Nielsen, 2003].

The amount of rehabilitative training is a tradeoff between reaching a high enough amount of movement repetitions, and assuring a high degree of similarity between individual repetitions, in order to induce hebbian synaptic learning [Murphy and Corbett, 2009; Woldag and Hummelsheim, 2002]. The level of rehabilitative training was based on observations from the pilot experiment, where it was seen that the quality of the gait performance declined after 25 beam traversions and 3 x 1 minutes of treadmill walking. The amount was believed to be high enough to envoke hebbian synaptic learning, since the results documented that functional performance level post stroke returned to baseline level.

The duration of rehabilitation is a tradeoff between electrode functionality and stability of terminal results. The quality of IC signals might decline over time. However, Vetter et al. [2004] documented IC signals of sufficient quality for spike detection up to 127 days post stroke. A timespan of 28 days of rehabilitative training was chosen, since physiological conditions have previously shown to reach

a stable level within this time [Metz et al., 2005]. However, large differences were seen, for firing rate modulation sizes between the last two recording days prior to termination of the experiment. Therefore, it would be interesting to prolong the rehabilitative timespan, in order to investigate if a stable level could be achieved.

Results from IC microstimulation tests were obtained on the basis of observed muscle movements, elicited by the electrical stimulations. Classification of channels was based on single movement observations, and thus it was not verified if the response could be elicited with consecutive identical stimulations. Previous studies e.g. Neafsey et al. [1986] have utilised an approach, where two to three consecutive identical stimulations were applied, upon observation of muscle activation, due to the IC microstimulation. This approach could have been used in the present study, in order to minimise the risk of misclassifying IC channels. Classification upon one observation of IC microstimulation resulting in muscle activation, was though chosen since the level of physical stress increased as a function of the number of electrical stimulations.

When assessing the results from the tracked marker trajectories it is necessary to consider the artefact caused by skin movement. However, in a study by Reinschmidt et al. [1996], it was found that the average angle difference in knee flexion and extension, obtained between skeletal and skin markers, was 2.1° . The skin movement artefact does not have significant effects on the results in the present study, since all results are calculated relatively to the baseline level, and thus the artefact is equally present on all recording days.

In the beam walking test, foot drops were counted for each hindlimb during each traversal. The results were calculated as the sum of foot drops for both hindlimbs. A disadvantage of this method is the lack of possibility to detect, whether the main compensation is apparent on one hindlimb or distributed on both. However, the main focus of the test was to verify that stroke had been induced, and thus the site of compensation was less important.

The x-axis of the PSTHs was transformed from time to percent of gait cycle duration. The advantage of this transformation is that individual gait cycles are aligned in the percent of gait cycle duration domain. Though, this advantage is obtained with a reduction in temporal resolution determined by the length of the individual gait cycles. In this way, the determination of modulation timing is compromised, but the modulation amount across gait cycles is more representative for the general neuronal firing within the recorded cortical area.

11.2 Results

The results of the marker trajectories revealed fluctuations of the CoG x-coordinates in both intervention groups. These fluctuations might not represent an actual instability in hindlimb movement across recording days, but could instead be caused by altered positioning of the abdomen marker or inconsistent camera positioning across recording days. Altered abdomen marker positioning would induce a lowering or an increase in the CoG x-coordinate depending on the displacement distance

in the horizontal plane. Incorrect placement of the camera across recording days, i.e. the camera is not placed perpendicular to the treadmill, leads to inconsistency of the calculated lengths between the markers. Though, it is believed that the CoG for x-coordinates reflect physiological alterations, since it is unlikely that possible alterations in abdomen marker positioning were equal for each rat within the intervention group. Furthermore, misplacement of the camera is also unlikely, since the camera was attached on a frame, which was not moved during the experiment. The SEM, calculated for the CoG of the marker trajectories, were very low, due to the large amount of samples, since a CoG was calculated for every gait cycle. Thus, only minor changes in the position of the CoG were required, in order to induce significant differences across recording days. Though, on several recording days the difference between and within groups for the CoG for marker trajectories were so large, that they most likely reflect physiological alterations during the course of the experiment.

One issue, in relation to ensemble recordings and analysis of hebbian plastic learning, is verification of correlated firing between neurons. Since PSTHs are possibly composed of the net sum of firing of several neurons, within the recording site of the IC electrode array, correlation analysis is troublesome. One approach to discriminate between the firing pattern of different neurons is to implement continuous recording of IC signals, hereby enabling spike sorting. This would enable verification of the source of firing rate modulation, e.g. one or multiple neurons [Nicoletis, 2008].

The results from the residuals for both intervention groups revealed that the main site for changes during gait was the knee-ground angle, even though this angle has a smaller range of values, compared to the ankle joint angle. The possible reason, for the lack of significant changes in the ankle joint angle, might have been a combination of variability on the baseline recordings and the low sample size, giving rise to large SEMs.

The aim of the present work was to assess if gait function post stroke was affected by different onset times of rehabilitation, through development and utilisation of a novel rat model of ischemic stroke. The results obtained from the beam walking test revealed that both intervention groups had gait deficits post stroke, hereby verifying that damage to the CMA had occurred. Further, the results showed expansion of the hindlimb representation within the CMA, and an increased firing rate modulation post stroke for intervention group 1. In contrast, for intervention group 2, these parameters were not significantly changed compared to baseline level. Results related to residuals and CoG for marker trajectories revealed a significant change pre to post stroke for both intervention groups. However, this difference was higher for intervention group 1, compared to intervention group 2. In summary the results showed that gait function post stroke is affected by onset time of rehabilitative training, indicated by a more effective rehabilitation and less behavioral compensation, when initiating rehabilitation on day seven compared to day one post stroke intervention. In this way, the novel rat model of ischemic stroke made it possible to discriminate between the effect, on both neuronal and peripheral level, of the two rehabilitative onset times, assessed in the present study. Therefore it can be concluded that a novel rat model of ischemic stroke was successfully developed.

12.1 Future Perspectives

Several new approaches, for improving the method for obtaining and analysing data in future work, can be introduced. These approaches are:

- Detection of midswing event of the gait cycle
- Integration of phase durations in CoG calculations
- Inclusion of another intervention group with rehabilitation onset after the critical period
- 3D recording during treadmill walking test
- Continuous time recording of IC signals

Detection of the midswing event of the gait cycle would increase the level of detail in the analysis of the IC signals, since addition of the midswing event would provide a third anchoring point, which could be used in comparison of activity recorded from different channels.

Phase durations of the gait cycle in CoG calculations could be integrated, in order to enable weighting of marker trajectories according to the swing and stance duration. This would eliminate the unequally distributed amount of data points in the stance and swing phase, which can distort the CoG position, and thus complicating the interpretation of the CoG results.

Inclusion of additional intervention group with rehabilitation onset after the critical period would enable verification of the suggested end time of the critical period, by using the currently developed rat model of ischemic stroke to assess the effect of the rehabilitative training.

3D recording during the treadmill walking test would enable assessment of compensatory movements post stroke through abduction/adduction of the hindlimb. Hereby, also eliminating the issue concerning variations in segmental distances calculated between markers.

Continuous time recording of IC signals would enable spike sorting and inclusion of methods for correlation between firing patterns of individual neurons. Hereby, enabling discrimination between individual neuronal firing characteristics, providing possibility for assessment of single-unit firing modulations.

Bibliography

- D. M. Armstrong and T. Drew. Discharges of pyramidal tract and other motor cortical neurones during locomotion in the cat. *The Journal of Physiology*, 346:471–495, 1984.
- A. Arvidsson, T. Collin, D. Kirik, Z. Kokaia, and O. Lindvall. Neuronal replacement from endogenous precursors in the adult brain after stroke. *Nature Medicine*, 8:963–970, 2002.
- S. Barbay, E.J. Plautz, K.M. Friel, S.B. Frost, N. Dancause, A.M. Stowe, and R.J. Nudo. Behavioral and neurophysiological effects of delayed training following a small ischemic infarct in primary motor cortex of squirrel monkeys. *Experimental Brain Research*, 169:106–116, 2006.
- Basler Inc. *BASLER A600f USER'S MANUAL*, 2005. Downloaded: 19.05.11.
- J. Biernaskie, G. Chernenko, and D. Corbett. Efficacy of Rehabilitative Experience Declines with Time after Focal Ischemic Brain Injury. *Journal of Neuroscience*, 24:1245–1254, 2004.
- M.H. Canu and C. Garnier. A 3D analysis of fore- and hindlimb motion during overground walking and ladder walking: Comparison of control and unload rats. *Experimental Neurology*, 218: 98–108, 2009.
- S.T. Carmichael. Rodent Models of Focal Stroke: Size, Mechanism, and Purpose. *The Journal of the American Society for Experimental NeuroTherapeutics*, 2:396–409, 2005.
- A. Despopoulos and S. Silberagl. *Color Atlas of Physiology*. 5th edition. Thieme, 2003. ISBN 3-13-545005-8.
- U. Dirnagl, C. Iadecola, and M.A. Moskowitz. Pathobiology of ischaemic stroke: an integrated view. *Trends in Neurosciences*, 22:391–397, 1999.
- B.H. Dobkin. Strategies for stroke rehabilitation. *The Lancet*, 3:528–536, 2004.
- J.P. Donoghue and S.P. Wise. The Motor Cortex of the Rat: Cytoarchitecture and Microstimulation mapping. *The Journal of Comparative Neurology*, 212:76–88, 1982.
- R.J. Douglas and K.A.C. Martin. Neuronal Circuits of the Neocortex. *The Annual Review of Neuroscience*, 2004.
- T. Drew. Motor cortical cell discharge during voluntary gait modification. *Brain Research*, 457: 181–187, 1988.

- A.W. Dromerick, C.E. Lang, R.L. Birkenmeier, J.M. Wagner, J.P. Miller, T.O. Videen, W.J. Powers, S.L. Wolf, and D.F. Edwards. Very Early Constraint-Induced Movement during Stroke Rehabilitation (VECTORS): A single-center RCT. *Neurology*, 73(3):195–201, 2009.
- P.W. Duncan, S.M. Lai, and J. Keighley. Defining post-stroke recovery: implications for design and interpretation of drug trials. *Neuropharmacology*, 39:835–841, 2000.
- J.J. Grome, G. Gojowczyk, W. Hofmann, and D.I. Graham. Quantitation of photochemically induced focal cerebral ischemia in rats. *Journal of Cerebral Blood Flow and Metabolism*, 8:89–95, 1988.
- Hjerteforeningen. *Fakta om apopleksi*. URL:
http://www.hjerteforeningen.dk/hjertestatistik/fakta_om_apopleksi/, 2011.
Visited: 21.05.12.
- T.A. Jones, J.A. Kleim, and W.T. Greenough. Synaptogenesis and dendritic growth in the cortex opposite unilateral sensorimotor cortex damage in adult rats: a quantitative electron microscopic examination. *Brain Research*, 733:142–148, 1996.
- E. Kandel, J.H. Schwartz, and T.M. Jessel. *Principles of Neural Science*. 4th edition. McGraw-Hill, 2000. ISBN 0-8385-7701-6.
- J.A. Kleim and T.A. Jones. Principles of Experience-Dependent Neural Plasticity: Implications for Rehabilitation After Brain Damage. *Journal of Speech, Language, and Hearing Research*, 51: 225–239, 2008.
- J.A. Kleim, S. Barbay, N.R. Cooper, T.M. Hogg, C.N. Reidel, M.S. Remple, and R.J. Nudo. Motor Learning-Dependent Synaptogenesis Is Localized to Functionally Reorganized Motor Cortex. *Neurobiology of Learning and Memory*, 272:1791–1794, 2002.
- B. Kolb, J. Cioe, and I.Q. Whishaw. Is there an optimal age for recovery from motor cortex lesions? I. Behavioral and anatomical sequelae of bilateral motor cortex lesions in rats on postnatal days 1, 10, and in adulthood. *Brain Research*, 882:62–74, 2000.
- Bryan Kolb and Richard C. Tees. *The Cerebral Cortex of the Rat*. 1. edition. The MIT Press, 1990. ISBN 0-262-61064-7.
- D. Lanens, N. Spanoghe, J. Dan Audekerke, A. Oksendal, A. Van der Linden, and R. Dommissie. Complimentary use of T2-weighted and postcontrast T1 and T2*-weighted imaging to distinguish sites of reversible and irreversible brain damage in focal ischemic lesions in the rat brain. *Magnetic Resonance Imaging*, 13:185–192, 1995.
- V.M. Lee, G.B. Newman, A. Carpenter, L.D. Hall, P.S. Pambakian, S. Patel, N.I. Wood, and M.F. James. Evolution of Photochemically Induced Focal Cerebral Ischemia in the Rat. *Stroke*, 27: 2110–2119, 1996.
- G.A. Metz, I. Antonow-Sclorke, and O.W. Witte. Motor improvements after focal cortical ischemia in adult rats are mediated by compensatory mechanisms. *Experimental Neurology*, 162:71–82, 2005.
- T.H. Murphy and D. Corbett. Plasticity during stroke recovery: from synapse to behaviour. *Neuroscience*, 10:861–872, 2009.

- E.J. Neafsey, E.L. Bold, G. Haas, K.M. Hurley-Gius, G. Quirk, C.F. Sievert, and R.R. Terreberry. The Organization of the Rat Motor Cortex: A Microstimulation Mapping Study. *Brain Research Reviews*, 11:77–96, 1986.
- Miguel A. L. Nicolelis. *Methods for Neural Ensemble Recordings*. 2nd edition. CRC-Press, 2008. ISBN 978-0-8493-7046-5.
- J.B. Nielsen. How we Walk: Central Control of Muscle Activity during Human Walking. *The Neuroscientist*, 9:195–204, 2003.
- M. Nieto-Sampedro and M. Nieto-Diaz. Neural plasticity: changes with age. *Journal of Neural Transmission*, 112:3–27, 2005.
- J. Nolte. *The Human Brain: An Introduction to its Functional Anatomy*. 6th edition. Elsevier Inc., 2009. ISBN 978-0-323-04131-7.
- R.J. Nudo. Postinfarct Cortical Plasticity and Behavioral Recovery. *Stroke*, 38:840–845, 2007.
- G. Paxinos. *The Rat Nervous System*. 3rd edition. Elsevier Inc., 2004. ISBN 978-0-12-547638-6.
- J. Raber, Y. Fan, Y. Matsumori, Z. Liu, P.R. Weinstein, J.R. Fike, and J. Liu. Irradiation attenuates neurogenesis and exacerbates ischemia-induced deficits. *Annals of Neurology*, 55:381–389, 2004.
- C. Reinschmidt, A.J. van den Bogert, A. Lundberg, B.M. Nigg, N. Murphy, A. Stacoff, and A. Stano. Tibiofemoral and tibio-calcaneal motion during walking: external vs. skeletal markers. *Gait and Posture*, 6:98–109, 1996.
- L.B. Rowell and J.T. Shepherd. *Handbook of Physiology - section 12: Exercise: Regulation and Integration of Multiple Systems*. 1st edition. Oxford University Press, 1997. ISBN 0195091744.
- T. Schallert, M.T. Woodlee, and S.M. Fleming. Disentangling multiple types of recovery from brain injury. *Pharmacology of Cerebral Ischemia*, pages 201–216, 2002.
- M. Schroeter, K. Schiene, M. Kraemer, G. Hagemann, H. Weigel, U.T. Eysel, O. Witte, and G. Stoll. Astroglial responses in photochemically induced focal ischemia of the rat cortex. *Exp Brain Res*, 106:1–6, 1995.
- Sigma-Aldrich. *Safety Data Sheet*. URL: <http://www.sigmaaldrich.com/catalog/product/sigma/r3877?lang=en®ion=DK>, 2006. Downloaded: 15.05.12.
- Sundhed.dk. *Apopleksi, rehabilitering*. URL: <http://laegehaandbogen.dk/legehaandbogen/hjerte-kar/apopleksi-rehabilitering-13084.html>, 2010. Visited: 21.05.12.
- P. Thored, A. Arvidsson, E. Cacci, H. Ahlenius, T. Kallur, V. Darsalia, C.T. Ekdahl, Z. Kokaia, and O. Lindvall. Persistent Production of Neurons from Adult Brain Stem Cells During Recovery after Stroke. *Stem Cells*, 24:739–747, 2006.
- Tucker-Davis Technologies Inc. *System 3 Manual*, 2011. Downloaded: 19.05.11.
- M. Ueno and T. Yamashita. Kinematic analyses reveal impaired locomotion following injury of the motor cortex in mice. *Experimental Neurology*, 230:280–290, 2011.

- R.J. Vetter, J.C. Williams, J.F. Hetke, E.A. Nunamaker, and D.R. Kipke. Chronic neural recording using silicone-substrate microelectrode arrays implanted in cerebral cortex. *IEEE Transactions on Biomedical Engineering*, 51:896–904, 2004.
- W.F. Walker Jr and D.G. Homberger. *Anatomy and Dissection of the Rat*. 3. edition. W. H. Freeman and Company, 1997. ISBN 0-7167-2635-1.
- Y. Wang-Fischer. *Manual of Stroke Models in Rats*. 1st edition. CRC Press, 2008. ISBN 978-0-8493-9578-9.
- B.D. Watson, W.D. Dietrich, R. Busto, M.S. Wachtel, and M.D. Ginsberg. Induction of reproducible brain infarction by photochemically initiated thrombosis. *Annals of Neurology*, 17:497–504, 1985.
- P. Wester, B.D. Watson, R. Prado, and M.D. Ginsberg. A Photothrombotic ‘Ring’ Model of Rat Stroke-in-Evolution Displaying Putative Penumbra Inversion. *Stroke*, 26:444–450, 1987.
- T. Wieloch and K. Nikolich. Mechanisms of neural plasticity following brain injury. *Current Opinion in Neurobiology*, 16:258–264, 2006.
- O.W. Witte, H. Bidmon, K. Schiene, C. Redecker, and G. Hagemann. Functional Differentiation of Multiple Perilesional Zones After Focal Cerebral Ischemia. *Journal of Cerebral Blood Flow & Metabolism*, 20:1149–1165, 2006.
- H. Woldag and H. Hummelsheim. Evidence-based physiotherapeutic concepts for improving arm and hand function in stroke patients. *Journal of Neurology*, 249:518–528, 2002.
- T.M. Woodruff, J. Thundyil, S. Tang, C.G. Sobey, and S.M. Taylor. Pathophysiology, treatment, and animal and cellular models of human ischemic stroke. *Molecular Neurodegeneration*, 6:1–19, 2011.
- W. Yonggang, B. Bontempi, S.M. Hong, K. Mehta, P.R. Weinstein, G.M. Abrams, and J. Liu. A comprehensive analysis of gait impairment after experimental stroke and the therapeutic effect of environmental enrichment in rats. *Journal of Cerebral Blood Flow and Metabolism*, 28:1936–1950, 2008.
- K.J. Zilles. *The Cortex of the Rat. A Stereotaxic Atlas*. 1st edition. Springer-Verlag, 1985. ISBN 9780387155708.